

THE NODAL BOUNDARY CONDITION METHOD
WAVE FUNCTIONS AND TRANSITION PROBABILITIES
FOR ATOMS WITH TWO VALENCE ELECTRONS

Thesis by
Thomas M. Helliwell

In Partial Fulfillment of the Requirements
For the Degree of
Doctor of Philosophy

California Institute of Technology
Pasadena, California
1963

ACKNOWLEDGMENTS

The author is particularly grateful to Professor R. F. Christy for continued help and encouragement in the preparation of this thesis. Several conversations with Professor R. B. King on experimental results were very useful. Numerous discussions on astrophysical applications with Professors J. L. Greenstein and W. A. Fowler, and also with Dr. W. L. W. Sargent and Dr. J. Jugaku, provided one of the chief motivations for this work.

ABSTRACT

A method is presented for computing valence atomic wave functions and transition probabilities. This method, called the "nodal boundary condition method", is a modified self-consistent-field approach which makes some use of experimental term-values in order to eliminate the need for calculating wave functions for the core electrons. As an application, the method is used to compute eigenvalues, wave functions, and transition probabilities for several atoms and ions having two valence electrons.

Various other approaches to the problem of calculating atomic wave functions are reviewed, so that the assumptions and approximations of the nodal boundary condition method may be placed in perspective. The results of the present calculations are compared in detail with previous results whenever possible. Finally, possible applications and extensions of the method are briefly discussed.

TABLE OF CONTENTS

I. INTRODUCTION	1
II. DEFINITIONS AND PROPERTIES OF OSCILLATOR STRENGTHS	5
III. METHODS OF CALCULATING ATOMIC WAVE FUNCTIONS	9
A. Atomic Wave Functions	9
B. The Hartree-Fock Method	15
C. Polarization of the Core	19
D. Analytic Variational Methods	24
E. The Nuclear Charge - Expansion Method	27
IV. THE COULOMB APPROXIMATION	31
A. The Method of Bates and Damgaard	31
B. Valence Wave Functions	35
C. Coulomb, SCF, and Experimental Oscillator Strengths	39
V. THE NODAL BOUNDARY CONDITION METHOD	43
A. Nodal Stability	45
B. Coulomb Nodes	52
1. Hydrogen and Ionized Helium	56
2. Alkali Atoms and Ions	59
3. $d^{10}s^2$ Atoms and Ions	75
4. s^2p Atoms and Ions	85
C. The Method with Calcium as an Example	92
1. Location of the Coulomb Nodes	92
2. The s^2 Ground-State Energy and Wave Function	93

3. The Excited $sp\ ^1P_1$ State	94
4. Calculation of Oscillator Strengths	95
D. Intercombination Lines	96
VI. RESULTS AND APPLICATIONS	105
A. The S-Squared Calculations	105
B. Eigenvalues and Oscillator Strengths	106
C. Comparison with the Coulomb Approximations and with Experimental Results of the National Bureau of Standards	163
D. General Conclusions	169
E. Astrophysical Applications	171
F. Extensions and Further Applications of the Nodal Boundary Condition Method	176
1. Configuration Interactions	176
2. Additional Electron Configurations	178
3. Other Applications	179
REFERENCES	182
APPENDIX A: Numerical Solution of the Equations	186
A. The Schrödinger Equation in a Coulomb Field	186
B. The $s^2\ ^1S_0$ Hartree-Fock Equation	188
C. The $sl\ ^1L$ and 3L Hartree-Fock Equations	189
APPENDIX B: The Computer Programs	195
Input Data Cards	197
The Subroutines	205
The Fortran Programs	223

I. INTRODUCTION

At the present time, there is an increasing need for reasonably accurate atomic transition probabilities, or "oscillator strengths." In contrast to atomic energy levels, which have been measured with great accuracy for most important atoms and ions, and which can often be well predicted theoretically, transition probabilities are usually only poorly known. Both experiments and theoretical calculations are rather difficult to perform.

From the very incomplete existing knowledge of oscillator strengths, it is clear that more effort is required, both experimentally and theoretically. Aside from the valuable comparisons between measurements and calculations, in some important cases only one method may be practicable. Experiments can be carried out on very complex atoms which may be nearly impossible to compute. On the other hand, ionized atoms are no more difficult to understand theoretically than neutral ones, while there are numerous experimental difficulties in making measurements with ions, because of the high temperatures involved. In addition, there are a number of neutral atoms, having inconvenient properties in the laboratory, which may be calculable.

This thesis will present a method for computing radial atomic wave functions which are often suitable for the calculation of oscillator strengths. The method, which is essentially a simplified self-consistent-field approach, will be called the "nodal boundary condition method." New approaches to the computation of transition probabilities are a practical necessity. In all but the simplest atoms, accurate calculations of atomic

wave functions are generally difficult and tedious. In Section III, various approaches to the problem of computing accurate transition probabilities will be discussed in some detail. It is appropriate here to mention two of these, which serve as a background to the introduction of the nodal boundary condition method.

The most generally accurate practical method for calculating atomic wave functions is the variational self-consistent-field (SCF) method. This general approach may assume many forms. In any case, computations are lengthy and the work proceeds atom by atom, sometimes only for the ground state, but seldom for more than two or three excited states. Thus only a limited number of SCF transition probabilities are available.

In 1949, the problem of computing accurate oscillator strengths for atoms with one valence electron was effectively and simply solved by Bates and Damgaard (1). Their method has been extensively applied to many kinds of atoms, but can only be consistently trustworthy for those with one valence particle. The great advantage of their approach is that the inner electron shells can be eliminated from the problem by the use of experimental term values. Results obtained by this simple method are as good or better than full self-consistent-field calculations for the appropriate atoms.

An important class of atoms and ions are those having two electrons outside closed shells, such as magnesium and calcium. Compared to our knowledge of atoms with one valence electron, data for two-electron atoms is rather meagre. A few experiments have been per-

formed. Also a handful of SCF calculations have been completed, particularly on the resonance lines.

The nodal boundary condition method was devised in an effort to obtain a large number of oscillator strengths for atoms and ions having two valence electrons. The method involves a technique for making some use of experimental energies in order to simplify the problem, principally by making unnecessary the calculation of wave functions for the inner electron shells. Although considerably more complicated than the one-electron situation, in a sense this new method can be viewed as an extension of the Bates-Damgaard method to a more complex system.

Among the most important application of oscillator strengths are various problems in astrophysics. Spectrographic measurements of line intensities, from stars or other objects, can reveal a great deal about the physical conditions under which the line was formed. Also, a considerable amount of work is currently being done on the element abundances in stars. Accurate cosmic abundances can provide detailed knowledge of stellar evolution, by comparison with theories of element formation. A crucial stage in the reduction of the observed line intensities of an element to an abundance value is the use of appropriate oscillator strengths. There are a number of approximate steps in this reduction, such as the use of model solar atmospheres and often difficult line intensity measurements, but particularly as the analysis improves, there will be a growing need for accurate transition probabilities.

The application of these oscillator strengths to the element

abundance problem will be discussed further in Section VI. Also, there are a number of extensions and other applications of the nodal boundary method which will be briefly outlined.

The remaining sections are organized as follows: In Section II, various important definitions and properties of oscillator strengths will be reviewed. Then, in Section III, several methods of computing atomic wave functions and transition probabilities will be discussed. Section IV will deal entirely with the coulomb approximation and atoms with one valence electron. The nodal boundary condition method will be explained and justified in Section V. Finally, the results of applying the method will be presented in Section VI. This will include eigenvalues and oscillator strengths for atoms and ions with two valence electrons. Appendices A and B will discuss the numerical methods and computer programs used in the solution of the Hartree-Fock equations.

II. DEFINITIONS AND PROPERTIES OF OSCILLATOR STRENGTHS

The oscillator strength, or "f-value," for a transition from an initial state i to a final state f , is given by the formula

$$f_{fi} = \frac{2}{3} \frac{\mu\omega}{\hbar} \frac{1}{(2J_i+1)} \sum_{m, m'} |\langle \Psi_f^{m'} | \vec{r} | \Psi_i^m \rangle|^2$$

where ω is the frequency of transition, μ is the electron mass, J_i is the total angular momentum of the initial state, and $e \langle \Psi_f^{m'} | \vec{r} | \Psi_i^m \rangle$ is the dipole moment matrix element connecting the initial and final wave functions of the atom. The subscripts of f are usually suppressed. It is convenient to introduce the line-strength S , defined as

$$S = \sum_{m, m'} |\langle \Psi_f^{m'} | \vec{r} | \Psi_i^m \rangle|^2$$

If we also define the quantity g by

$$g = 2J_i + 1$$

the product gf can be written

$$gf = \frac{\Delta E}{3} S$$

where ΔE is the transition energy in Rydbergs, and the line-strength S is expressed in units of the first Bohr radius squared. The product gf has the advantage of being symmetrical between the initial and final states.

In terms of the oscillator strength, the transition probability, or Einstein "A," is written

$$A = \frac{2e^2 \omega^2}{3mc^3} f$$

It has become a wide-spread custom to speak of the f -value, rather than the transition probability, because the oscillator strength is a dimensionless quantity, often of order unity, obeying a number of sum-rules.

There are alternative definitions of the oscillator strength, in terms of the so-called dipole "velocity" and dipole "acceleration" matrix elements. These definitions are related to the dipole moment form by the expressions

$$\langle \Psi_f | \frac{\partial}{\partial z_j} | \Psi_i \rangle = -\Delta E \langle \Psi_f | z_j | \Psi_i \rangle$$

and

$$\langle \Psi_f | \frac{\partial V}{\partial z_j} | \Psi_i \rangle = (\Delta E)^2 \langle \Psi_f | z_j | \Psi_i \rangle$$

respectively. V is the potential energy acting on the electron making the transition, and $\Delta E = E_f - E_i$. These definitions are all equivalent if the wave functions used are exact solutions of the Schrodinger equation, but the three forms for the matrix element may give quite different results using approximate functions. It is evident that in going from the dipole moment through the dipole velocity to the dipole acceleration forms, the parts of the radial wave functions at small radii become successively more important. The wave functions developed in this thesis are most accurate at medium-to-large radii, so we shall use the dipole moment form exclusively.

The most important sum-rule obeyed by oscillator strengths is the Thomas-Reiche-Kuhn sum-rule, or "f sum-rule,"

$$\sum_{n'} f_{n'n} = N$$

which maintains that the sum of f-values from any one state to all others allowed by the dipole selection rules (including transitions to the continuum) is equal to the number of electrons in the atom. Oscillator strengths for transitions to lower energy are to be taken with a minus sign. This rule is of rather limited usefulness in the analysis of atomic spectra. In practice it is necessary to write the approximate relation

$$\sum_{n'} f_{n'n} \approx N_v$$

where N_v is the number of valence electrons, and we include only transitions of these particles. Unfortunately, we must include jumps down into the core which are allowed by the selection rules, but forbidden by the exclusion principle. For example, an approximate sum-rule for neutral sodium is $\sum_{n'} f_{n',3s} = 1.0$ which involves the f-values for the valence 3s electron. It is necessary to include the f-value for the 3s-2p transition, which cannot actually occur. Nevertheless, in order to apply the rule, we must formally calculate this quantity.

The f sum-rule has been used to check the accuracy of calculated values, and also to normalize a set of oscillator strengths whose relative values are known. These applications are generally unreliable

except in the roughest sense. Unfortunately, it does not follow that the better of two calculated sets of oscillator strengths is that which most nearly satisfies the sum-rule. For example, Green, Weber, and Krawitz (2) have calculated f-values for transitions involving the 3d level of Ca II. This was done using both SCF functions with and without exchange (see Section III), giving thereby two sets of f-values. Although the individual oscillator strengths were quite different in the two cases, the sum-rule was about equally satisfied for both sets.

Further sum-rules and other properties of f-values are reviewed and proved in (for example) "Quantum Mechanics of One and Two Electron Atoms" by Bethe and Salpeter.

III. METHODS OF CALCULATING ATOMIC WAVE FUNCTIONS

In this section, several approaches to the problem of calculating atomic wave functions will be reviewed. Part A outlines the problem and discusses various properties of wave functions. The Hartree-Fock self-consistent-field method is summarized in Part B. Part C discusses the way in which polarization of the atomic core can be taken into account. Part D reviews briefly various "analytic variational" methods for computing accurate wave functions. Finally, the nuclear charge-expansion method of Layzer is discussed in Part E.

A. Atomic Wave Functions

The Schrodinger equation for a many-electron atom,

$$\left[-\frac{\hbar^2}{2m} \sum_{i=1}^N \nabla_i^2 - Ze^2 \sum_{i=1}^N \frac{1}{r_i} + e^2 \sum_{i<j} \frac{1}{r_{ij}} \right] \Psi(1, \dots, N) = E\Psi(1, \dots, N),$$

cannot be separated exactly into the sum of simpler equations; the electrons are all coupled to one another. Therefore, the corresponding wave function depends on the variables of all the electrons, and cannot be written as the product of several functions, each involving only a small number of variables.

Except in the case of very few electrons, it appears that in order to make any progress at all, separable wave functions must be used. In fact, it is generally not only necessary to assume that the total wave function can be approximately written as a product or sum of products of one-electron functions, but also that each one-electron

function is a product of radial, angular, and spin functions. It has been shown (3) that for closed shells of electrons in the Hartree-Fock SCF theory, the requirement that the total function be a product or anti-symmetric product of one-electron functions also implies that each one-electron function is a product of radial, angular, and spin functions.

Some very important work with non-separable variational wave functions has been carried out by Hylleraas (4) and others, mostly for helium-like ions. This work is mentioned briefly in part D of this section. Since calculations of the Hylleraas type appear to be too complicated to extend beyond ions with 3 or 4 electrons, a great deal of effort has been expended to develop accurate methods of computing separable functions. In general, these are written as finite sums of products of a radial function, a spin function, and an angular function. The latter is invariably taken to be a spherical harmonic possessing a definite orbital angular momentum quantum number l , or a simple trigonometric function.

The Schrödinger equation as written on the previous page includes in the potential energy only the electrostatic interaction between all the atomic particles. There is another term in the Hamiltonian which sometimes becomes important enough, for our purposes, to treat as a first-order perturbation. This is the spin-orbit effect, caused by the relativistic Thomas precession, and by the action of an effective magnetic field on the electron's spin. If the spin-orbit interaction is negligible for a given atom, that atom is said to obey Russell-Saunders (or LS) coupling, for which the total orbital angular momentum \underline{L} and

the total spin S (or multiplicity $2S + 1$) are good quantum numbers. It is found experimentally that light atoms are described very well by LS-coupling, but that heavier atoms often show marked deviations. If the spin-orbit interaction is large, it may be that an atom obeys more nearly the so-called jj coupling, for which the total angular momentum j of each electron is a good quantum number. Since the majority of atoms show only small or moderate deviations from LS coupling, it is common to label a particular state by the Russell-Saunders notation: $2S+1L_J$ where L is written as $S, P, D, F \dots$ for $L = 0, 1, 2, 3, \dots$ respectively. In actual fact, particularly for heavy atoms, we must apply intermediate coupling, which mixes the functions of different L and S , but which have the same total angular momentum J . Thus for example a state written " 1P_1 " for an sp -configuration may contain an appreciable amount of the 3P_1 function for the same configuration. This effect gives rise to the "intercombination" lines, involving a change in multiplicity between the initial and final states. Transitions of the type $(s^2)^1S_0 - (sp)^3P_1$ could not occur if both wave functions were purely LS-coupled, but in many atoms these transitions are observed, and are caused by an admixture of a 1P_1 function in the 3P_1 function. Oscillator strengths for a number of intercombination lines are calculated and listed in Section VI.

The spin-orbit interaction produces a splitting of the energy levels for different values of J within the same multiplet. Therefore a qualitative criterion for judging whether strong intercombination lines might exist for a particular change of configuration is to compare this splitting with the difference in term values between the multiplets of

the initial or final configuration. For example, if the splitting among the states ${}^3P_{0,1,2}$ is very small compared to the energy difference between the states 3P_1 and 1P_1 , all in the sp -configuration, the intercombination line $(s^2)1S_0 - (sp)3P_1$ must be very weak.

A number of methods for obtaining approximate product wave functions will be discussed in the following pages of this section. It is appropriate first to define the complete problem, and how these various methods can approach the exact solution. We wish to obtain the solution of the non-separable Schrödinger equation neglecting spin effects, the finite nuclear size, relativity, and all interactions except the point-charge non-relativistic electrostatic Coulomb potential between all the particles. If needed, some other effects may be included at the end by perturbation theory, but the initial problem can be restricted, without necessarily reducing the difficulties to reasonable proportions, to the non-relativistic Schrödinger equation with Coulomb forces. The exact wave-function Ψ can be expanded in terms of an infinite complete set of orthonormal N -electron basis functions, and the total energy for this state Ψ proceeds from the diagonalization of the energy matrix

$$H = \begin{vmatrix} \langle \phi_1 | H | \phi_1 \rangle & \langle \phi_1 | H | \phi_2 \rangle & \dots \\ \langle \phi_2 | H | \phi_1 \rangle & \langle \phi_2 | H | \phi_2 \rangle & \dots \\ \vdots & \vdots & \ddots \\ \vdots & \vdots & \ddots \end{vmatrix}$$

where the ϕ_i are the basis functions, and H is the Hamiltonian

$$H = -\frac{\hbar^2}{2m} \sum_{i=1}^N \nabla_i^2 - Ze^2 \sum_{i=1}^N \frac{1}{r_i} + e^2 \sum_{i<j} \frac{1}{r_{ij}} .$$

The most extensive work has been carried out using the Hartree and the Hartree-Fock SCF methods, with or without exchange forces. The goal of this method is to find those separated functions ϕ which minimize the off-diagonal elements in the energy matrix. These wave functions are then the most accurate single-function approximations to a given state as far as the variational procedure is concerned. It should be emphasized that this does not imply that variational functions are necessarily superior for computing matrix elements of operators other than the Hamiltonian, but in practice they are used for the lack of better criteria. The inclusion of off-diagonal elements is known as "configuration interaction" or "superposition of configurations." This matter will be reviewed in part B of this section.

Other methods relinquish the requirement that the off-diagonal elements be as small as possible for general product functions, but require only that they be as small as possible for product functions of a definite algebraic form. While these off-diagonal elements are larger in this case, it may be that both they and also the diagonal elements can be more easily calculated, whereupon a diagonalization of a finite block of the energy matrix can be performed. This is the viewpoint of various analytic variational methods reviewed in part D.

The use of approximate wave functions, whose N-electron eigenvalues are only an approximation to the true state energies, has

raised an interesting and important question in the calculation of f -values. The dipole-moment definition of the oscillator strength involves the product of the transition energy and the matrix element squared:

$$gf = \frac{\Delta E}{3} \sum_{m', m} |\langle \Psi_f^{m'} | \vec{r} | \Psi_f^m \rangle|^2$$

Is it better to use the experimental value of ΔE , or the difference in the calculated energies corresponding to the approximate functions Ψ_f and Ψ_i ? Hartree and Hartree (5) have suggested that there is no reason to expect the calculated value to compensate for errors in the wave functions, so they use the experimental ΔE . On the other hand, Trefftz (6) has computed f -values in neutral calcium by both the dipole-moment and dipole-velocity definitions, and finds that the agreement is improved if calculated values are used for ΔE . Green, Webber, and Krawitz (2) have analyzed f -values in the ion Ca II in some detail, and find that more consistent results are obtained if the calculated ΔE 's are used. In particular, the approximate f sum-rules seem to be better satisfied in this case. The question has still not been satisfactorily answered and deserves further study. The nodal boundary condition method to be presented in Section V will employ experimental transition energies. This is consistent with its semi-empirical nature and the relative inaccuracy of energies calculated by this approach.

B. The Hartree-Fock Method

In 1928, Hartree (7) first introduced the self-consistent-field (SCF) method. This method, with its later refinements, has provided most of our knowledge of accurate atomic wave functions. We begin by assuming that each electron moves in a potential caused by the nucleus and a spherically symmetrized charge density of other electrons. Then from classical electrostatics

$$V_i = -\frac{2Z}{r_i} + \frac{2}{r_i} \sum_{j \neq i} \int_0^{r_i} dr_j P_j^2(r_j) + 2 \sum_{j \neq i} \int_{r_i}^{\infty} dr_j \frac{P_j^2(r_j)}{r_j}$$

where V_i is the potential acting on the i 'th electron (in Hartree's atomic units, with radii in terms of the first Bohr radius, and energies in Rydbergs), $P_j(r_j)$ is the radial wave function of the j 'th electron, and $P_j^2(r_j)$ is its charge density. Therefore Schrödinger's equation for one of the electrons in helium (for example) becomes approximately

$$P_\ell''(1) = \left[\epsilon_\ell - \frac{2Z}{r} + \frac{\ell(\ell+1)}{r^2} + \frac{2}{r} \int_0^r dr P_{\ell, (2)}^2 + 2 \int_r^\infty dr \frac{P_{\ell, (2)}^2}{r} \right] P_\ell \quad (1)$$

which is the Hartree equation.

It was shown somewhat later that this equation follows from the variational procedure, if it is assumed that the many-particle wave function of an atom may be approximately written as a product of one-electron functions,

$$\Psi(1, 2, \dots, N) = u_1(1)u_2(2)\dots u_N(N)$$

subject to the condition of orthonormality of all distinct orbitals u_i .

Therefore the Hartree function represents the best wave function possible as far as the variational procedure is concerned, as long as a simple product form is assumed. In addition, we have also required that each one-electron function be separable into products of radial and angular parts.

Subsequently Fock (8) added the important condition that the wave functions should obey the Pauli principle, i. e. that they should be written in the form of antisymmetric products or Slater determinants. We then apply the variational method to these functions Ψ :

$$\delta [\langle \Psi | H | \Psi \rangle - \sum_{i,j} \lambda_{ij} \langle u_i | u_j \rangle] = 0$$

where H is the "exact" Hamiltonian (neglecting spin forces)

$$H = - \sum_i \nabla_i^2 - \sum_i \frac{ZZ}{r_i} + \sum_{i<j} \frac{z}{r_{ij}}$$

and the λ_{ij} are Lagrange multipliers constraining the one-electron orbitals u_i to be normalized (diagonal λ 's) and orthogonal (off-diagonal λ 's). The Hartree-Fock equations then become

$$\begin{aligned} & - \nabla^2 V_i - \frac{ZZ}{r} V_i + \left[\sum_j \int d\tau V_j^* \frac{z}{r_{12}} V_j \right] u_i \\ & - \sum_j \delta(m_{si} m_{sj}) \left[\int d\tau V_j^* \frac{z}{r_{12}} V_i \right] u_j = - \sum_j \lambda_{ij} \delta(m_{si} m_{sj}) V_j \end{aligned}$$

The Kronecker delta $\delta(m_{si} m_{sj})$ contains as arguments the spin projections of functions V_i and V_j .

These equations are sometimes referred to as the "SCF equations with exchange," in contrast to the Hartree equations, or "SCF equations without exchange." The inclusion of exchange effects produces a substantial lowering of the total energy, indicating that the wave functions are definitely superior to those calculated without exchange.

Two other assumptions have been made in the SCF methods: first, that each state corresponds to a definite electron configuration, and second, that LS coupling holds. Departures from these assumptions can be accounted for approximately at the end of a calculation. The influence of other configurations is included by the so-called "superposition of configurations." The Hartree-Fock functions form a complete orthonormal set, so the true wave function can be expanded in terms of them. This is accomplished by diagonalizing the energy matrix using wave functions of all configurations which can contribute to a particular state, having the correct parity, orbital, spin, and total angular momenta. The process appears to converge slowly, however, so in order to obtain functions a great deal better than the single-configuration approximation, a large number of configurations should be included. It is apparently more practical to follow an analytic variational method for this expansion, as discussed in part D.

Deviations from LS coupling may be accounted for by mixing two or more pure LS states for a particular configuration, so that the observed spin-orbit splittings are reproduced. This procedure will be treated in detail in Section V.

Also in Section V we will need the Hartree-Fock radial equations

for the states $(s^2)^1S$, $(sl)^1L$, and $(sl)^3L$ of a helium-like ion. If we write the one-electron orbitals as products of radial, angular, and spin functions, we are left with an integrodifferential equation for the radial function $P(r)$. For an s^2 state, this is

$$P''(r) = \left[\epsilon - \frac{2Z}{r} + \frac{2}{r} \int_0^r dr P^2(r) + 2 \int_r^\infty dr \frac{P^2(r)}{r} \right] P(r)$$

which is identical with the Hartree equation (without exchange) for this state, since the antisymmetry of the $s^2^1S_0$ function is provided by the singlet spinor. For the sl configuration, we obtain

$$\begin{aligned} P_s''(r) &= \left[\epsilon_s - \frac{2Z}{r} + \frac{2}{r} \int_0^r dr P_l^2(r) + 2 \int_r^\infty dr \frac{P_l^2(r)}{r} \right] P_s(r) \\ &\pm \left[\frac{2}{2l+1} \right] \left[\frac{1}{r^{l+1}} \int_0^r dr P_s r^l P_l + r^l \int_r^\infty dr \frac{P_s P_l}{r^{l+1}} \right] P_l(r) \end{aligned}$$

and

$$\begin{aligned} P_l''(r) &= \left[\epsilon_l - \frac{2Z}{r} + \frac{l(l+1)}{r^2} + \frac{2}{r} \int_0^r dr P_s^2(r) + 2 \int_r^\infty dr \frac{P_s^2(r)}{r} \right] P_l(r) \\ &\pm \left[\frac{2}{2l+1} \right] \left[\frac{1}{r^{l+1}} \int_0^r dr P_s r^l P_l + r^l \int_r^\infty dr \frac{P_s P_l}{r^{l+1}} \right] P_s(r) \end{aligned}$$

where the + and - signs refer to the singlet and triplet states, respectively. The off-diagonal Lagrange multipliers have not been included in these equations, so there is no assurance that all functions are orthogonal. It has been found that the off-diagonal terms are small, so that for example the $1s$ and $2s$ radial functions for the states $(1s2s)^1S$ or 3S are nearly orthogonal. The departures are often neglected, since their systematic inclusion may take much more effort

without making appreciable difference.

For much more thorough and lucid accounts of the SCF theory, the reader is referred to recent books by Hartree (9) and by Slater (10).

C. Polarization of the Core

The Hartree-Fock method as described in part B assumes among other things that the closed shells of an atom are spherically symmetric. Aside from exchange effects, one pictures a valence electron as moving in a spherical potential produced by a stationary spherical charge distribution. There is at least one physical effect of importance which is neglected by this approximation, and this is the polarization of the core by the valence electrons. An electron in the valence shell will attract the nucleus and repel the core electrons, causing a polarization effect which in turn produces an additional attractive potential on the valence particle. Classically, this potential is given for large radii by $V = \alpha e^2 / r^4$, where α is the polarizability.

The influence of core polarization on atomic energy levels and transition probabilities has been studied particularly by Biermann and his collaborators. In a series of articles in the Journal Zeitschrift für Astrophysik (11, 12, 13), the method has been developed and applied to a number of atoms and ions with one or two valence electrons.

The procedure as set forth in the original article of Biermann (11) can be briefly summarized. It is assumed that the polarization potential can be written (in Hartree units)

$$2 \Delta V = \frac{ae^2}{r^2} (1 - e^{-(r/r_0)^5})$$

This is correct at large radii, and the exponential term is included in order to cut off the potential inside some radius r_0 , which is taken to be the outer turning-point of the outermost shell of the core. The polarizability a is taken from experiment. Using this potential and known SCF wave-functions, the energy correction due to polarization can be estimated from first-order perturbation theory. This was done for Ca II, K I, Si IV, and Na I, and the results added to the previously calculated Hartree-Fock eigenvalues. It is clear that the change is in the right direction to approach the experimental results, since the variational method must underestimate the one-electron binding energies, at least for monovalent ions with nearly stationary cores. In fact the final predicted energies agree with experiment within 1%, except in two or three of the states examined.

New valence wave-functions were then found by integrating Schrödinger's equation

$$P'' + (2V - \epsilon - \frac{l(l+1)}{r^2})P = 0$$

using experimental term values for ϵ , and the potential

$$2V = 2V_{\text{Hartree}} (1 + \Delta\beta re^{-(r/r_0)^5}) + \frac{a}{r^2} (1 - e^{-(r/r_0)^5})$$

The parameter $\Delta\beta$ is determined from the solution, since the boundary conditions must be satisfied. Oscillator strengths for a few transitions in Na I, K I, and Mg II were calculated from these functions, and were pronounced in good agreement with experimental values.

After the war, Biermann and Lübeck (12) published some further work on core polarization, including calculations on both the alkalis Na I, KI, and Mg II, and also the ions C II, Al I, and Si II, which have an s^2p configuration in the valence shell. The polarization corrections were calculated by perturbation theory as before, but it was found that to get sensible results a new polarization potential was necessary:

$$2\Delta V = \frac{ae^2}{r^4} (1 - e^{-(r/r_0)^8})$$

which differs from Biermann's original potential in that the eighth power rather than the fifth power is used in the exponent. The change made little difference in the alkalis, but was quite important in the s^2p ions.

A large number of wave functions were computed using the same method as in the original article, except that $(r/r_0)^8$ was used. Oscillator strengths were found from these functions. The lack of experiments on the s^2p ions precludes any check on the reliability of the calculated values, but the alkali results agreed well with experiment.

The core polarization method was subsequently extended to atoms with two electrons outside closed shells, in particular Mg I and Ca I. Biermann and Trefftz (13) calculated wave functions for several states in Mg I, and oscillator strengths for the transitions

$$\begin{aligned} (3s^2)^1S - (3s3p)^1P & \quad \lambda 2852, \\ (3s3p)^3P - (3s3d)^3D & \quad \lambda 3832, \end{aligned}$$

and

$$(3s3d) \ ^3D - (3s4f) \ ^3F \quad \lambda 14877.$$

The polarization potential $\frac{ae^2}{r^4} (1 - e^{-(r/r_0)^8})$ was included in the Hartree-Fock equations, which were then solved by usual methods. The oscillator strength derived in this way for the resonance line $\lambda 2852$ was $f = 2.21$.

A more detailed analysis of Mg I was undertaken by Trefftz (14), by the inclusion of term mixing or superposition of configurations as well as core polarization. In particular, the effects of the configuration $(3p^2)^1D$ on the terms $(3s, nd)^1D$ were calculated, and also the influence of $(3p^2)^1S$ on the ground-state $(3s^2)^1S$ was investigated. This partial diagonalization of the energy matrix brought the calculated and observed energies into better agreement than with the usual single-configuration approximation. The term mixing also exercised a substantial effect on the oscillator strengths. The resonance line was computed to give an f -value of 1.606, considerably different than the value 2.21 found without term mixing.

Trefftz has also treated Ca I (15) by the same kind of calculation, for the states 4^1S , 4^1P , 4^3P , and 3^3D . Oscillator strengths were found for the resonance line $\lambda 4227$ ($f = 1.458$) and for the transition $4^3P - 3^3D$ $\lambda 19310$ ($f = 0.010$). Both the dipole moment and dipole velocity matrix elements were evaluated, and f -values derived from each. It was discovered that the use of calculated rather than observed transition frequencies in the f -value formulas improved the agreement between the two results, so the calculated values were used. This is

in contrast to the previous work on magnesium, and on the majority of other SCF f -value calculations, for which the experimental frequencies are employed (and in which the dipole moment form is almost universal). It is not clear that the greater consistency in the calcium result should serve as a valid criterion for the use of calculated frequencies. In this particular instance the experimental frequency (in Rydbergs) is 0.2155, while the calculated value is 0.2305. In other calculations the discrepancies are sometimes much larger, so the question of which to use is important and deserves consideration.* The oscillator strengths for the resonance lines of Mg and Ca obtained by Trefftz agree very well with the latest experiments, as given in Section VI. It should be emphasized that this agreement is probably more the result of using "superposition of configurations" than of including polarization effects.

The result of this work on core polarization has undoubtedly demonstrated its importance, and has provided one of the most important physical mechanisms neglected in the standard SCF approach. The question of exactly how this effect should be included is a difficult question, since there remain ambiguities. Some elements, as pointed out by Biermann and Lübeck, seem to be sensitive to the form of the polarization potential cut-off inside the core, and also the way in which polarizabilities are to be chosen is not very clear. It seems likely that in the (perhaps somewhat distant) future calculations will run more along the line of the analytic variational methods described in part D, which are not as physically appealing, but are very well defined.

* See Section IIIA.

By the use of a large number of configurations involving the core as well as the valence electrons, the polarization phenomenon should be taken into account.

D. Analytic Variational Methods

In contrast to the Hartree-Fock method, which requires the solution of a set of coupled non-linear differential-integral equations, a variety of analytic methods have been introduced which assume definite algebraic forms for the wave-functions. Most of these methods use finite sums of products of one-electron functions, but for very light atoms, with only two or three electrons, considerable work has been done with functions depending explicitly on r_{ij} , the distance between electrons i and j . It is clear that the inclusion of such a term should bring about a substantial lowering of the energy, since it can describe very efficiently the electrostatic correlation between the two electrons. The first calculations of the type were made by Hylleraas (4), but since that time various authors (16) have expanded and improved the method, determining the ionization potential of helium to within 0.01 cm^{-1} . A discussion of the efforts in this direction, along with an extensive bibliography, is contained in Chapter 18 of the Quantum Theory of Atomic Structure by J. C. Slater.

Since the number of terms involving r_{ij} 's rises quadratically with the number of electrons, the work involved with finding Hylleraas-type functions for many-electron atoms is prohibitive, so we must have recourse to other methods. The first simple analytic product wave

functions were published by Zener (17), Eckart (18), and by Morse, Young and Haurwitz (19). They have the same structure (product of single-particle radial and angular functions) as the Hartree-Fock functions with exchange, so cannot be as accurate, since the analytic functions are restricted to a particular algebraic form. They are nevertheless useful, because they are relatively easy to find, and because integrals over them can be explicitly performed. The Morse function for the 1s level, for example, is $(\mu^3 a^2/\pi)^{1/2} e^{-\mu a r}$, where a is to be varied. Other orbitals are in general products of exponentials and polynomials in the radius, and are similar in form to the hydrogenic functions.

Within the past few years it has become generally recognized that analytic variational methods may be the best way of obtaining wave-functions of arbitrary accuracy. Several superposition-of-configuration calculations have been performed with the Hartree-Fock equations, as reviewed briefly in part B, but the calculations for each configuration are lengthy, and the process converges slowly. An advantage of using analytic wave functions is that the solution for each configuration involves an algebraic expansion, rather than the numerical integration of a differential equation. By clever choice of the functions the results may converge more rapidly, but the principal advantage is the facility with which algebraic functions can be manipulated.

Such a configuration interaction calculation has been performed for the ground state of helium by Nesbet and Watson (20), who used 20

configurations. The one-electron orbitals were of the form $\Psi_l = r^{A+l} e^{-ar} Y_l^m(\theta, \phi) v(m_s)$, where A is an integer, and $v(m_s)$ is a spinor. While their results are not as accurate as those using Hylleraas-type wave functions, it is clear that they are superior to a single-configuration approximation, and that in principle any atom can be solved to arbitrary accuracy by this procedure. Watson (21) has made a 37-configuration calculation for the ground state of beryllium by the same method.

A large number of papers have been published by Boys and collaborators (22), who use a roughly similar approach. They have investigated the mathematical framework very thoroughly, and the steps toward obtaining highly accurate functions have been set forth in detail. The complete calculation is separated into eight distinct stages, each of which can be precisely defined. Tentative estimates can be given of the effect involved in programming and performing the computation of each stage. The best source for these developments is an article by Boys in the Reviews of Modern Physics (23) which reviews all his procedures. The results for only a few atoms treated by this method have been published thus far, notably beryllium, boron and carbon.

Several other authors have made contributions to the analytic methods for both atoms and molecules, much of which was presented at a conference on molecular quantum mechanics as reported in the Reviews of Modern Physics, Vol. 32. It is apparent that procedures are being developed which will substantially increase our knowledge

of atomic wave-functions, although at this point comparatively few individual atoms have been calculated.

E. The Nuclear Charge-Expansion Method

In 1959, Layzer (24) proposed a new formulation of the atomic structure problem. He noted that while the conventional SCF method generally gives satisfactory eigenvalues and transition probabilities, it is unable to reproduce certain observed regularities in spectra. In SCF theory, there is no simple way to get wave functions and eigenvalues for N electrons around a nucleus Z in terms of those for N electrons around a nucleus $Z + 1$. Each atom and ion must be individually treated. There are some well-known regularities in the spectra of isoelectronic sequences which are left unexplained in the usual theory, since the calculations do not follow the experimental data in some respects. In particular, there are two experimental "laws" which state that along an isoelectronic sequence

- 1) the square root of the ionization potential varies linearly with Z (the generalized Moseley's Law)
- 2) the difference in energy between two terms in the same configuration (e. g. 1D and 3P in the p^2 configuration) varies linearly with Z (the generalized "screening doublet law")

Layzer's theory is specifically designed to explain these approximate experimental regularities, and this is accomplished by retaining the nuclear charge Z as a dynamical variable.

Beginning with the Hamiltonian for N electrons (in atomic units)

$$H(N, Z) = \sum_i \left(\frac{p_i^2}{2} - \frac{Z}{r_i} \right) + \sum_{i < j} \frac{1}{r_{ij}}$$

we can write

$$H(N, Z) = E(N, Z) + V(N)$$

where

$$E(N, Z) = \sum_{i=1}^N \left(\frac{p_i^2}{2} - \frac{Z}{r_i} \right)$$

and

$$V(N) = \sum_{i < j} \frac{1}{r_{ij}}$$

If a new unit of length is adopted, equal to the Bohr radius divided by Z , we have

$$H(N, Z) = Z^2 \{ E(N, 1) + Z^{-1} V(N) \}$$

which may be treated by perturbation theory if Z is sufficiently large so that the second term is small. The result is that the eigenvalues of H can be written in the form

$$H' = W_2 Z^2 + W_1 Z + W_0 + O(Z^{-1})$$

where

$$W_2 = - \sum_{i=1}^N \frac{1}{2n_i^2}$$

and W_1 are eigenvalues of the matrices V_{npSL} whose elements are taken between terms having the same radial quantum number, parity, total spin and total orbital angular momentum. These matrices are to be evaluated using hydrogenic wave-functions with $Z = 1$, and the operator $V = \sum_{i < j} \frac{1}{r_{ij}}$. The fact that such simple functions are used

follows from the fact that the zero-order Hamiltonian $Z^2 E(N, 1)$ is a sum of single-particle hydrogenic Hamiltonians. The notation $O(Z^{-1})$ means that the product $Z \cdot O(Z^{-1})$ remains smaller than some fixed constant for arbitrarily large Z .

From the above expression for H' , the ionization potential can be written

$$\text{I. P.} = \frac{(Z - \sigma)^2}{2n^2} + C + O(Z^{-1})$$

if W_0 is defined to be $\frac{\sigma^2}{2n^2} + C$. The theory of Layzer does not predict the size of the last term $O(Z^{-1})$, so the usefulness of the expression for the ionization potential rests on the fact that this term seems to be small experimentally. Both the generalized Moseley's Law and the screening doublet law then follow immediately from the equation. The screening constants σ can be found from the variational principle, using hydrogenic functions. The wave functions used in this method are therefore these screened hydrogen wave-functions. It should be mentioned that the screening theory has recently been extended to include the effects of relativity (25).

Varsavsky (26) has attacked the problem of calculating f -values from the standpoint of Layzer's theory. Since the work was of an exploratory nature, only the first-order wave-functions were used, and it was further assumed that each state belonged to a definite configuration. The full first-order theory takes account of some effects of configuration mixing, because all configurations for a given set of radial quantum numbers are included. The results are not uniformly successful, and often disagree with experiment by large factors (almost all

f-value theories do!). Transitions in which there is no change in the radial quantum numbers seem to be fairly well predicted. This is probably principally due to the fact that there is usually a good "overlap" of the initial and final wave functions for such a transition so the matrix element is not highly sensitive to the details of the functions.

Oscillator strengths usually require very accurate functions, so one expects that the use of screened hydrogenic functions would be inadequate for most transitions. The method does have the great advantage of simplicity, so it might be feasible to include higher perturbations. However, the theory was not designed for the purpose of obtaining accurate wave functions, and the addition of higher orders in the perturbation expansion becomes difficult.

IV. THE COULOMB APPROXIMATION

In this section we will be concerned with atoms having only one electron outside closed shells. This configuration provides the least complicated situation for the calculation of f -values, and in fact very simple theories give excellent results. We will concentrate on a description and evaluation of the Coulomb approximation, or method of Bates and Damgaard. It is interesting to explore the assumptions in this approach, since its success for monovalent atoms is quite striking. The analysis will provide much of the motivation for the nodal boundary condition method for more complex atoms. Part A of this section discusses the Coulomb approximation, part B relates these Coulomb wave functions to the more sophisticated SCF functions, and part C compares various computed and laboratory f -values.

A. The Method of Bates and Damgaard

In 1949, Bates and Damgaard (1) effectively solved the problem of calculating transition probabilities for atoms with one valence electron. The results are probably the most accurate so far obtained for fairly light atoms or ions having a ground state with an s electron outside a closed s or p shell, such as neutral lithium, sodium, or potassium. This fact is somewhat surprising at first, since the method is very simple.

Bates and Damgaard use a Coulomb approximation: that is, the valence electron is assumed to move in a pure Coulomb field.

Therefore, this method is expected to supply a satisfactory wave function outside the electron core, but to deviate strongly for small radii. Fortunately, the greatest part of the valence function is outside the core for alkali atoms. Coupling this with the fact that the dipole moment matrix element stresses the parts of the initial and final wave functions at large radii, we have one reason for the success of the Bates-Damgaard method with these atoms. Another reason has to do with the eigenvalues chosen for the valence electron. From SCF theory, Koppman's theorem (27) states that the eigenvalue of an electron in the Hartree-Fock equation will be equal to its ionization energy if and only if the wave functions of all other electrons are constrained not to change (i. e. "settle") in the process of removing the electron in question. Now in an actual SCF problem, the other wave functions do change, more or less, as evidenced by many calculations. The removal of one electron reduces the shielding for all the others, causing them to be pulled in toward smaller radii. However, this effect is usually negligible for the inner shells, which are all that remain for alkali atoms, aside from the valence particle. Hartree and Hartree (28), for example, have computed wave functions for neutral, first-ionized, and negatively ionized sodium. The eigenvalues of the inner shells $1s^2$, $2s^2$, and $2p^6$ are all affected somewhat by the presence of valence electrons, but the core wave functions themselves are essentially the same in all three cases.

In contrast to the stability shown for the inner shells, we can present the results of Hartree and Hartree (28) for neutral and first-

ionized calcium. Neutral calcium has a one-electron eigenvalue $\epsilon = 0.3891$ Ryd. for the $4s^2$ ground state, while the single $4s$ electron of ionized calcium has an eigenvalue $\epsilon = 0.8295$ Ryd. The removal of one of the s -electrons has a large effect on the second, causing it to collapse toward the nucleus.

As exemplified by the sodium calculation, the inner shell wave functions of alkali atoms are negligibly affected by the presence of the valence particle. Koopman's theorem then testifies that for these atoms, SCF eigenvalues are also SCF ionization energies. In addition, calculated values agree fairly well with experimental results. For example,

$$\epsilon_{\text{Li}}(2s) = 0.3964 \qquad \text{I. P.} = 0.3965$$

$$\epsilon_{\text{Na}}(3s) = 0.361 \qquad \text{I. P.} = 0.3778$$

The remaining discrepancy may be due principally to core polarization, as suggested by Biermann (11). For these reasons it is permissible, and perhaps better, to use experimental term values rather than the (usually unknown) SCF energies as the eigenvalues for the Coulomb wave functions of Bates and Damgaard.

The actual wave functions used are asymptotic series representations of Coulomb functions, depending on several parameters. They depend upon the effective charge \underline{C} acting on the valence electron, which is equal to the degree of ionization if the active

electron is removed. The functions also depend on the angular momentum l , and on the effective radial quantum number $n^* = C/\sqrt{E}$, where E is the ionization energy of the level, in Rydbergs. The radial functions are:

$$P(r) = \frac{\left(\frac{2rC}{n^*}\right)^{n^*} \left[\exp(-rC/n^*)\right] \left[1 + \sum_{t=1}^{\infty} \frac{a_t}{r^t}\right]^*}{\left[(n^*)^2 \Gamma(n^* + l + 1) \Gamma(n^* - l) / C\right]^{1/2}}$$

where

$$a_1 = \frac{n^*}{2C} [l(l+1) - n^*(n^*-1)]$$

and

$$a_t = a_{t-1} \left(\frac{n^*}{2tC} [l(l+1) - (n^*-t)(n^*-t+1)]\right)$$

Bates and Damgaard evaluate the dipole-moment matrix elements by forming the integral $\int dr P_f r P_i$ and then interchanging the sums and integral. The integral is then simple. Finally, the double sums can be (laboriously) computed as a function of n_f^* and n_i^* , and tabulated.

The relative simplicity of the Bates-Damgaard method has come about because the inner shells have been separated from the problem by making use of experimental energies. These core wave functions have not had to be computed, since there has been no need to apply the usual boundary condition that the valence function go to zero at the origin.

* There are several typographical errors in these formulas in the Bates-Damgaard article.

Unfortunately, the method cannot be confidently used for atoms with more than one valence electron, for two reasons. First, the active electron no longer moves in a Coulomb field, because of the presence of other valence particles. Second, it is not sufficiently accurate to use experimental term energies for the one-electron eigenvalues, since the other valence electrons are strongly affected by the motion of the active one. The Coulomb approach has been used rather extensively for complex atoms for want of something better. The results are often rather good, but in other cases are wrong, so application of the Bates-Damgaard tables to atoms with more than a single valence particle must be viewed with caution.

B. Valence Wave Functions

It is interesting to compare the Coulomb functions with the more sophisticated results of a SCF calculation, to see exactly where the differences become important. The Coulomb functions are expected to be correct at large radii, but to become inaccurate as they move through the inner electron shells toward the nucleus. The one-electron eigenvalues in the Bates-Damgaard method are taken from experiment, so we do not expect the Coulomb functions to agree perfectly with the usual SCF results even for large radii, since the latter have different (purely theoretical) eigenvalues. According to the work of Biermann and collaborators, the energy discrepancy may be largely due to the neglect (in SCF theory) of the polarization of inner electron shells by the valence electron.

Figures IV-A and IV-B illustrate the similarities and differences of the Coulomb and SCF radial functions. Figure IV-A shows the 3s valence function for sodium as computed by the Coulomb approximation using the experimental term value as an eigenvalue, superimposed on the SCF function of Hartree (28). The SCF 2p function is drawn also to indicate the position of the core electrons. It is apparent that serious deviations of the Coulomb function do not occur until the valence particle is well within the core. Figure IV-B shows the same 3s function of sodium in the Coulomb approximation and in the SCF calculation of Biermann (11), which includes polarization of the core. The agreement is somewhat better in this case, since the eigenvalues are the same for each function. The polarization potential in itself only slightly changes the shape of the SCF radial function, but the associated change in eigenvalue draws the electron into smaller radii, agreeing more closely with the Coulomb function.

The Coulomb functions used in these comparisons were calculated by the computer program described in the Appendices. It should be noted that they are computed numerically from Schrodinger's equation, while Bates and Damgaard use the series representation given in part A. The results are the same within the accuracy of the two methods.

Figure IV-A

Comparison of the Coulomb with the SCF radial function for the
3s state of Na I.

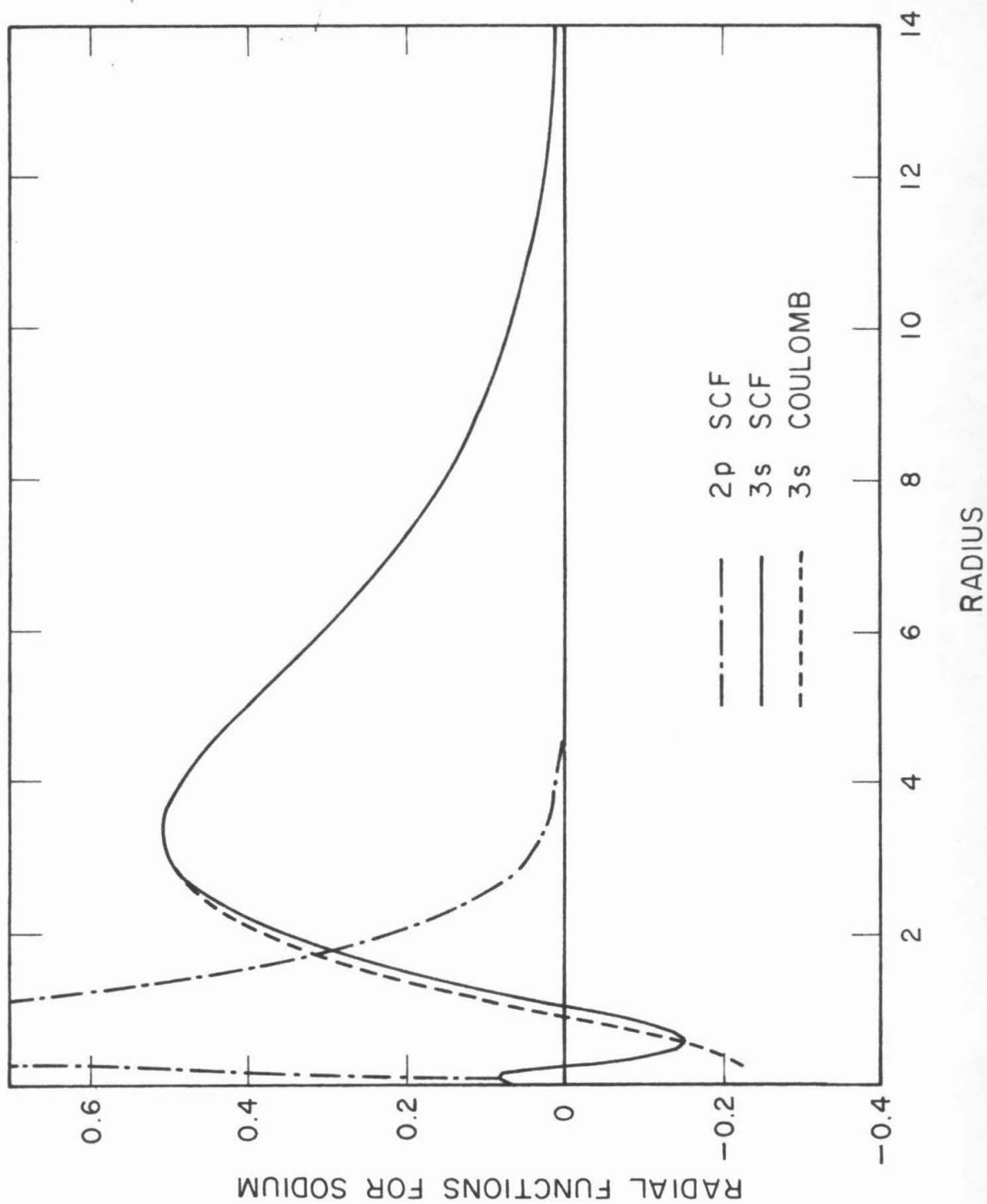
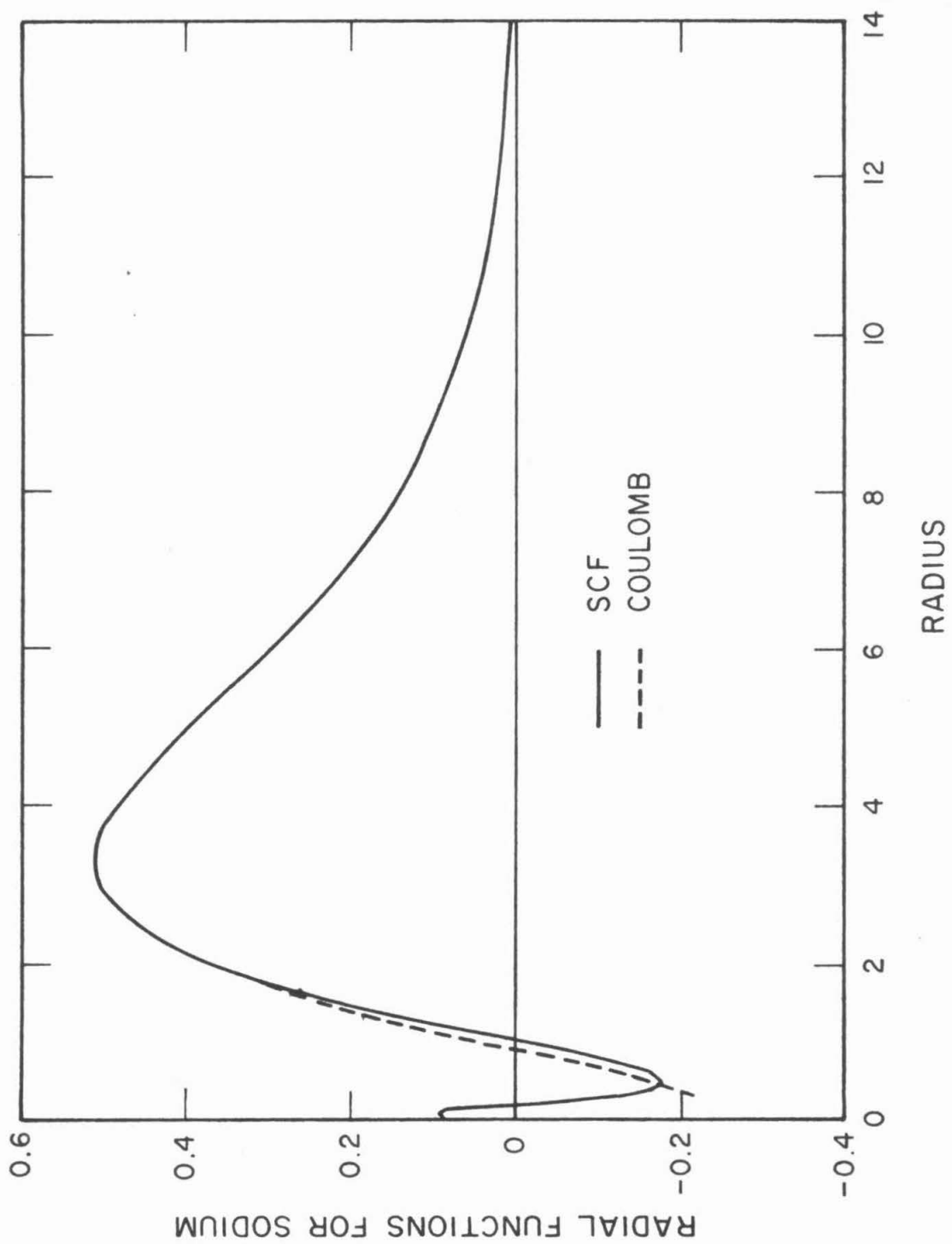


Figure IV-B

Comparison of the coulomb with the SCF radial function (including core polarization) for the 3s state of NaI.



C. Coulomb, SCF, and Experimental Oscillator Strengths

The Bates-Damgaard approximation should give accurate f -value results for atoms with one valence electron, particularly the alkali metals, for which the stationary core approximation is most nearly satisfied. A great deal of effort, both experimental and theoretical, has been expended in the determination of transition probabilities for some of these atoms. It will therefore be particularly instructive to compare the results of experiment and of self-consistent field calculations with the simple Coulomb approximation. As examples, we will list and discuss oscillator strengths for Li I, Na I, and Ca II.

1) Li I

More than 25 papers dealing with theoretical and experimental oscillator strengths of neutral lithium have appeared since 1926. Table IV-A compares several results for four lines to the ground state. Two sets of SCF calculations are listed, those of Hargreaves (29) without exchange, and of Fock and Petrashen (30) with exchange. Also given are the results of Varsavsky (26) using the charge expansion method, and of Bates and Damgaard. The experimental f -value for the resonance line is from Stephenson (31), and the other results are the relative values of Filippov (32) normalized to Stephenson's scale. From an examination of the table, one comes to admire the Bates-Damgaard results, which are expected to be very good for such an alkali atom.

TABLE IV-A

<u>Transition</u>	<u>Hargreaves</u>	<u>Varsavsky</u>	<u>Fock and Petrashen</u>	<u>Bates and Damgaard</u>	<u>Experiment</u>
2s-2p	0.700	0.819	0.769	0.750	0.72 ± 0.03
2s-3p	0.014	0.0358	0.0037	0.00565	0.0055
2s-4p	0.0147	0.0177	0.0035	0.00501	0.0047
2s-5p	0.0051	-	0.0015	0.00245	0.00253

2) Na I

An awesome array of about 100 papers have dealt with f -values for Na I. Self-consistent-field calculations have been made, for example, by Fock and Petrashen (33) and by Biermann (11) and Biermann and Lübeck (12). The latter two papers include the effects of core polarization. Table IV-B lists f -values from these calculations along with those of Bates and Damgaard. Among the most recent experiments on the resonance 3p-3s transition are those of Stephenson (34) and of Ostrovskii and Penkin (35). Their results are $f = 0.975 \pm 0.034$ and $f = 1.15 \pm 0.03$, respectively. The experimental values listed in the table are the relative f -values measured by Filippov and Prokofiev (36) normalized to a compromise $f = 1.00$ for the resonance line.

TABLE IV-B

<u>Transition</u>	<u>Fock-Petraschen</u> <u>Length</u>	<u>Velocity</u>	<u>Biermann</u>	<u>Bates-</u> <u>Damgaard</u>	<u>Experiment</u>
3p-3s	1.04	0.97	0.99	0.94	1.0
4p-3s	0.014	0.010	0.014	0.014	0.0144
5p-3s				0.0021	0.0021
6p-3s				0.00064	0.000645

3) Ca II

A discussion and analysis of much of the work on Ca II is contained in the thesis of Varsavsky (26). Oscillator strengths for several lines have been computed in many different ways: by SCF with exchange, SCF with exchange and core polarization, by the Coulomb approximation, and by the nuclear charge expansion method. Studies have been made of the effect of using the dipole length, velocity, and acceleration forms of the matrix element. The result of using experimental or calculated transition energies has also been investigated.

Table IV-C contains several computed and one experimental f -value for the resonance (4p-4s) line of Ca II. Other results are listed in Varsavsky's thesis (26). The SCF results (with exchange) agree very well with experiment. The Bates-Damgaard value appears to be somewhat small. It is to be expected that the Coulomb approximation will become poorer for heavy atoms, so this discrepancy may

indicate that the method is beginning to fail.

TABLE IV-C

	<u>SCF without exchange</u>	<u>SCF with exchange</u>	<u>Other Calculations</u>	<u>Experiment</u>
Hartree and Hartree	1.42	1.19		
Green and Weber	1.36	1.19		
Biermann and Trefftz		1.10		
Varsavsky			1.25	
Bates and Damgaard			0.93	
Ostrovskii and Penkin				1.27

V. THE NODAL BOUNDARY CONDITION METHOD

In this section we will introduce a method for calculating wave functions, eigenvalues, and transition probabilities. It is here applied to atoms and ions with two valence electrons, but the general approach has wider applications, which will be discussed in Section VI.

The purpose of the previous two sections was partly to review various theoretical attacks on the atomic structure and f -value problems, but was also intended to serve as an introduction to some aspects of the present method. The nodal boundary condition method uses some of the simplifying assumptions of the Bates-Damgaard approach so that the calculation of wave functions for the core electrons becomes unnecessary. It also uses the Hartree-Fock equations to calculate the valence wave functions.

Two of the basic assumptions of the Bates-Damgaard method are that the valence electron moves in a Coulomb field and that its eigenvalue is the experimental term value. These two approximations are very good for the alkali atoms, and are often adequate for other monovalent atoms. The support for the assumptions comes from comparison of Bates-Damgaard Coulomb functions with SCF functions, from comparison of experimental ionization energies with SCF eigenvalues for such atoms, and from the agreement between Bates-Damgaard f -values with experiment. Neither approximation is valid, however, for more complex atoms. A valence particle then does not move in a Coulomb field, and its eigenvalues are not necessarily close to experimental term values, due to the adjustment in position of other valence

electrons. Nevertheless the implications of the two assumptions for monovalent atoms is important for the treatment of more complicated situations. The Coulomb field approximation means that the valence electron spends most of the time outside the core. The eigenvalue approximation implies that the core is nearly unaffected by the position of the valence electron. These facts are about equally valid for atoms with two or more electrons outside closed shells. When combined with the effect of a deep core potential, they provide the motivation for the nodal boundary condition method.

In part C of this section the method will be described in detail, including particular examples. It will be useful at this point to give a brief outline of the principal features.

It will first be established that the inner nodes of many valence radial wave functions are insensitive to their eigenvalues. This is here called "nodal stability," and is explained and verified in parts A and B. The positions of these nodes can be found for any atom with two electrons outside closed shells by a study of the corresponding ion with a single valence particle, for which the two Bates-Damgaard assumptions are valid. Nodal positions are then used as the inner boundary conditions on the wave functions of the Hartree-Fock equations for the two-electron situation. This provides sufficient information to determine eigenvalues and wave functions. Just as in the Bates-Damgaard method, these wave functions are adequate outside the core, but are incorrect at small radii because of our neglect of the true core potential. Many atomic processes depend almost entirely on the main

part of the valence functions at intermediate and large radii, and this is the case with oscillator strengths, if the dipole-moment matrix element is employed.

A. Nodal Stability

The nodal boundary condition method depends on the near-independence of node positions with energy. For example, the 3s ground-state radial wave function of sodium has two nodes. We will make use of the fact that the 4s, 5s, ... excited states of sodium have nearly the same two inner nodes, the higher levels merely adding on additional loops and nodes at large radii.

There is nothing special about using the node positions; the slope-to-value ratio of any part of the valence wave function inside the electron core could be used instead. The wave functions inside the core (except for normalization) are almost the same for any degree of excitation of electrons with a given angular momentum. Specifying the node position is particularly appropriate because it is easily visualized, and because it is convenient to use in calculations, involving a change in sign of the wave function.

The idea of nodal stability can be understood in several ways. The kinetic energy of a valence electron when it falls into the deep potential within the core is so large that it "forgets" how much it had when it was out on the limb of the potential, where it spends most of its time. Looked at in terms of Schrödinger's equation

$$P''(r) = [V(r) - E]P(r)$$

it is seen that if the potential $V(r)$ is large compared to the eigenvalue E , the wave function is nearly independent of E . A small change in energy of the valence electron, due to excitation, the presence of other electrons, external fields, or other causes, may radically alter the outer parts of the valence function, but the inner nodes remain quite stable. The nodal boundary condition method leans heavily on this stability. We will use in particular the fact that (for example) the nodes for the single valence s -electron of Ca II are very close to those for the two valence s -electrons in Ca I. That is, an atom and its ion have almost identical core potentials.

If the nodes for a particular atom are found to be stable, two things are implied. First, that the potential inside the core is large compared to the eigenvalue. Second, it must be true that the positions of the core electrons are not much affected by the condition of the valence particle.

Before presenting the evidence for nodal stability, it is necessary to consider just how much stability is required. For no atom are the nodes absolutely stable for the whole range of energies for which data is available. The criterion which will be used is that we should be able to determine the nodes sufficiently accurately so that varying their position within the range of possible error produces only a small change in the calculated oscillator strength. This means also that the change in calculated eigenvalues for a two-electron function will be small.

The first line of evidence for nodal stability comes from all previously calculated Hartree and Hartree-Fock functions. Many

atoms and ions, both ground and excited states, have been solved by the full self-consistent field method. We may investigate the positions of the nodes for such an atom for electrons of a particular angular momentum (s, p, d, ...). The known results for several atoms and ions having one or two ground-state "s" or "p" electrons are given in Table V-A. In brief, one finds that atoms or ions having one or two "s" or "p" electrons outside closed "p" shells are particularly stable. Because of the large centrifugal potential which tends to reduce the deep central potential well, "d" electrons and those of higher angular momentum do not usually have sufficiently stable nodes. It is only for heavy atoms that the method can be used for "d" electrons, since in this case the potential is large enough. Atoms with "s" or "p" electrons outside closed "d" shells are not as stable as those outside closed "p" shells. This is due to the fact that the "d" shell is quite sensitive (owing to the shallow potential in which it moves) to movements of the valence electrons. This in turn changes somewhat the potential acting on the valence particle, thus changing their nodes.

We can leave to experimental term-values (and the criterion previously mentioned) whether a given $d^{10}s$ or $d^{10}s^2$ atom (e. g. Cu I, Zn II) can be treated by the nodal boundary condition method. One or two electrons outside a closed "s" shell (e. g. Al I, Si II) are rather unstable, probably due to the influence of the valence particles on this s-shell. In this case the important influence is not due to the potential in which the inner shell moves, which in the case of an s-shell is very deep, but is due rather to there being only two particles in the shell,

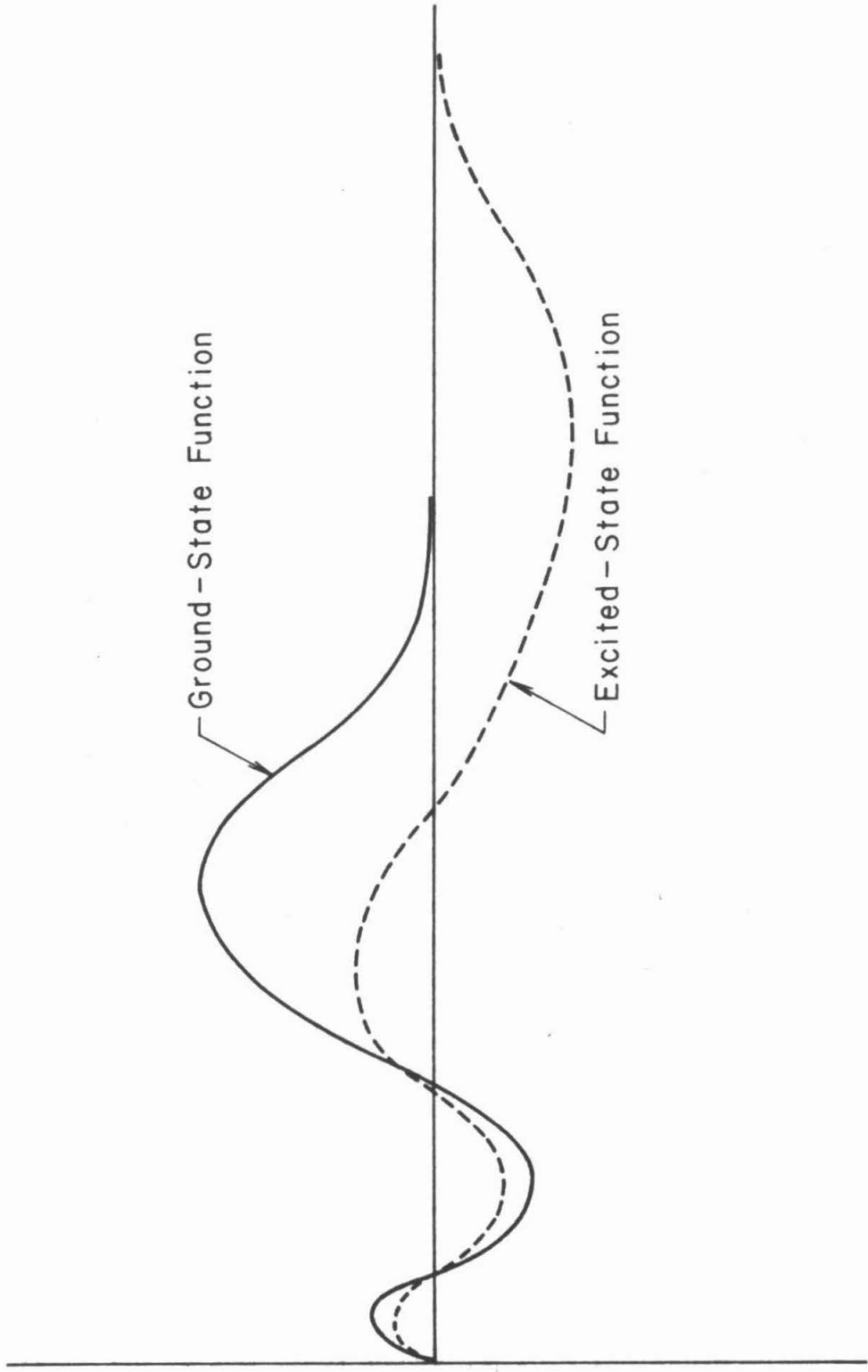
so that a perturbation in the potential can have a relatively large effect. For an inner p-shell, a small change in potential is less effective in moving the electrons, as a change in one of the six tends to shield the others from further change.

The second line of evidence for stable nodes, which serves to find the atoms for which the method can be used, and also the "Coulomb node" positions, comes from experimental term values for atoms and ions with one valence electron. This procedure will be discussed in part B.

From the available SCF data and the Coulomb node results to be given in part B, it is apparent that for most atoms the shift of inner nodes is small, if an electron is excited or if another valence electron is added. The direction of these shifts are easily understood. For a monovalent ion, the greater the degree of excitation, the more the nodes shift inward (see figure V-A). For smaller binding energies, the quantity $|V - E|$ becomes larger, increasing the curvature of the radial function for small radii, and decreasing it for large radii past the classical turning point $V = E$. Therefore for smaller binding energies, the nodes move inward. The addition of another electron produces two effects. First of all, the valence binding energies are different, and less than that of the single electron in the ion ground-state; therefore the nodes will shift inward slightly. Secondly, the introduction of another electron, particularly an "s" electron, produces an added shielding on the original electron which was not present in the ion. That is, a certain amount of the wave function of the new electron

Figure V-A

A schematic diagram showing a ground-state and an excited-state ($l = 0$) radial wave function for a monovalent ion. The figure illustrates the near-independence of the node positions with excitation energy, and also the direction in which deviations occur.



is inside the core, which means that the first electron does not move in exactly the same core potential as before. In turn, the original electron shields the added electron more than one would expect from the ionic situation. The effect of this shielding is to reduce the net core potential a certain amount, which will be small for the medium-to-heavy atoms possessing nodal stability. But the reduction in core potential pushes the nodes outward slightly. Therefore the correct nodes for a neutral atom are somewhat further out (about 1%) than what one would deduce from an interpolation of the energy versus node curve obtained from the ionic functions. For example, Hartree and Hartree (37) have calculated wave functions for Ca II ($3p^6 4s$) and for Ca I ($3p^6 4s^2$). As taken from Table V-A, the outermost s -node for Ca II ($4s$) is at $r = 1.433$ corresponding to an energy $\epsilon = 0.8295$ Ryd, while the node of Ca I ($4s^2$) is at $r = 1.442$ for $\epsilon = 0.3891$. If there were no added shielding, the s^2 node would have shifted inward slightly.

Table V-A presents the SCF node positions for Na I, Na⁻, Mg I, Si IV, K I, K⁻, Ca II, and Ca I, as taken from the wave functions published by various investigators. These results provide an idea of the nodal stability to be expected when moving from the ground state to excited states of atoms with one or two valence electrons, and also indicate the expected stability when passing from ionized to neutral atoms.

Table V-A

<u>Ion</u>	<u>State</u>	<u>s-node</u>	<u>ϵ_s</u>	<u>p-node</u>	<u>ϵ_t</u>	<u>Reference</u>
Na I	3s	1.034	.361			(28)
Na ⁻	3s ² 1S	1.038	.0268			(28)
Mg II	3s, 3p	.899	1.1055	.953	.780	(12)
Mg I	3s ² 1S	.896	.520			(13, 14)
	3s3p 1P	.890	.650	.9545	.2485	
	3s3p 3P	.896	.6969	.9545	.4297	
	3s4s 3S	.893	.8420			
	4s:	.877	.1930			
Si IV	3s, 3p	.709	3.275	.698	2.639	(42)
	4s, 4p	.685	1.538	.672	1.319	
	5s, 5p	.677	.893	.663	.793	
K I	4s	.4733	.2915			(28)
K ⁻	4s ² 1S	.4721	.02025			(28)
Ca II	4s, 4p	1.433	.8295	1.610	.6193	(5)
Ca I	4s ² 1S	1.442	.3891			(5)
	4s4p 1P	1.433	.5052	1.650	.1720	
	4s4p 3P	1.441	.5177	1.622	.3058	

B. Coulomb Nodes

It was shown in part A that the results of SCF calculations provide evidence for nodal stability. The second line of evidence for this method comes from a study of the ground and excited states in atoms or ions with one valence electron. There are many ions of this general type which have not been computed by a SCF method. Therefore, if in some way the wave functions of a large number of monovalent ions could be investigated, an idea as to their nodal stability could be attained. In particular, it is necessary to study the stability of various atomic configurations, such as p^6s , $d^{10}s$, and s^2p . We will now proceed to show how this program can be accomplished, and give the results.

The problem of a single valence electron was treated in section IV. It was shown why the Bates-Damgaard wave functions are good outside the core, and why the method is justified in using experimental term values for the eigenvalues. The node positions in which we are interested are all within the core, because it is only these which are stable. Nodes for highly excited states at large radii are in a region where the potential is too small to insure stability.

Since the Bates-Damgaard Coulomb approximation does not take into account the influence of the core potential on the valence wavefunctions, the inner node positions of this method cannot agree with SCF results. In fact, for a given eigenvalue, the nodes obtained by the Bates-Damgaard approach will invariably be at smaller radii than those of a SCF calculation (see figures IV-A and IV-B). This situation prevails because the true potential is deeper than the asymptotic Coulomb

potential, so the SCF function, which is identical with the Coulomb function for large radii, "curves over" more rapidly as it enters the core.

There is a second interesting difference between the "Coulomb nodes" and the "SCF nodes." The inner node of an excited state function may be at a slightly larger radius than that of the ground state function, when calculated by the Coulomb approximation. That is, the dependence of the node position on energy, using a Coulomb potential, can be opposite to that indicated in part A for SCF functions. This difference can be understood when one thinks of the Coulomb functions as being computed numerically by integrating inward from large to small radii. A smaller eigenvalue (i. e. the excited state) means that the function will curve less quickly at a given radius to the right of the classical turning point (where $E < V$) and more quickly for small radii (where $E > V$).

Now the position of the turning point for the excited states is nearly the same whether the Coulomb or Hartree potential is used, since this turning point is at a large radius where the potentials are almost the same. However, the turning point for the ground-state function will be at a smaller radius for the Coulomb potential than for the Hartree potential, because of the latter's greater depth. Therefore the region to the left of the turning point is relatively less important for the ground state in the Coulomb approximation, than for the SCF calculation. This fact implies that it is possible for the Coulomb ground-state node to be at a smaller radius than for the corresponding Coulomb excited-state node. Some of the ions in the following tables exhibit this behavior.

One of the purposes of these calculations was to investigate the validity of the nodal stability approximation for various kinds of atoms (i. e. $d^{10}s$, p^6s , s^2p configurations). The second purpose was to find the nodes to be used in a subsequent two-electron calculation. There is an apparent ambiguity in the eigenvalue to be used for "p" and "d" electrons, since there are two states for each configuration, corresponding to $j = l \pm 1/2$. For example, the splitting of the p-wave ${}^2P_{1/2}$ and ${}^2P_{3/2}$ states, caused by the spin-orbit interaction, is small for the lightest atoms, but becomes very significant for heavier atoms. If we were only interested in testing nodal stability, we could merely consistently use just one function, e. g. ${}^2P_{3/2}$, and use the experimental term values for this state. However, since we will use the nodes for two-electron calculations, the absolute values of the nodes are needed. So it is an important matter to find the right choice of p - and d-wave eigenvalues.

This problem is not difficult to solve, because evidently we should use the energy corresponding to the absence of the spin-orbit interaction. That is, the correct zero-order valence radial function would be an eigenfunction of the Hamiltonian including only the central potential. A better wave-function and eigenvalue could then be obtained by using the spin-orbit interaction in perturbation theory. This new wave function, however, would no longer be the product of radial and angular parts, but would be a mixture of many such functions. It therefore only makes sense to find a particular radial function from an eigenvalue corresponding to the purely central potential. This eigenvalue is

the "center-of-mass" of the experimental energies of the states ${}^2P_{1/2, 3/2}$ for a p-electron, or ${}^2D_{3/2, 5/2}$ for a d-electron.

The well-known relation for computing the spin-orbit matrix element between states of definite L, S, and J is

$$\langle {}^{2s+1}L_J | \vec{L} \cdot \vec{S} | {}^{2s+1}L_J \rangle = \frac{1}{2} [J(J+1) - L(L+1) - S(S+1)]$$

from which one finds

$$\langle {}^2P_{1/2} | \vec{L} \cdot \vec{S} | {}^2P_{1/2} \rangle = -1$$

$$\langle {}^2P_{3/2} | \vec{L} \cdot \vec{S} | {}^2P_{3/2} \rangle = \frac{1}{2}$$

$$\langle {}^2D_{3/2} | \vec{L} \cdot \vec{S} | {}^2D_{3/2} \rangle = -\frac{3}{2}$$

$$\langle {}^2D_{5/2} | \vec{L} \cdot \vec{S} | {}^2D_{5/2} \rangle = 1.$$

These matrix elements are proportional to the first-order energy splitting. Therefore the eigenvalue for a p-electron in the absence of a spin-orbit interaction will be

$$\epsilon_p = E_p\left(\frac{1}{2}\right) + \frac{2}{3} [E_p\left(\frac{3}{2}\right) - E_p\left(\frac{1}{2}\right)]$$

where $E\left(\frac{1}{2}\right)$ and $E\left(\frac{3}{2}\right)$ are the experimental ${}^2P_{1/2}$ and ${}^2P_{3/2}$ energies. The eigenvalue for a d-electron is

$$\epsilon_d = E_d\left(\frac{3}{2}\right) + \frac{3}{5} [E_d\left(\frac{5}{2}\right) - E_d\left(\frac{3}{2}\right)].$$

The following tables present eigenvalues and Coulomb nodes for 32 monovalent atoms and ions. The nodes were found for the lowest

three or four s, p, and d states except when experimental energies were lacking. Excited states in general have more than one Coulomb node: in this case the innermost node position is given first. Whenever there is a significant p- or d-wave spin-orbit splitting, three energies are quoted: that corresponding to $j = l + 1/2$, the "center of mass" energy, and that corresponding to $j = l - 1/2$, in order. In every case the center-of-mass energy was used for the eigenvalue in the calculation. The first table gives the results for hydrogen and ionized helium. Since these wave functions are known exactly, a comparison with the computed nodes gives an indication of the accuracy of the numerical integration. For convenience of analysis, the remaining atoms and ions are collected into three groups: those whose ground states have the configurations $p^6 s$ (or $s^2 s'$), $d^{10} s$, and $s^2 p$ respectively. At the beginning of each group, a discussion will be given of the results obtained.

1. Hydrogen and Ionized Helium

Wave functions for hydrogen and ionized helium were computed in order to test the accuracy of the numerical method used in the computer program. As evidenced by the close agreement between exact and calculated nodes, as given in the next table, the method is sufficiently accurate for s- and p-wave electrons. The only significant discrepancies occur for d-wave nodes close to the origin, where the rapidly varying centrifugal potential $l(l+1)/r^2$ introduces considerable truncation error. Therefore d-electron wave functions must be computed with caution, and small-radii Coulomb nodes considered unreliable.

Calculations were performed for a variety of spacings and maximum radii, but the node positions for s - and p -wave functions varied a negligible amount unless the spacing became so large that truncation error was important ($h = \text{spacing} \geq 0.1$).

Hydrogen

13.59 ev

1.0 Ryd

109,680 cm^{-1}

<u>state</u>	<u>ϵ(Ryd)</u>	<u>Computed nodes</u>	<u>Exact nodes</u>
1s	1.0	none	none
2s	0.25	2.00002	2.0
3s	0.11111	1.90213, 7.09821	1.90193, 7.09807
2p	0.25	none	none
3p	0.11111	6.0001	6.0
3d	0.11111	0.349	none
4d	0.0625	0.2903, 12.000002	12.0

He II

54.40 ev

4.0 Ryd

438,900 cm^{-1}

<u>state</u>	<u>ϵ(Ryd)</u>	<u>Computed nodes</u>	<u>Exact nodes</u>
1s	4.0	none	none
2s	1.0	1.00004	1.0
3s	0.44444	0.95107, 3.54911	0.95096, 3.54903
2p	1.0	none	none
3p	0.44444	3.00007	3.0
3d	0.44444	none	none

2. Alkali Atoms

a) Li I, Be II, B III ($1s^2 2s$ configuration)

These three ions have fairly stable s-nodes, but the p- and d-wave Coulomb nodes are not sufficiently stable to use for a two-electron calculation. This instability is caused by the fact that the innermost p- and d-wave nodes are far outside the tiny $1s^2$ core. As a result, the $2s^2$ ground-state energies and wave functions of Be I and B II can be computed, but any transition probabilities calculated by the nodal boundary condition method would be unreliable.

b) Na I, Mg II, Al III ($2p^2 3s$)

K I, Ca II, Sc III ($3p^6 4s$)

Rb I, Sr II, Y III ($4p^6 5s$)

Cs I, Ba II, La III ($5p^6 6s$)

These ions exhibit greater nodal stability than any other group. In general the stability is greater for the heavier than for the lighter elements, so that even the d-states become fairly stable by the time one reaches barium. Therefore, in principle, oscillator strengths can be computed for s-p transitions of all the corresponding two-electron atoms. However, the experimental term values are not sufficiently complete for Sc III, Y III, or La III, so that Coulomb nodes cannot be accurately determined for these ions. Transition probabilities were computed for Mg I, Al II, Ca I, Sr I, and Ba I.

Li I

5.390 ev

0.3965 Ryd

43,487 cm^{-1}

<u>state</u>	<u>ϵ(Ryd)</u>	<u>Coulomb nodes</u>
2s	0.3965	0.819
3s	0.1485	0.806, 4.643
4s	0.07727	0.803, 4.364, 11.719
2p	0.2606	none
3p	0.1145	5.698
4p	0.06398	5.240, 14.003
3d	0.1113	none
4d	0.06258	11.973
5d	0.04004	10.862, 24.080

Be II

18.21 ev

1.339 Ryd

146, 882 cm^{-1}

<u>state</u>	<u>ϵ(Ryd)</u>	<u>Coulomb nodes</u>
2s	1.3390	0.5816
3s	0.5348	0.5667, 2.715
4s	0.2865	0.5626, 2.543, 6.484
2p	1.048	none
3p	0.4594	2.834
4p	0.2564	2.608, 6.983
3d	0.4452	none
4d	0.2504	5.983
5d	0.1602	5.428, 12.036

B III

37.92 ev

2.7894 Ryd

305,931 cm^{-1}

<u>state</u>	<u>ϵ(Ryd)</u>	<u>Coulomb nodes</u>
2s	2.7894	0.4504
3s	1.1464	0.4366, 1.943
4s	0.6221	0.4324, 1.818, 4.532
2p	2.3484	none
3p	1.0300	1.901
4p	0.5753	1.750, 4.674
3d	1.0017	none
4d	0.5634	3.989
5d	0.3605	3.617, 8.022

Na I

5.138 ev

0.3778 Ryd

41,450 cm^{-1}

<u>state</u>	<u>ϵ(Ryd)</u>	<u>Coulomb nodes</u>
3s	0.3778	0.9081
4s	0.1432	0.9114, 4.903
5s	0.07521	0.9105, 4.611, 12.151
3p	0.2232	1.033
4p	0.10194	1.033, 6.929
5p	0.05843	1.031, 6.413, 15.895
3d	0.1119	none
4d	0.06292	11.859
5d	0.04024	10.742, 23.909

Mg II

15.03 ev

1.108 Ryd

121, 267 cm^{-1}

<u>state</u>	<u>ϵ(Ryd)</u>	<u>Coulomb nodes</u>
3s	1.1057	0.8360
4s	0.4692	0.8245, 3.284
5s	0.2597	0.8197, 3.077, 7.382
3p	0.7804	0.8838
	0.7799	
	0.7796	
4p	0.3706	0.8673, 4.043
	0.3704	
	0.3703	
5p	0.2170	0.8603, 3.745, 8.799
3d	0.4538	none
4d	0.2549	5.797
5d	0.1627	5.244, 11.772

Al III

28.44 ev

2.092 Ryd

229, 454 cm^{-1}

<u>state</u>	<u>ϵ(Ryd)</u>	<u>Coulomb nodes</u>
3s	2.0921	0.7560
4s	0.9418	0.7375, 2.576
5s	0.5363	0.7308, 2.407, 5.504
3p	1.6026	0.7651
	1.6012	
	1.6005	
4p	0.7825	0.7416, 2.976
	0.7820	
	0.7818	
5p	0.4652	0.7321, 2.755, 6.268
	0.4650	
	0.4649	
3d	1.0348	none
4d	0.5805	3.782
5d	0.3700	3.412, 7.729

K I

4.339 ev

0.3192 Ryd

35,010 cm^{-1}

<u>state</u>	<u>ϵ(Ryd)</u>	<u>Coulomb nodes</u>
4s	0.3192	1.2767
5s	0.1275	1.3058, 5.821
6s	0.0689	1.3134, 5.488, 13.653
4p	0.2008	1.6136
	0.2005	
	0.2003	
5p	0.09399	1.6327, 7.913
	0.09388	
	0.09382	
6p	0.05481	1.6350, 7.352, 17.381
	0.05475	
	0.05472	
3d	0.1229	none
4d	0.06941	9.902
5d	0.0440	8.715, 21.003
6d	0.0302	8.226, 18.934, 35.437

Ca II

11.87 eV

0.8730 Ryd

95,748 cm⁻¹

<u>state</u>	<u>ε(Ryd)</u>	<u>Coulomb nodes</u>
4s	0.8730	1.2614
5s	0.3974	1.2541, 4.155
6s	0.2286	1.2504, 3.897, 8.715
4p	0.6433 0.6420 0.6413	1.473
5p	0.3211 0.3206 0.3203	1.451, 5.047
6p	0.1939 0.19364 0.1935	1.441, 4.690, 10.259
3d	0.7485 0.7482 0.7480	none
4d	0.3548 0.3547 0.3546	2.850
5d	0.2099	2.610, 8.029
6d	0.1388	2.507, 7.294, 14.683

Sc III

24.75 ev

1.8207 Ryd

199,693 cm^{-1}

<u>state</u>	<u>ϵ(Ryd)</u>	<u>Coulomb nodes</u>
4s	1.5879	0.1355, 1.1869
5s	0.7734	0.1511, 1.1621, 3.383
6s	0.4599	0.1576, 1.1553, 3.168, 6.707
4p	1.2545 1.2516 1.2502	1.328
5p	0.6520 0.6509 0.6504	1.292, 3.916
6p	no data	
3d	1.8207 1.8196 1.8189	none
4d	0.7972 0.7970 0.7968	1.907
5d	0.4689 0.4688 0.4687	1.785, 5.414
6d	no data	

Rb I

4.176 ev

0.3072 Ryd

33,691 cm^{-1}

<u>state</u>	<u>ϵ(Ryd)</u>	<u>Coulomb nodes</u>
5s	0.3072	1.3741
6s	0.1236	1.4274, 6.091
7s	0.06729	1.4376, 5.746, 14.085
5p	0.1925	1.8829
	0.1910	
	0.1903	
6p	0.09096	1.9083, 8.384
	0.09049	
	0.09025	
7p	0.05339	1.9121, 7.801, 18.083
	0.05318	
	0.05307	
4d	0.1307	none
5d	0.07286	9.007
	0.07284	
	0.07283	
6d	0.04562	7.955, 19.914
	0.04561	
	0.04561	
7d	0.03110	7.521, 17.968, 34.100
	0.03109	
	0.03108	

Sr II

11.027 ev

0.8111 Ryd

88, 964 cm⁻¹

<u>state</u>	<u>ϵ(Ryd)</u>	<u>Coulomb nodes</u>
5s	0.8111	0.0938, 1.4244
6s	0.3759	0.1184, 1.4278, 4.489
7s	0.21882	0.1267, 1.4263, 4.215, 9.219
5p	0.5949	1.7684
	0.5900	
	0.5876	
6p	0.3027	1.7433, 5.545
	0.3009	
	0.3000	
7p	0.1853	1.7197, 5.140, 10.940
	0.18436	
	0.1839	
4d	0.6784	none
	0.6769	
	0.6759	
5d	0.3253	3.563
	0.3248	
	0.3245	
6d	0.1955	3.295, 8.984
	0.19527	
	0.1951	
7d	0.1308	3.190, 8.207, 15.969
	0.13066	
	0.1306	

Y III

20.5 ev

1.5070 Ryd

165, 289 cm^{-1}

<u>state</u>	<u>ϵ(Ryd)</u>	<u>Coulomb nodes</u>
5s	1.4390	0.2052, 1.3831
6s	0.7164	0.2316, 1.3678, 3.753
7s	no data	
5p	1.1300 1.1203 1.1154	1.637
6p	no data	
7p	no data	
4d	1.5071 1.5031 1.5004	none
5d	0.7012 0.7001 0.6994	2.616
6d	no data	

Cs I

3.893 ev

0.2864 Ryd

31,407 cm⁻¹

<u>state</u>	<u>ϵ (Ryd)</u>	<u>Coulomb nodes</u>
6s	0.2864	1.5669
7s	0.1175	1.6414, 6.553
8s	0.06464	1.6649, 6.205, 14.849
6p	0.1844	2.1897
	0.1811	
	0.1794	
7p	0.08790	2.2327, 8.943
	0.08680	
	0.08625	
8p	0.05195	2.2387, 8.333, 18.910
	0.05145	
	0.05120	
5d	0.1542	none
	0.1537	
	0.1533	
6d	0.08040	7.338
	0.08017	
	0.08001	
7d	0.04886	6.617, 18.006
	0.04875	
	0.04867	
8d	0.03279	6.336, 17.353, 31.850
	0.03272	
	0.03268	

Ba II

10.001 ev

0.7357 Ryd

80,687 cm⁻¹

<u>state</u>	<u>ε(Ryd)</u>	<u>Coulomb nodes</u>
6s	0.7357	0.1661, 1.6670
7s	0.3495	0.2038, 1.6809, 4.961
8s	0.2066	0.2174, 1.6835, 4.667, 9.928
6p	0.5509	2.106
	0.5406	
	0.5355	
7p	0.2854	2.078, 6.109
	0.2816	
	0.2797	
8p	0.1764	2.058, 5.678, 11.748
	0.17461	
	0.1737	
5d	0.6912	none
	0.6868	
	0.6839	
6d	0.3167	3.803
	0.3156	
	0.3149	
7d	0.1904	3.569, 9.373
	0.18992	
	0.1896	
8d	0.1278	3.474, 8.593, 16.507
	0.12748	
	0.1273	

La III

19.17 ev

1.4099 Ryd

154,630 cm⁻¹

<u>state</u>	<u>ϵ(Ryd)</u>	<u>Coulomb nodes</u>
6s	1.2859	0.3061, 1.6400
7s	0.65907	0.3414, 1.6220, 4.1974
8s	0.37505	0.5183, 1.948, 4.471, 8.678
6p	1.0268	1.973
	1.0080	
	0.9986	
7p	no data	
8p	no data	
5d	1.4099	none
	1.4011	
	1.3953	
6d	0.6588	2.995
	0.6564	
	0.6548	
7d	no data	

3. Cu I, Zn II, Ga III	(3d ¹⁰ 4s)
Ag I, Cd II, In III	(4d ¹⁰ 5s)
Au I, Hg II, Tl III	(5d ¹⁰ 6s)

On the whole, the Coulomb nodes for this group of ions are not as stable as those for the alkali metals with the p^6 ground-state configuration. As previously explained, this is due to the sensitivity of the d^{10} shell to the excitation energy of the valence electron. Some wave functions and/or transition probabilities were calculated for all of the following two-electron ions: Zn I, Ga II, Cd I, In II, Hg I, and Tl II. In some cases, either the p - or d -wave states were unstable or the experimental term-values inadequate.

Cu I

7.724 ev

0.5682 Ryd

62, 317 cm^{-1}

<u>state</u>	<u>ϵ(Ryd)</u>	<u>Coulomb nodes</u>
4s	0.5682	0.331
5s	0.1749	0.423, 3.610
6s	0.08633	0.440, 3.451, 10.087
4p	0.2898	none
	0.2883	
	0.2875	
5p	0.1179	5.414
6p	0.06868	4.665, 13.061
	0.06720	
	0.06646	
4d	0.1129	none
5d	0.06317	11.776
6d	0.04033	10.689, 23.833

Zn II

17.96 ev

1.3211 Ryd

144, 891 cm^{-1}

<u>state</u>	<u>ϵ(Ryd)</u>	<u>Coulomb nodes</u>
4s	1.3211	0.5972
5s	0.5147	0.6356, 2.872
6s	0.2771	0.6429, 2.715, 6.778
4p	0.8790	0.5756
	0.8737	
	0.8710	
5p	0.3969	0.6286, 3.643
	0.3954	
	0.3946	
6p	0.2280	0.6407, 3.396, 8.248
	0.2275	
	0.2273	
4d	0.4375	0.9457
	0.4372	
	0.4370	
5d	0.2455	0.9853, 6.201
	0.24534	
	0.2452	
6d	0.1574	0.9878, 5.649, 12.351
	0.15731	
	0.1573	

Ga III

30.70 ev

2.2584 Ryd

247, 700 cm^{-1}

<u>state</u>	<u>ϵ(Ryd)</u>	<u>Coulomb nodes</u>
4s	2.2584	0.6624
5s	0.9752	0.6761, 2.452
6s	0.5483	0.6799, 2.311, 5.348
4p	1.6643 1.6538 1.6486	0.7015
5p	0.7927 0.7894 0.7878	0.7167, 2.933
6p	no data	
4d	0.9448 0.9441 0.9437	0.9709
5d	0.5335 0.5332 0.5330	0.9589, 4.387
6d	no data	

Ag I

7.574 ev

0.5572 Ryd

61, 107 cm⁻¹

<u>state</u>	<u>ε(Ryd)</u>	<u>Coulomb nodes</u>
5s	0.5572	0.351
6s	0.1691	0.490, 3.805
7s	0.08407	0.516, 3.655, 10.458
5p	0.2877 0.2821 0.2793	none
6p	0.1168 0.1155 0.1149	5.612
7p	0.06443 0.06394 0.06370	5.247, 14.016
5d	0.1127 0.1126 0.1125	none
6d	0.06295 0.06290 0.06826	11.866
7d	0.04018 0.04015 0.04013	10.796, 23.986

Cd II

16.904 ev

1.2434 Ryd

136,375 cm⁻¹

<u>state</u>	<u>ε(Ryd)</u>	<u>Coulomb nodes</u>
5s	1.2434	0.6717
6s	0.4867	0.7458, 3.116
7s	0.2651	0.7606, 2.958, 7.185
5p	0.8410	0.7271
	0.8259	
	0.8184	
6p	0.3800	0.8136, 3.952
	0.3758	
	0.3737	
7p	0.2190	0.8354, 3.705, 8.735
	0.21817	
	0.2178	
5d	0.4257	1.3256
	0.4249	
	0.4243	
6d	0.2389	1.3667, 6.510
	0.23849	
	0.2382	
7d	0.1537	1.3697, 5.958, 12.792
	0.15344	
	0.1533	

In III

28.03 ev

2.0615 Ryd

226, 100 cm^{-1}

<u>state</u>	<u>ϵ(Ryd)</u>	<u>Coulomb nodes</u>
5s	2.0615	0.7752
6s	0.9047	0.8130, 2.725
7s	0.5167	0.8219, 2.577, 5.776
5p	1.5401 1.5138 1.5006	0.880
6p	0.7432 0.7351 0.7310	0.912, 3.270
7p	0.4153 0.4116 0.4098	1.180, 3.480, 7.375
5d	0.8903 0.8887 0.8877	1.329
6d	0.5067 0.5057 0.5050	1.314, 4.792
7d	0.3288 0.3283 0.3279	1.311, 4.409, 9.150

Au I

9.22 ev

0.6784 Ryd

74,410 cm⁻¹

<u>state</u>	<u>ε(Ryd)</u>	<u>Coulomb nodes</u>
6s	0.6784	0.182
7s	0.1817	0.353, 3.399
8s	0.08815	0.384, 3.297, 9.803
6p	0.3378	none
	0.3146	
	0.3030	
7p	0.1311	4.749
	0.1268	
	0.1247	
8p	0.07116	4.323, 12.494
	0.06931	
	0.06838	
6d	0.1136	none
	0.1131	
	0.1128	
7d	0.06328	11.813
	0.06306	
	0.06291	
8d	0.04047	10.724, 23.884
	0.04027	
	0.04014	

Hg II

18.751 ev

1.3793 Ryd

151,280 cm^{-1}

<u>state</u>	<u>ϵ(Ryd)</u>	<u>Coulomb nodes</u>
6s	1.3793	0.5481
7s	0.5066	0.6657, 2.939
8s	0.2723	0.6880, 2.809, 6.936
6p	0.9099	0.6358
	0.8544	
	0.8267	
7p	0.3919	0.8753, 4.057
	0.3696	
	0.3584	
8p	0.2219	0.8669, 3.756, 8.815
	0.21672	
	0.2146	
6d	0.4221	1.4752
	0.4188	
	0.4166	
7d	0.2367	1.5168, 6.662
	0.23527	
	0.2343	
8d	0.1524	1.5164, 6.104, 13.000
	0.15168	
	0.1512	

Tl III

29.8 ev

2.194 Ryd

240,600 cm^{-1}

<u>state</u>	<u>ϵ(Ryd)</u>	<u>Coulomb nodes</u>
6s	2.194	0.6968
7s	0.9254	0.7699, 2.640
8s	0.5235	0.7897, 2.5161, 5.679
6p	1.6088	0.874
	1.5187	
	1.4737	
7p	0.7545	0.973, 3.374
	0.7200	
	0.7027	
8p	no data	
6d	0.8684	1.499
	0.8612	
	0.8564	
7d	0.4946	1.493, 5.022
	0.4914	
	0.4892	
8d	no data	

4. BI, CII	($2s^2 2p$)
Al I, Si II	($3s^2 3p$)
Ga I, Ge II	($4s^2 4p$)

The Coulomb nodes for this group of ions are found to be less stable than for either of the previous groups, except for the s- and p-wave states of Al I, Ga I, and Ge II, and the s-wave states of Si II. Therefore the only reasonably reliable transition probabilities that could be computed for a two-electron situation are those for Ge I. As a result, no two-electron calculations at all were made for this group, because previous theoretical and experimental results are almost entirely lacking. No basis for reliability can be established within the group. There is also evidence that there is strong interaction between various configurations involving all three of the outer electrons, so that it is probably not a good approximation to treat these ions as having a stationary s^2 shell and one valence electron.

B I

8.296 ev

0.6101 Ryd

66,930 cm^{-1}

<u>state</u>	<u>ϵ(Ryd)</u>	<u>Coulomb nodes</u>
3s	0.2452	2.069
4s	0.1087	2.012, 7.323
5s	0.06185	1.939, 6.741, 15.731
2p	0.6101	none
3p	no data	
4p	no data	
3d	0.1109	1.0538
4d	0.06329	- 11.737
5d	0.04056	- 10.554, 23.640

C II

24.376 ev

1.7931 Ryd

196,659 cm^{-1}

<u>state</u>	<u>ϵ(Ryd)</u>	<u>Coulomb nodes</u>
3s	0.7305	0.1721, 1.686
4s	0.3595	0.1687, 1.580, 4.774
5s	0.2125	0.1699, 1.552, 4.439, 9.573
2p	1.7931 1.7927 1.7925	none
3p	0.5920	1.756
4p	0.3113	1.584, 5.274
5p	0.19484	1.407, 4.635, 10.175
3d	0.4660	none
4d	0.2602	5.587
5d	0.1656	5.038, 11.477

Al I

5.984 ev

0.4402 Ryd

48,279 cm⁻¹

<u>state</u>	<u>ε(Ryd)</u>	<u>Coulomb nodes</u>
4s	0.2091	0.150, 2.709
5s	0.09656	0.184, 2.682, 8.646
6s	0.05593	0.196, 2.670, 8.102, 17.921
3p	0.4402	none
	0.4395	
	0.4392	
4p	0.1398	3.948
	0.1397	
	0.1396	
5p	0.07301	3.786, 11.597
	0.07297	
	0.07295	
6p	0.04508	3.722, 10.731, 22.564
	0.04506	
	0.04505	
3d	0.1444	none
4d	0.08525	6.336
	0.08522	
	0.08520	
5d	0.05512	4.310, 14.844
	0.05510	
	0.05508	
6d	0.03750	3.317, 12.514, 26.436
	0.03748	
	0.03747	

Si II

16.34 ev

1.2019 Ryd

131,818 cm^{-1}

<u>state</u>	<u>ϵ(Ryd)</u>	<u>Coulomb nodes</u>
4s	0.6047	0.3785, 2.260
5s	0.3086	0.4047, 2.189, 5.872
6s	0.1882	0.4139, 2.162, 5.477, 11.173
3p	1.2019	none
	1.1993	
4p	0.3705	
	0.3701	0.8703, 4.048
	0.3699	
5p	0.2550	
	0.2548	- , 2.646, 7.045
	0.2547	
6p	0.1620	
	0.1619	- , 2.588, 6.508, 12.979
	0.1619	
3d	0.4785	
	0.4784	none
	0.4784	
4d	0.2808	4.844
5d	0.17715	4.288, 10.402
6d	0.12127	- , 9.412, 17.646

Ga I

6.00 ev

0.4411 Ryd

48,380 cm^{-1}

<u>state</u>	<u>ϵ(Ryd)</u>	<u>Coulomb nodes</u>
5s	0.2151	2.585
6s	0.09843	0.150, 2.564, 8.418
7s	0.05673	0.162, 2.558, 7.898, 17.596
4p	0.4411	none
	0.4361	
	0.4336	
5p	0.1398	3.981
	0.1391	
	0.1388	
6p	0.07298	3.821, 11.655
	0.07272	
	0.07259	
7p	0.04503	3.766, 10.082, 22.670
	0.04490	
	0.04484	
4d	0.1239	none
5d	0.06908	10.004
	0.06904	
	0.06901	
6d	0.04381	8.824, 21.159
	0.04378	
	0.04376	
7d	0.03016	8.275, 19.001, 35.530
	0.03014	
	0.03012	

Ge II

15.93 ev

1.1718 Ryd

128,518 cm^{-1}

<u>state</u>	<u>ϵ(Ryd)</u>	<u>Coulomb nodes</u>
5s	0.6028	0.383, 2.270
6s	0.3078	0.410, 2.200, 5.892
7s	0.18767	0.421, 2.178, 5.503, 11.214
4p	1.1718 1.1611 1.1557	none
5p	0.4514 0.4493 0.4482	2.945
6p	0.24868	0.152, 2.797, 7.290
7p	0.15958	0.125, 2.697, 6.675, 13.224
4d	0.4347 0.4337 0.4331	1.073
5d	0.2592 0.2590 0.2588	- , 5.634
6d	0.1654 0.1653 0.1652	- , 5.059, 11.508

C. The Method with Calcium as an Example

In parts A and B of this section, evidence has been presented for the nodal stability of several types of ions. It is now possible to show how this property can be used to calculate radial wave functions for atoms with two valence electrons. At medium to large radii, these functions will compare in accuracy to those calculated from the full SCF treatment with exchange. To be definite, the method will be explained by referring to the resonant $\lambda 4227$ line ($4s^2\ ^1S_0 - 4s4p\ ^1P_1$) of neutral calcium. An example of the calculation of an intercombination line (singlet to triplet) will be given in part D.

1. Location of the Coulomb Nodes

The first stage in the calcium calculation is the preparation of the table of Coulomb nodes for Ca II (p. 67). These are found by solving the one-electron Schrödinger equation numerically, using experimental term-values for the eigenvalues. The results, taken from p. 67, show the inner s- and p-wave nodes to be stable:

<u>state</u>	<u>ϵ (Ryd)</u>	<u>Coulomb node</u>
4s	0.8730	1.2614
5s	0.3974	1.2541
6s	0.2286	1.2504
4p	0.6420	1.473
5p	0.3206	1.451
6p	0.19364	1.441

The p-wave energies correspond to the "center-of-mass" of the $^2P_{1/2}$ and $^2P_{3/2}$ states, as explained in part B.

2. The s^2 Ground-State Energy and Wave Function

The second stage in the calculation of the calcium resonance line is the determination of the $4s^2$ ground-state energy, using the Ca II s -wave Coulomb node data just quoted, and also the s^2 energy-node table on p. 107. The latter table was prepared with the assistance of the s -squared program discussed in the appendices. Nodes for s^2 states were found as a function of the eigenvalue ϵ , by solving the Hartree-Fock equation

$$P''(r) = \left[\epsilon - \frac{2C}{r} + \frac{2}{r} \int_0^r dr P^2 + 2 \int_r^\infty dr \frac{P^2}{r} \right] P(r)$$

Therefore we have available two curves of energy vs. node: that from the s -states of Ca II, and also the s^2 curve. If we neglect the effects of the small change in core potential as another s -electron is added to Ca II, then the correct s^2 energy and node for the ground state of Ca I can be read from the intersection of the two curves.

In practice this was accomplished in the following way: The Ca II energies 0.8730 and 0.3974 with corresponding nodes 1.2614 and 1.2541 define a linear variation of node with energy. Using also a linear interpolation between the s^2 energies 0.40 and 0.41 from p. 107 one finds the intersection at $\epsilon_{s^2} = 0.4093$ with node at 1.2542. Another linear relation for Ca II comes from using the two energies 0.3974 and 0.2286 with nodes 1.2541 and 1.2504. This line has a somewhat different slope than that used before, but not enough to change the point of intersection with the s^2 curve by an appreciable amount. We therefore conclude that $\epsilon_{s^2} = 0.4093$ with a Coulomb node at 1.2542.

The result derived by Hartree and Hartree (37) from a full SCF calculation is $\epsilon_{s_2} = 0.3891$. The SCF electrons are thus not quite so tightly bound. Part of this difference is due to the neglect of core polarization in the usual SCF method. Core polarization is roughly accounted for in the nodal boundary condition method by the use of empirical nodes. Another part of the difference is due, in the nodal boundary condition method, to a neglect of the slight reduction in core potential when a second valence electron is added to a monovalent ion. The order of magnitude of the influence of this effect on the node positions can be estimated from the SCF node data of table V-A. This table suggests that the radius of the node should be increased by about 1% when passing from the monovalent to the divalent situation. Using then a Coulomb node of 1.266 instead of 1.2542, the one electron energy is found to decrease from 0.4093 to 0.4070. This change is small, amounting to only 1/2 %. Therefore it is likely that the full SCF calculation, perhaps because of the neglect of core polarization, underestimates the binding energy by 3 to 4%.

3. The Excited sp^1p_1 State

The most difficult calculation is that for the sp -configuration. This involves solving simultaneously the two non-linear Hartree-Fock equations given in Section III-B and Appendix A. Coulomb nodes are extracted from the Ca II data, assuming a linear relation between energy and node. A fair guess can be made of the s - and p -wave eigenvalues expected, so that for a preliminary run, nodes corresponding to these energies are used as inner boundary conditions on the wave

functions. If the derived eigenvalues differ significantly from those guessed, the nodes are readjusted and the whole calculation repeated.

In the case of calcium, the initial 4s and 4p Coulomb nodes were chosen to be 1.263 and 1.438, respectively. The $4s4p\ ^1P_1$ calculation resulted in the eigenvalues $\epsilon_s = 0.555$ and $\epsilon_p = 0.180$. From these energies, better nodes can be found by interpolating the Ca II data. These are: s-node 1.256; p-node 1.440. The final resulting energies are $\epsilon_s = 0.533$ and $\epsilon_p = 0.1792$.

Hartree and Hartree (37) have calculated the $4s4p\ ^1P_1$ state of Ca I by the full SCF method with exchange, and obtained $\epsilon_s = 0.5052$ and $\epsilon_p = 0.1720$. As with the s^2 configuration, these eigenvalues are less than those obtained by the nodal boundary condition method. It is again our contention that the discrepancy is due largely to the neglect of core polarization or other correlation effects in the SCF method, which are implicitly accounted for roughly in the nodal boundary condition method by the use of experimental energies.

4. Calculation of Oscillator Strengths

Once the initial and final wave functions have been determined, the calculation of the dipole moment matrix element requires only the evaluation of two numerical integrals by Simpson's rule. The computer program calculates both of the two electron functions, the radial integrals, the line strengths, and the gf-value.

D. Intercombination Lines

The effects of a deviation from LS-coupling were reviewed in section III-A. The resulting mixture of the LS basis functions provides a means by which the so-called "intercombination lines" can occur. These are transitions involving a change of multiplicity or total spin S , which means for two-electron functions that triplet to singlet transitions are possible. For the configurations s^2 , ss' , and sp , which we have been considering, the following intercombination lines can occur:

$$(s^2) {}^1S_0 - (sp) {}^3P_1$$

$$(ss') {}^1S_0 - (sp) {}^3P_1$$

$$(ss') {}^3S_1 - (sp) {}^1P_1$$

To find oscillator strengths for these transitions, it is first necessary to calculate the amount of mixing from observed spin-orbit splittings. These wave functions can then be inserted in the dipole moment matrix element. For example, if the experimentally designated $(sp) {}^3P_1$ state is actually

$${}^3P_1 = a {}^3P_1 + b {}^1P_1$$

where $a^2 + b^2 = 1$, then for the transition $(s^2) {}^1S_0 - (sp) {}^3P_1$.

$$\langle \Psi_f | \vec{r} | \Psi_i \rangle = \langle a {}^3P_1 + b {}^1P_1 | \vec{r} | {}^1S_0 \rangle = b \langle {}^1P_1 | \vec{r} | {}^1S_0 \rangle$$

Condon and Shortley (38) give a complete discussion of intermediate coupling. The energy matrix for the sp -configuration is

	3P_2	3P_1	1P_1	3P_0
3P_2	$\zeta/2 - G_1$			
3P_1		$-\zeta/2 - G_1$	$\lambda\zeta/\sqrt{2}$	
1P_1		$\lambda\zeta/\sqrt{2}$	G_1	
3P_0				$-\zeta - G_1$

where G_1 and ζ denote electrostatic and spin-orbit matrix elements. Following King and Van Vleck (39), the parameter λ has been inserted to try to account empirically for the ratio of the off-diagonal to the diagonal radial matrix elements of the spin-orbit interaction. In the more common approximation (as in Condon and Shortley), λ is set equal to unity, but King and Van Vleck point out that the ratio $\lambda = \int dr (R_3 R_1 / r^3) / \int dr (R_3^2 / r^3)$ (where R_3 and R_1 are the triplet and singlet radial functions) is unlikely to be unity, because of imperfect overlap of R_1 and R_3 . The $1/r^3$ factor weights small radii so heavily that only the inmost parts of the wave functions contribute to the integrals. But in this region the overlap is almost perfect (in the SCF approximation) between the singlet and triplet functions, i. e., the nodes coincide. However, the normalization differs considerably between the two, the singlet function being smaller for small radii, so that the ratio λ should be less than one.

By diagonalizing the matrix exactly, one finds the following energies for the four states (apart from a single additive constant):

$${}^3P_2 : \zeta/2 - G_1$$

$${}^3P_1 : -\zeta/4 - \frac{1}{8} [4G_1^2 + 2G_1\zeta + (1 + 8\lambda^2)\zeta^2/4]^{1/2}$$

$${}^1P_1 : -\zeta/4 + \frac{1}{2}[4G_1^2 + 2G_1\zeta + (1 + 8\lambda^2)\zeta^2/4]^{\frac{1}{2}}$$

$${}^3P_0 : -\zeta - G_1$$

Several relations then follow:

$${}^3P_2 - {}^3P_0 = 3/2 \zeta$$

$${}^3P_1 + {}^1P_1 - {}^3P_2 - {}^3P_0 = 2 G_1$$

and

$${}^1P_1 - {}^3P_1 = [4G_1^2 + 2G_1\zeta + (1 + 8\lambda^2)\zeta^2/4]^{\frac{1}{2}} .$$

Using experimental term values, ζ , G_1 , and λ can be determined from these three equations.

The wave functions corresponding to an energy matrix

$$\begin{vmatrix} v_{11} & v_{12} \\ v_{21} & v_{22} \end{vmatrix} \quad (v_{12} = v_{21})$$

with eigenvalues

$$E = \frac{1}{2}[(v_{11} + v_{22}) \pm \{(v_{11} - v_{22})^2 + 4(v_{12})^2\}^{\frac{1}{2}}]$$

are

$$\psi = C_1 \psi_1 + C_2 \psi_2$$

where

$$C_1 = \left\{ \frac{v_{12}}{2|v_{12}|} \left[1 \mp \frac{v_{11} - v_{22}}{\{(v_{11} - v_{22})^2 + 4(v_{12})^2\}^{\frac{1}{2}}} \right] \right\}^{\frac{1}{2}}$$

and

$$C_2 = \pm \left\{ \frac{v_{12}}{2|v_{12}|} \left[1 \mp \frac{v_{11} - v_{22}}{\{(v_{11} - v_{22})^2 + 4(v_{12})^2\}^{\frac{1}{2}}} \right] \right\}^{\frac{1}{2}}$$

so that one obtains (defining $\Delta \equiv v_{22} - v_{21} = 2G_1 + \zeta/2$)

$${}^1P_1 = \frac{1}{\sqrt{2}} \left(1 - \frac{\Delta}{(\Delta^2 + 2\lambda^2 \zeta^2)^{\frac{1}{2}}} \right)^{\frac{1}{2}} {}^3P_1 + \frac{1}{\sqrt{2}} \left(1 + \frac{\Delta}{(\Delta^2 + 2\lambda^2 \zeta^2)^{\frac{1}{2}}} \right)^{\frac{1}{2}} {}^1P_1$$

$${}^3P_1 = \frac{1}{\sqrt{2}} \left(1 + \frac{\Delta}{(\Delta^2 + 2\lambda^2 \zeta^2)^{\frac{1}{2}}} \right)^{\frac{1}{2}} {}^3P_1 - \frac{1}{\sqrt{2}} \left(1 - \frac{\Delta}{(\Delta^2 + 2\lambda^2 \zeta^2)^{\frac{1}{2}}} \right)^{\frac{1}{2}} {}^1P_1$$

which are correctly normalized. These wave function mixings were calculated for the lowest and next-to-lowest sp-configurations of the atoms and ions treated.

For the lowest sp-configuration of CaI, ZnI, SrI, CdI, BaI, and HgI, King and Van Vleck obtain λ 's varying between 0.758 and 0.841, agreeing with our expectation that $\lambda < 1$. The same analysis can be carried through for the lowest sp-configurations of MgI, AlII, GaII, InII, and TlII, and also the excited sp-configurations of all the divalent atoms and ions. The results are given in Table V-B. The numbers were computed using the recent term-value tables of Moore (40), so they differ somewhat from those of King and Van Vleck. The values of λ for the lowest sp-configuration of all elements considered from CaI through TlII fall between the limits 0.747 and 0.891. MgI and AlII have anomalously high λ 's: 1.778 and 1.349, respectively, as previously noted by Rubenstein (41) for MgI (who obtained $\lambda = 2.4$). The λ -results for the next-higher sp-configuration are larger than unity for almost all ions, which may indicate that the simple single-configuration assumption has broken down.

Experimental evidence supports the introduction of the λ - ratio for the lowest sp-configurations of CaI through TlII as reviewed by King and Van Vleck, and as displayed in Table V-C, which gives

the ratios of singlet to triplet resonance f -values. There is no experimental data for the next excited sp -configurations, so it was judged very dubious to calculate intercombination lines involving these configurations, for which $\lambda > 1.0$. Therefore, only two or three intercombination lines were computed for each ion, all arising from the lowest sp -configuration. Table V-B gives the calculated values of ζ , G_1 , and λ , along with the previously published λ 's of King and Van Vleck (39) (CaI, ZnI, SrI, CdI, BaI, HgI) and of Rubenstein (41) (MgI). The last two columns contain the coefficients "a" and "b" for the expressions

$${}^1P_1 = a {}^1P_1 + b {}^3P_1$$

and

$${}^3P_1 = a {}^3P_1 - b {}^1P_1 .$$

As an example of a complete calculation of an intercombination line, consider the transition $(4s4p) {}^3P_1 - (4s^2) {}^1S_0$ in neutral calcium. From Moore's tables (40), the excitation energies of the $4s4p$ states are:

<u>state</u>	<u>energy (cm⁻¹)</u>
1P_1	23652.324
3P_0	15157.910
3P_1	15210.067
3P_2	15315.948

From the equation ${}^3P_2 - {}^3P_0 = 3/2 \zeta$ one obtains $\zeta = 105.36$, and from ${}^3P_1 + {}^1P_1 - {}^3P_2 - {}^3P_0 = 2G_1$ one finds that $G_1 = 4194.27$.

The factor λ is then found from

$${}^1P_1 - {}^3P_1 = [4G_1^2 + 2G_1\zeta + (1 + 8\lambda^2)\zeta^2/4]^{1/2}$$

to be $\lambda = 0.891$. The constants "a" and "b" are then 0.99997 and 0.007867, respectively. To find the ${}^3P_1 - {}^1S_0$ matrix element, we have

$$\langle {}^3P_1 | \vec{r} | {}^1S_0 \rangle = -0.00787 \langle {}^1P_1 | \vec{r} | {}^1S_0 \rangle.$$

The latter matrix element has already been computed in the course of finding the oscillator strength for the $4s^2 {}^1S_0 - 4s4p {}^1P_1$ transition, so the work is completed.

TABLE V-B

Ion	Configuration	ζ	G	λ	$\lambda_{\text{previous}}$	a	b
MgI	3s3p	40.513	6580.1	1.778	2.4	1.0	.00386
	3s4p	2.733	747.4	3.409		1.0	.0302
AlII	3s3p	124.9	11166.1	1.349		1.0	.00532
	3s4p	28.93	732.3	1.139		1.0	.0158
CaI	4s4p	105.36	4194.3	.891	.8126	1.0	.00787
	4s5p	18.307	2555.5	8.017		1.0	.0203
ZnI	4s4p	386.0	7022.6	.747	.7702	1.0	.0143
	4s5p	55.27	803.3	1.000		1.0	.0239
CaII	4s4p	920.0	11198.0	.870		1.0	.0247
	4s5p	199.3	951.5	1.040		.997	.0726
SrI	5s5p	387.36	3493.4	.810	.807	1.0	.0309
	5s6p	79.71	70.09	1.271		.944	.330
CdI	5s5p	1141.99	6203.8	.759	.7618	1.0	.0471
	5s6p	163.8	670.75	1.049		.996	.0845
InII	5s5p	2368.0	9140.4	.876		1.0	.0748
	5s6p	511.77	764.6	1.043		.980	.1988
BaI	6s6p	832.48	2458.1	.842	.8414	.9958	.0917
	6s7p	162.50	815.91	1.097		.997	.0730

TABLE V-B (continued)

Ion	Configuration	ζ	G	λ	$\lambda_{\text{previous}}$	a	b
HgI	6s6p	4265.3	5896.5	.758	.7578	.9875	.1579
	6s7p	1127.2	116.4	.894		.8625	.5061
TlII	6s6p	8182.67	8438.5	.871		.9750	.2222
	6s7p	1778.67	282.5	.953		.8714	.4905

TABLE V-C

Resonance Line Ratios

$$f(s^2 1S - sp^1 P) / f(s^2 1S - sp^3 P)$$

Ion	King and Van Vleck	Present Calculation	Experiment
Ca I	30180	25200	33000 (P) 36000 (OP)
Zn I	6757	7000	7200 (W)
Ga II		2420	
Sr I	1582	1570	1660 (P)
Cd I	637	641	680 \pm 100 (W)
In II		260	
Ba I	169	170	146 (P) 164 (OP)
Hg I	53.4	55	46.8 \pm 2 (W)
Tl II		29.3	

References: P = Prokofiev; OP = Ostrovskii and Penkin; W = Wolfsohn

References quoted after each element in Section VI-B, or in the paper of King and Van Vleck (ref. 39).

VI. RESULTS AND APPLICATIONS

Evidence for nodal stability and the details of applying the nodal boundary condition method have been given in Section V. Calcium was used as an example, and the eigenvalues, eigenfunctions, and oscillator strengths were compared with those found from a complete SCF calculation. In this section, the entire results of calculating with the method will be tabulated. In Part A, the s^2 configuration is discussed, and tables of the variation in Coulomb node with energy are given. Part B collects together eigenvalues and oscillator strengths for transitions in thirteen atoms and ions with two valence electrons. The application of these results to astronomically observed lines, and to the problem of element abundances, is treated briefly in Part C. Finally, in Part D, possible extensions of the technique are outlined, along with other uses of the nodal boundary condition method.

A. The S-Squared Calculations

The s -squared program discussed in the appendices computes wave functions for given one-electron eigenvalues. Therefore, a table of energy versus node can be constructed for this configuration. From this table, if the Coulomb nodes are known for a particular atom, the s^2 one-electron energy can be interpolated. The details of making this interpolation were treated in Section V-C. If one subsequently wishes to compute a transition probability involving this s^2 ground-state, the eigenvalue is known, so that the wave-function is determined.

The eigenvalues found from these calculations can be compared with SCF results for various atoms. For example, the Coulomb s -node for magnesium (from the data of Section V-B) is at $r = .825$. From the node versus energy curve for the s^2 configuration of neutral atoms (Table VI-A), one finds a one-electron energy for the ground-state valence function of magnesium to be .5194 Ryd. This is close to the result (.520) of Biermann and Trefftz (13) using SCF with core polarization. The case of the ground state of neutral calcium was discussed in Section V-C. A systematic comparison with previous results is given atom by atom in Part B of this section.

B. Eigenvalues and Oscillator Strengths

The following tables contain the results of all the computations made for atoms with two valence electrons. Altogether, some calculations were carried out for thirteen atoms and ions:

<u>Ion</u>	<u>Configuration</u>
He I, Li II	($1s^2$)
Mg I, Al II	($2p^6 3s^2$)
Ca I	($3p^6 4s^2$)
Zn I, Ga II	($3d^{10} 4s^2$)
Sr I	($4p^6 5s^2$)
Cd I, In II	($4d^{10} 5s^2$)
Ba I	($5p^6 6s^2$)
Hg I, Tl II	($5d^{10} 6s^2$)

TABLE VI-A

Neutral Atoms

ϵ = one-electron energy for the s^2 configuration.

<u>ϵ</u>	<u>Coulomb node</u>	<u>ϵ</u>	<u>Coulomb node</u>
1.00	.1933	.50	.8842
.90	.2567	.49	.9169
.80	.3417	.48	.9513
.70	.4592	.47	.9875
.69	.4735	.46	1.0256
.68	.4881	.45	1.0658
.67	.5034	.44	1.1081
.66	.5192	.43	1.1529
.65	.5356	.42	1.2002
.64	.5527	.41	1.2503
.63	.5704	.40	1.3033
.62	.5889	.39	1.3597
.61	.6081	.38	1.4195
.60	.6281	.37	1.4832
.59	.6490	.36	1.5510 , .1186
.58	.6707	.35	1.6235 , .1396
.57	.6939	.34	1.7009 , .1630
.56	.7171	.33	1.7837 , .1890
.55	.7419	.32	1.8726 , .2180
.54	.7678	.31	1.9681 , .2503
.53	.7949	.30	2.0709 , .2863
.52	.8232	.29	2.1818 , .3263
.51	.8530	.28	2.3017 , .3711

TABLE VI-B

First - Ionized Atoms

<u>e</u>	<u>Coulomb node</u>	<u>e</u>	<u>Coulomb node</u>
3.0	.1342	1.45	.6447
2.8	.1617	1.40	.6858
2.6	.1950	1.35	.7307
2.4	.2358	1.30	.7798
2.3	.2597	1.25	.8336
2.2	.2864	1.20	.8927
2.1	.3163	1.175	.9246
2.0	.3501	1.150	.9580
1.9	.3883	1.125	.9933
1.8	.4318	1.100	1.0304
1.7	.4818	1.075	1.0696
1.6	.5395	1.050	1.1109
1.5	.6068	1.025	1.1547

The ions Sc II, Y II, and La II following Ca I, Sr I, and Ba I could not be treated because of the lack of sufficient experimental data for the monovalent ions Sc III, Y III, and La III. The various isoelectronic sequences, beginning with the neutral atom on the left, could be extended to arbitrary degrees of ionization, if enough data were available from the corresponding monovalent ions to establish the Coulomb nodes. The same method and the same computer programs are applicable.

Two tables are given for each ion. The first table lists the levels calculated, the experimental excitation energy of these levels in inverse centimeters, the s- and p-wave Coulomb nodes used, and finally the resulting eigenvalues. For the first four ions, He I, Li II, Mg I, and Al II, the eigenvalues for the various configurations calculated without exchange are included for comparison.

The second table for each ion lists the transitions calculated (including some intercombination lines), the transition energy in cm^{-1} , and the wavelength for each line. Then, in order, the following quantities are given:

a)
$$\int_1 \equiv \int P_\ell(r) r P_{\ell-1}(r) dr$$

b)
$$\int_1 \int_2 \equiv \int P_s'(r) P_s(r) dr \int P_\ell(r) r P_{\ell-1}(r) dr$$

c) S, the line strength, defined as

$$S = \sum_{m, m'} |\langle \psi_f^{m'} | e \vec{r} | \psi_i^m \rangle|^2$$

d) $gf = \frac{\Delta E}{3} S$ where f is the oscillator strength, $g = 2J_i + 1$ is the multiplicity of the initial state, and ΔE is the transition

energy in Rydbergs.

Following the tables for each ion, a comparison is made with previous experimental and theoretical results, whenever such exist. An attempt was made to locate all the appropriate papers, those which quote relevant f -values, or those which only compute wave functions. The exceptions to this are papers wherein analytic functions are calculated which cannot be directly compared with nodal boundary condition functions. For example, Hylleraas-type wave functions do not possess one-electron eigenvalues, so they cannot be compared in this way. A list of references follows the results for each ion, with a brief indication of the contents of each paper.

HeI

<u>state</u>	<u>\bar{w}</u>	<u>s-node</u>	<u>ϵ_s</u>	<u>l-node</u>	<u>ϵ_l</u>
1s ² 1S	0	0	-	-	-
1s2p (no X)	-	0	3.480	0	.2521
1s2p 1P	171129	0	3.502	0	.2448
1s2p 3P	169081	0	3.460	0	.2636
1s2s (no X)	-	0	3.460	0	.3068
1s2s 1S	166272	0	3.633	0	.1735
1s2s 3S	159850	0	-	0	-
1s3p (no X)	-	0	3.750	0	.1100
1s3p 1P	186204	0	3.777	0	.1103
1s3p 3P	185559	0	3.744	0	.1136

<u>Transition</u>	<u>$\Delta\bar{\nu}$</u>	<u>λ</u>	<u>\int_1</u>	<u>$\int_1 \int_2$</u>	<u>s</u>	<u>gf</u>
$(1s^2)^1S_0 - (1s2p)^1P_1$	171129	584	.508	.500	.499	.259
$(1s^2)^1S_0 - (1s3p)^1P_1$	186204	537	.249	.245	.120	.0679
$(1s2s)^1S_0 - (1s2p)^1P_1$	4857.4	20589	-4.245	-4.245	18.017	.265

Comparison with Previous Results

The $1s^2$ ground-state function for He I could not be found accurately by the s^2 computer program (described in Appendix B), because the "node" is at the origin. The method of inward integration can give only a lower limit to the eigenvalue in this case, since any eigenvalue greater than or equal to the correct value will result in no node. Therefore the eigenvalue $\epsilon = 1.836$ as calculated by Wilson (Helium reference 5) was used in the program. This differs only slightly from the earlier calculation $\epsilon = 1.835$ of Hartree (1). All excited states could be calculated by the programs, so that only the ground-state was taken from previous work.

The $1s2s$ and $1s2p$ states have been computed without exchange by Wilson, and the eigenvalues compare as follows with the present calculations if exchange is neglected:

$1s2s$		$1s2p$		
ϵ_{1s}	ϵ_{2s}	ϵ_{1s}	ϵ_{2p}	
3.469	.3068	3.496	.2522	Wilson
3.460	.3068	3.480	.2521	Present Calculation

SCF functions with exchange have been computed by Trefftz

et al:

	<u>Trefftz</u>	<u>Present Calculation</u>
1s2p ¹ P	$\epsilon_{1s} = 3.5127$	3.502
	$\epsilon_{2p} = .2450$.2448
1s3p ¹ P	$\epsilon_{1s} = 3.7816$	3.777
	$\epsilon_{3p} = .1095$.1103
1s2p ³ P	$\epsilon_{1s} = 3.4675$	3.460
	$\epsilon_{2p} = .2631$.2636
1s3p ³ P	$\epsilon_{1s} = 3.7683$	3.744
	$\epsilon_{3p} = .1152$.1136

F-Value Comparisons:

<u>Author</u>	<u>$1s^2 1S - 1s2p^1P$ ($\lambda 584$)</u>	<u>$1s^2 1S - 1s3p^1P$ ($\lambda 537$)</u>
Vinti	.349	.0928
Wheeler	.266	-
Hylleraas	.3555	.0722
Korwein	.365	.089
Dalgarno and Lynn	.239	.081
Dalgarno and Stewart	.275	.0746
Trefftz, et al.	.2719	.0720
Salpeter and Zaidi	.2717	.0706
Weiss	.2760	.0730
Present Calculation	.259	.068

<u>Author</u>	<u>$1s2s^1S - 1s2p^1P$</u>
Hylleraas	.3918
Goldberg	.389
Trefftz, et al.	.3578
Weiss	.377
Present Calculation	.265

References for Helium

A great deal of work has been done on helium by analytic variational methods and by Hylleraas-type wave functions (depending explicitly on r_{12}). We refer here (and also for all other atoms) only to SCF calculations and other theoretical or experimental results with which our eigenfunctions, eigenvalues, or transition probabilities can be directly compared.

- 1) Hartree, D.R.
Proc. Camb. Phil. Soc. 24, 111, '27
Computes the ground-state function and one-electron eigenvalue.
- 2) Vinti, J. P.
Phys. Rev. 42, 632, '32
Calculates f -values for single-excited, doubly-excited, and continuum states from screened wave functions.
- 3) Wheeler, J. A.
Phys. Rev. 43, 258, '33
Computes the $1s^2-1s2p$ f -value using variational functions.
- 4) Korwein, H.
Z. Physik 91, 1, '34
Computes $1s^2-1s2p$ and $1s^2-1s3p$ f -values from variational functions.
- 5) Wilson, W. S., and Lindsay, R. B.
Phys. Rev. 47, 681, '35
Computes SCF functions without exchange for the configurations $(1s)^2$, $(1s2s)$, $(1s2p)$, $(2s^2)$, $(2p^2)$, and $(2s2p)$. Wave functions and eigenvalues are given.
- 6) Wilson, W. S.
Phys. Rev. 48, 536, '35
The total atomic energies are computed for the states of reference 5).

- 7) Morse, P. M., Young, L. A., and Haurwitz, E. S.
Phys. Rev. 48, 948, '35
Analytic wave functions. Used by Veselov for f -value calculations (ref. 10).
- 8) Hylleraas, E. A.
Z. Physik 106, 395, '37
Computes oscillator strengths for many helium transitions using previously calculated wave functions.
- 9) Goldberg, L.
Ap. J. 90, 414, '39
Uses simple variational analytic-type wave functions to obtain f -values for the series $2s$ - np and $2p$ - nd .
- 10) Veselov, M. G.
Jour. Ex. and Theo. Phys. (USSR) 19, 959, '49
Computes f -values for the transitions $1s$ - $2p$ and $2s$ - $2p$ using Morse wave functions (from ref. 7).
- 11) Vizbaraitė, Ya. I., Kantserovichyua, A. I., and Yutsis, A. P.
Optika i Spek. 1, 9, 156
Computes the $1s2s$, $1s3s$, $1s4p$ states by SCF with exchange.
- 12) Heron, S., McWhirter, R. W. P., and Rhoderick, E. H.
Nature 234, 565, '56
Measures lifetime of the 3^1P state.
- 13) Dalgarno, A., and Lynn, N.
Proc. Phys. Soc. London A 70, 802, '57
Modifies previously calculated f -values to satisfy the f sum-rule.
- 14) Trefftz, E., Schlüter, A., Dettmar, K.-H., and Jörgens, K.
Z. f. Ap. 44, 1, '58
Calculates eigenvalues and eigenfunctions by an extended Hartree-Fock scheme. Oscillator strengths are given for many transitions.

- 15) Osherovich, A. L., and Savich, I. G.
Optika i Spek. 4, 715, '58
Measures lifetimes of 3^3P and 3^1P states.
- 16) Dalgarno, A., and Stewart, A. L.
Proc. Phys. Soc. London A 76, 49, '60
Gives f -values for $1s^2-1s2p$ and $1s^2-1s3p$ transitions.
- 17) Salpeter, E. E., and Zaidi, M. H.
Phys. Rev. 125, 248, '62
Calculates f -values using many-parameter functions.
- 18) Weiss, A. W.
National Bureau of Standards (private communication).

Li II

<u>state</u>	<u>$\bar{\nu}$</u>	<u>s-node</u>	<u>ϵ_B</u>	<u>l-node</u>	<u>ϵ_l</u>
1s ² 1S	0	0	-	-	-
1s2p (no X)	-	0	7.941	0	1.011
1s2p 1P	501816	0	7.962	0	.980
1s2p 3P	494273	0	7.961	0	1.051
1s2s (No X)	-	0	7.989	0	1.133
1s2s 1S	490079	0	7.550	0	.940
1s2s 3S	476046	0	8.061	0	1.211
1s3p (no X)	-	0	8.503	0	.448
1s3p 1P	561749	0	8.511	0	.439
1s3p 3P	559501	0	-	0	-

transition	$\Delta\bar{\nu}$	λ	\int_1	$\int_1 \int_2$	S	gf
$(1s^2)S_0 - (1s2p)^1P_1$	501816	1993	-	-	-	-
$(1s^2)S_0 - (1s3p)^1P_1$	561749	1780	-	-	-	-
$(1s2s)^1S_0 - (1s2p)^1P_1$	11737	3520	-2.562	-2.559	6.547	.23
$(1s2s)^1S_0 - (1s3p)^1P_1$	71670	1395	1.727	1.725	2.974	.65
$(1s2s)^3S_1 - (1s21)^3P_2^*$	18227	5486	-2.386	-2.386	9.489	.52
$-(1s2p)^3P_1$	18227	5486	-2.386	-2.386	5.69	.31
$-(1s2p)^3P_0$	18227	5486	-2.386	-2.386	1.90	.104

References for Li II

- (1) Veselov, M. G.
J. Expt. Theo. Phys. USSR 19, 959, '49
Calculates f-values for $1s^2\ ^1S - 1s2p\ ^1P$, $1s2s\ ^1S - 1s2p\ ^1P$,
and $1s2s\ ^3S - 1s2p\ ^3P$.

- (2) Yutsis, A. P., Ushpalis, K. K., Kavetskis, V. I., and
Levinson, I. B.
Optika i Spektroskopija 1, 601, '56
SCF calculations with exchange.

State	MJ I			
	\bar{v}	s-node	ϵ_s	ϵ_l
$3s^2$ $1S$	0	.825	.5194	-
$3s3p$ (no X)	-	.830	.6490	.2651
$3s3p$ $1P$	35051	.830	.7056	.2022
$3s3p$ $3P$	21870	.830	.6934	.3683
$3s4s$ (no X)	-	.834	.8507	.1641
$3s4s$ $1S$	43503	.834	.9286	.0946
$3s4s$ $3S$	41197	.833	.8547	.1799
$3s4p$ (no X)	-	.834	.9023	.1127
$3s4p$ $1P$	49347	.834	.9037	.09816
$3s4p$ $3P$	47848	.834	.9052	.1237

Transition	$\Delta\bar{\nu}$	λ	$\int I$	$\int \frac{I \cdot \sqrt{2}}$	s	$\frac{fI}{s}$
$(3s^2)^1S_0 - (3s3p)^1P_1$	35051.4	2852	3.014	2.951	17.42	1.85
$(3s^2)^1S_0 - (3s4p)^1P_1$	49347.6	2026	1.021	1.002	2.010	.30
$(3s4s)^1S_0 - (3s3p)^1P_1^*$	8451.6	11829	-.797	0.797	.635	.016
$(3s4s)^1S_0 - (3s4p)^1P_1$	5843.6	17113	14.42	14.41	207.7	3.68
$(3s4s)^3S_1 - (3s3p)^3P_2^*$	19286.3	5184	-2.705	-2.686	12.025	.70
$- (3s3p)^3P_1$	19327.0	5173	-2.705	-2.686	7.23	.42
$- (3s3p)^3P_0$	19347.0	5167	-2.705	-2.686	2.41	.14
$(3s4s)^3S_1 - (3s4p)^3P_2$	6654.4	15028	8.594	8.594	123.08	2.48
$- (3s4p)^3P_1$	6650.3	15037	8.594	8.594	73.9	1.49
$- (3s4p)^3P_0$	6650.3	15037	8.594	8.594	24.6	.496

Comparison with Previous Results

Eigenvalues:

State	Biermann and Trefftz (ref. 3)	Present Calculation
$3s^2 1S$	$\epsilon_{3s} = .520$	$\epsilon_{3s} = .5194$
$3s3p 1P$	$\epsilon_{3s} = .650$	$\epsilon_{3s} = .7056$
	$\epsilon_{3p} = .2485$	$\epsilon_{3p} = .2022$
$3s3p 3P$	$\epsilon_{3s} = .6969$	$\epsilon_{3s} = .6934$
	$\epsilon_{3p} = .4297$	$\epsilon_{3p} = .3683$

F- Values:

$3s^2 1S_0 - 3s3p 1P_1 \quad \lambda 2852$

Biermann and Trefftz (3)	Trefftz (4)	Ostrovskii et al	Demtröder	Present Calculation
2.21	1.606	1.2 + .3	1.11	1.85
	Trefftz (5)			
	1.674			

$3s4s 3S_1 - 3s3p 3P_0 \quad \lambda 5167$

Kersten and Ornstein	Trefftz (4)	Trefftz (5)	Present Calculation
.164	.128	.134	.14

References for Magnesium

- 1) Prokofiev, W.
Zeit. f. Ph. 50, 701, '28
Extrapolates lifetimes of the transitions $2^1P_1 - 1^1S_0$ and $2^3P_1 - 1^1S_0$ from measurements on the corresponding transitions in Ca, Sr, and Ba.
- 2) Kersten, J. A. H., and Ornstein, L. S.
Physica 8, 1124, '41
Measures relative transition probabilities for a large number of lines. Of interest to us are primarily the transitions $4^3S_1 - 3^3P_{0,1,2}$; $3^1P_1 - 3^1S_0$; and $3^3P_1 - 3^1S_0$.
- 3) Biermann, L. and Trefftz, E.
Zeit. f. Ap. 26, 213, '49
Calculates wave functions for the states $(3s)^2 1S$, $(3s)(3p)^1F$, $(3s)(3p)^3P$, $(3s)(3d)^3D$, and $(3s)(4f)^3F$ from the Hartree-Fock equations, including core polarization. Computes f-values for $\lambda 2852 \ 3^1S - 3^1P$, $\lambda 3832 \ 3^3P - 3^3D$, and $\lambda 14877 \ 3^3D - 4^3F$.
- 4) Trefftz, E.
Zeit. f. Ap. 26, 240, '49
Calculates functions and energies for the states $(3s)(3d)^1D$, $(3s)(4d)^1D$, $(3s, 5d)^1D$, $(3s)(4f)^1F$, $(3s)(4s)^3S$, $(3p)^2 1S$, and $(3p)^2 3P$, using SCF with exchange, and the effects of configuration interaction. That is, mixing is included between the states $(3p)^2 1D$ and $(3s)(nd)^1D$, and between the states $(3p)^2 1S$ and $(3s)^2 1S$. Gives f-values for several transitions, including $3^1S - 3^1P$ and $3^3P - 4^3S$.
- 5) Trefftz, E.
Zeit. f. Ap. 28, 67, '50
Calculations including both core polarization and term mixing. The usually designated $(3s)^2 1S_0$ state is expanded in terms of

the pure configurations $(3s)^2$, $(3s)(4s)$, $(3p)^2$, and $(3p)(4p)$. Similarly, for example, 4^1S is given in terms of the $(3s)^2$, $(3s)(4s)$, $(3p)^2$, and $(3p)(4p)$ configurations; 4^3S in terms of $(3s)(4s)$ and $(3p)(4p)$; 3^1P in terms of $(3s)(3p)$ and $(3p)(3d)$; and 3^3P in terms of $(3s)(3p)$, $(3s)(4p)$, $(3s)(5p)$, and $(3p)(3d)$. Oscillator strengths are quoted for $3^1S - 3^1P$, $3^1P - 4^1S$, and $3^3P - 4^3S$, among others.

- 6) Allen, C. W.
Monthly Notices, Royal Astron. Soc. 117, 622, '57
Measures absolute oscillator strengths and compares with previous experiments and with calculations of Treffitz and Bates-Damgaard.
- 7) Boldt, G.
Zeit. f. Phys. 150, 205, '58
Measurements of the absorption f-value for the intercombination line $\lambda 4571$ $3^1S_0 - 3^3P_1$.
- 8) Ostrovskii, Iu. I., Penkin, N. P., and Shabanova, L. N.
Sov. Phys. Doklady 3, 538, '58
Measurement of the resonance line $\lambda 2852$ $3^1S_0 - 3^1P_1$ by simultaneous measurement of total absorption and dispersion.
- 9) Varsavsky, C. M.
Thesis, Harvard University, 1958
Calculates various line-strengths by the charge-expansion method.
- 10) Brehm, B., Demtröder, W., and Osberghaus, O.
Z. Naturforsch. 16a, 843, '61
Measures the resonance line $\lambda 2852$.
- 11) Demtröder, W.
Z. Physik 166, 42, 162
Measures the resonance line $\lambda 2852$.

A/ II

State	\bar{v}	s-node	ϵ_s	l-node	ϵ_l
$3s^2 \ ^1S$	0	.744	1.3365	-	-
$3s3p \text{ (no X)}$	-	.745	1.424	.745	.906
$3s3p \ ^1P$	59849.7	.744	1.347	.741	.766
$3s3p \ ^3P$	37579.3 (3P_2)	.747	1.549	.750	1.060
$3s4s \text{ (no X)}$	-	.748	1.713	.731	.518
$3s4s \ ^1S$	95348.2	.746	1.494	.729	.482
$3s4s \ ^3S$	91271.2	.751	1.726	.731	.542
$3s4p \text{ (no X)}$	-	.751	1.759	.730	.405
$3s4p \ ^1P$	106918.2	.751	1.733	.730	.384
$3s4p \ ^3P$	105467.7 (3P_2)	.752	1.774	.731	.420

Transition	$\Delta\bar{\nu}$	λ	\int_1	$\int_1 \int_2$	S	gf
$(3s^2)^1S_0 - (3s3p)^1P_1$	59849.7	1671	2.487	2.464	12.15	2.20
$(3s^2)^1S_0 - (3s4p)^1P_1$	106918.2	935	.275	.273	.149	.048
$(3s4s)^1S_0 - (3s3p)^1P_1$	35498.5	2817	-1.403	-1.389	1.931	.208
$(3s4s)^1S_0 - (3s4p)^1P_1$	11570.0	8641	5.982	5.926	35.12	1.23
$(3s4s)^3S_1 - (3s3p)^3P_2$	53691.9	1862	-1.581	-1.576	4.141	.674
- (3s3p) ³ P ₁	53817.4	1858	-1.581	-1.576	2.48	.405
- (3s3p) ³ P ₀	53879.2	1856	-1.581	-1.576	.828	.135
$(3s4s)^3S_1 - (3s3p)^3P_2$	14196.5	7044	5.798	5.798	56.02	2.41
- (3s4p) ³ P ₁	14167.2	7059	5.798	5.798	33.6	1.45
- (3s4p) ³ P ₀	14153.1	7066	5.798	5.798	11.2	.482

Biermann and Harting have computed the ground state of Al II by SCF without exchange, obtaining $\epsilon_{3s} = 1.212$, compared with our result $\epsilon_{3s} = 1.336$.

Reference:

Biermann, L. and Harting, H.

Z. f. Ap. 22, 81, '43

Ca I

State	$\bar{\nu}$	s-node	ϵ_g	l-node	ϵ_l
4s ² 1S	0	1.254	.4093	-	-
4s4p 1P	23652.3	1.256	.5305	1.440	.1795
4s4p 3P	15315.9 (³ P ₂)	1.256	.5315	1.451	.3181
4s5s 1S	33317.3	1.259	.7178	1.247	.0842
4s5s 3S	31539.5	1.258	.6593	1.249	.1547
4s5p 1P	41679.0	1.259	.6915	1.433	.0903
4s5p 3P	36575.1 (³ P ₂)	1.259	.6969	1.435	.1114

Transition	$\Delta\bar{\nu}$	λ	$\int I$	$\int I \int Z$	$\frac{S}{g}$	$\frac{gf}{S}$
$(4s^2)^1S_0 - (4s4p)^1P_1^*$	23652.3	4227	3.832	3.755	28.20	2.02
$(4s^2)^1S_0 - (4s5p)^1P_1$	41679.0	2399	1.235	1.216	2.957	.37
$(4s5s)^1S_0 - (4s4p)^1P_1^*$	9665.0	10344	-.428	-.428	.183	.0054
$(4s5s)^1S_0 - (4s5p)^1P_1$	8631.7	11959	-	-	-	-
$(4s5s)^3S_1 - (4s4p)^3P_2^*$	16223.6	6164	-3.083	-3.054	15.55	.765
$- (4s4p)^3P_1$	16329.4	6124	-3.083	-3.054	9.34	.461
$- (4s4p)^3F_0$	16381.6	6103	-3.083	-3.054	3.11	.154
$(4s5s)^3S_1 - (4s5p)^3P_2$	5035.6	19859	10.022	10.021	167.4	2.56
$- (4s5p)^3F_1$	5015.2	19939	10.022	10.021	100.5	1.53
$- (4s5p)^3F_0$	5008.2	19967	10.022	10.021	33.5	.51
$(4s^2)^1S_0 - (4s4p)^3P_1$	15210.1	6573	3.832	3.755	$1.74 \cdot 10^{-3}$	$8.05 \cdot 10^{-5}$
$(4s5s)^3S_1 - (4s4p)^1P_1$	7887.2	12679	-3.083	-3.054	$5.77 \cdot 10^{-4}$	$1.38 \cdot 10^{-5}$

Comparison with Previous Results

Eigenvalues:

	$4s^2\ ^1S$	$4s4p\ ^1P$	$4s4p\ ^3P$
Hartree and Hartree (reference 5)	$\epsilon_{4s} = .3891$	$\epsilon_{4s} = .5052$ $\epsilon_{4p} = .1720$	$\epsilon_{4s} = .5177$ $\epsilon_{4p} = .3058$
Present calculation	$\epsilon_{4s} = .4093$	$\epsilon_{4s} = .5305$ $\epsilon_{4p} = .1795$	$\epsilon_{4s} = .5315$ $\epsilon_{4p} = .3181$

Resonance Line F-Value ($4\ ^1S_0 - 4\ ^1P_1\ \lambda 4227$)

<u>Author</u>	<u>gf</u>	
Steinhaüser	2.3	
Hartree and Hartree	2.2	
Treffitz	1.46	
Allen	1.6	
Ostrovskii and Penkin	$1.3 \pm .2$	(ref. 11)
Ostrovskii and Penkin	$1.49 \pm .04$	(ref. 13)
Present calculation	2.02	

F-Value ($4s4p\ ^3P_0 - 4s5s\ ^3S_1\ \lambda 6103$)

<u>Author</u>	<u>gf</u>
Olsen, Routly, King	.162
Allen	.085
Bates-Damgaard	.0795
Weinstein	.138
Present calculation	.154

References for Ca I

- 1) Prokofiev, V. K.
Z. Physik 50, 701, '28
measures relative f-values for the resonance lines
- 2) Filppov, A., and Kremenevsky, N.
Physik Z. Sowjetunion 1, 299, '32
measures relative f-values for the resonance lines
- 3) Hartree, D. R., and Hartree, W.
Proc. Roy. Soc. 149, 210, '35
calculates the ground-state wave functions and eigenvalues by SCF without exchange
- 4) Steinhäuser, A.
Z. Physik 95, 669, '35 and 99, 300, '36
measures the lifetime of the resonance line $\lambda 4227$
- 5) Hartree, D. R., and Hartree, W.
Proc. Roy. Soc. 164, 167, '37
calculates the ground and excited states by SCF with exchange, and the transition probability for the resonance line
- 6) Schuttevaer, J. W., De Bont, M. J., and Van Den Broek, Th. H.
Physica 10, 544, '43
measurement of some relative f-values for triplet lines, including $n^3S_1 - 4^3P_{0,1,2}$ where $n = 5, 6, 7$, and the intercombination line $4^3P_1 - 4^1S_0$ $\lambda 6573$.
- 7) Trefftz, E.
Z. f. Ap. 29, 287, '50
calculates the state 4^1S , 4^1P , 4^3P , and 3^3D by SCF with polarization and term mixing. F-values given for the transitions $4^1S - 4^1P$ $\lambda 4227$, and $4^3P - 3^3D$ $\lambda 19700$
- 8) Allen, C. W.
M. N., 117, 622, '57
measures absolute f-values for a number of lines, including

$\lambda 4227$ and $\lambda 6162$. Comparisons are made with other experiments and calculations.

- 9) Weinstein, L. A.
Optika i Spektr. 3, 313, '57
- 10) Olsen, K. H., Routly, P. M., and King, R. B.
Ap. J. 130, 688, '59
measures relative f-values for 107 lines
- 11) Varsavsky, C. M.
Thesis, Harvard University
calculates line-strengths for 4^1S-4^1P and 4^3P-3^3D by the charge expansion method
- 12) Ostrovskii, Yu. I., Penkin, N. P., and Shabanova, L. N.
Soviet Physics - Doklady 3, 538, '59
measures the f-value for the resonance line $\lambda 4227$
- 13) Ostrovskii, Yu. I., and Penkin, N. P.
Optics and Spectroscopy 10, 4, '61
measures relative f-values of 34 lines
- 14) Ostrovskii, Yu. I., and Penkin, N. P.
Optics and Spectroscopy 11, 307, '61
measures the f-value for the resonance line $\lambda 4227$

Zn I

State	$\bar{\nu}$	s-node	ϵ_s	l-node	ϵ_l
4s ² 1S ₀	0	.632	.5980	-	-
4s4p 1P	46745.4	.620	.8692	.642	.2124
4s4p 3P	32890.3 (3P ₂)	.621	.8259	.629	.3805
4s5s 1S	55789.2	.608	1.112	.648	.1025
4s5s 3S	53672.2	.613	1.028	.645	.1938
4s5p 1P	62910.0	.610	1.100	.650	.1007
4s5p 3P	61330.1 (3P ₂)	.610	1.093	.648	.1275

<u>transition</u>	<u>$\Delta\bar{\nu}$</u>	<u>λ</u>	<u>$\int I$</u>	<u>$\int \frac{I}{\lambda^2}$</u>	<u>s</u>	<u>gf</u>
$(4s^2)^1S_0 - (4s4p)^1P_1$	46745.4	2139	2.562	2.500	12.50	1.77
$(4s^2)^1S_0 - (4s5p)^1P_1$	62910.0	1590	.919	.898	1.614	.31
$(4s5s)^1S_0 - (4s4p)^1P_1$	9043.8	11057	-1.278	-1.277	1.631	.045
$(4s5s)^1S_0 - (4s5p)^1P_1$	7120.8	14043	14.02	14.02	196.5	4.24
$(4s5s)^3S_1 - (4s4p)^3P_2^*$	20781.9	4811	-2.733	-2.713	12.265	.77
$- (4s4p)^3P_1$	21170.8	4722	-2.733	-2.713	7.35	.47
$- (4s4p)^3P_0$	21360.9	4680	-2.733	-2.713	2.45	.16
$(4s5s)^3S_1 - (4s5p)^3P_2$	7657.9	13058	7.823	7.823	102.0	2.37
$- (4s5p)^3P_1$	7601.7	13155	7.823	7.823	61.2	1.42
$- (4s5p)^3P_0$	7575.0	13201	7.823	7.823	20.4	.47

Comparison with Previous Results

Eigenvalue: $4s^2 1S_0$ ground state

Hartree et al	$\epsilon_{4s} = .539$	(without exchange)
Present Calculation	$\epsilon_{4s} = .598$	

GF-values:

$4s^2 1S_0 - 4s4p^1P_1$ λ 2139 (resonance line)

Prokofiev	1.2
Filippov	1.2
Billeter	1.17
Present Calculation	1.77

$4s^2 1S_0 - 4s4p^3P_1$ λ 3076

Prokofiev	$1.3 \cdot 10^{-4}$
Filippov	$1.5 \cdot 10^{-4}$
Billeter	$1.6 \cdot 10^{-4}$
Soleillet	$2 \cdot 10^{-4}$
Present Calculation	$2.5 \cdot 10^{-4}$

$4s4p^3P - 4s5s^3S$	Schuttevaer & Smit	Bates-Damgaard	Present Calculation
2 - 1 λ 4811	.813	.603	.77
1 - 1 4722	.468	.346	.47
0 - 1 4680	.1445	.112	.16

References for Zn I

- 1) Prokofiev, V. K.
Z. Physik 50, 701, '28
Measures the resonance lines $\lambda 2139$ and $\lambda 3076$.
- 2) Filippov, A. N.
Phys. Z. Sowjetunion 1, 289, '32
Measures the resonance lines.
- 3) Billeter, W.
Helv. Phys. Acta 7, 505, '34 and 7, 841, '34
Measures the absolute f-value for the line $\lambda 3076$ and quotes an f-value for $\lambda 2139$ using previous relative measurements.
- 4) Soleillet, P.
Compt. Rend. 204, 253, '37
Measures the transition $\lambda 3076$.
- 5) Hartree, W., Hartree, D. R., and Manning, M. F.
Phys. Rev. 59, 299, '41
Calculates the ground-state by SCF without exchange.
- 6) Schuttevaer, J. W., and Smit, J. A.
Physica 10, 502, '43
Measures several relative f-values.
- 7) Penkin, N. P. and Red'ko, T. P.
Optics and Spectroscopy 9, 360, '60
Measures relative f-values.

Ga II

State	$\bar{\nu}$	s-node	ϵ_s	l-node	ϵ_l
$4s^2 \ ^1S_0$	0	.672	1.417	-	-
$4s4p \ ^1P$	70700	.671	1.477	.717	.769
$4s4p \ ^3P$	48750 (3P_2)	.669	1.659	.712	1.066
$4s5s \ ^1S$	106656	.670	1.582	.680	.487
$4s5s \ ^3S$	102943	.667	1.864	.680	.560
$4s5p \ ^1P$	120540	.667	1.881	.723	.380
$4s5p \ ^3P$	118726 (3P_2)	.666	1.921	.722	.421

<u>transition</u>	$\Delta\bar{\nu}$	λ	$\int I$	$\int I \sqrt{Z}$	s	$\frac{gf}{s}$
$(4s^2)^1S_0 - (4s4p)^1P_1$	70700	1414	2.334	2.309	10.66	2.29
$(4s^2)^1S_0 - (4s5p)^1P_1$	120540	830	.387	.382	.292	.107
$(4s5s)^1S_0 - (4s4p)^1P_1$	35956	2781	-1.442	-1.426	2.032	.22
$(4s5s)^1S_0 - (4s5p)^1P_1$	13884	7203	5.893	5.820	33.87	1.43
$(4s5s)^3S_1 - (4s4p)^3P_2$	54193	1845	-1.662	-1.655	4.568	.75
$- (4s4p)^3P_1$	55127	1814	-1.662	-1.655	2.740	.46
$- (4s4p)^3P_0$	55573	1799	-1.662	-1.655	.915	.15
$(4s5s)^3S_1 - (4s5p)^3P_2$	15783	6336	5.559	5.558	51.49	2.46
$- (4s5p)^3P_1$	15573	6421	5.559	5.558	30.8	1.46
$- (4s5p)^3P_0$	15484	6458	5.559	5.558	10.3	.48
$(4s^2)^1S_0 - (4s4p)^3P_1$	47816	2091	2.334	2.309	$6.5 \cdot 10^{-3}$	$9.45 \cdot 10^{-4}$
$(4s5s)^1S_0 - (4s4p)^3P_1$	58840	1700	-1.442	-1.426	$1.24 \cdot 10^{-3}$	$2.2 \cdot 10^{-4}$
$(4s5s)^3S_1 - (4s4p)^1P_1$	32243	3101	-1.662	-1.655	$1.67 \cdot 10^{-3}$	$1.6 \cdot 10^{-4}$

Hartree, Hartree, and Manning have calculated the ground-state functions of Ga II by SCF without exchange. They obtain $\epsilon = 1.28$ for the $4s^2 1S$ state, compared to our $\epsilon = 1.417$.

Reference:

Hartree, W., Hartree, D.R., and Manning, M.F.

Phys. Rev. 59, 299 '41

Sr I

State	$\bar{\nu}$	s-node	ϵ_s	l-node	ϵ_l
5s ² 1S	0	1.426	.379	-	-
5s5p 1P	21698.5	1.426	.490	1.717	.1706
5s5p 3P	14898.6 (³ P ₂)	1.427	.488	1.742	.2940
5s6s 1S	30591.8	1.425	.668	1.425	.0816
5s6s 3S	29038.8	1.425	.608	1.425	.1471
5s6p 1P	34098.4	1.425	.638	1.700	.0869
5s6p 3P	33973.1 (³ P ₂)	1.425	.642	1.700	.1065

transition	$\Delta\bar{\nu}$	λ	$\int I$	$\int I \lambda^2$	s	gf
$(5s^2)^1S_0 - (5s5p)^1P_1^*$	21698.5	4607	4.100	4.018	32.29	2.12
$(5s^2)^1S_0 - (5s6p)^1P_1$	34098.4	2932	1.332	1.313	3.447	.356
$(5s6s)^1S_0 - (5s5p)^1P_1$	8893.3	11244	-.483	-.482	.233	.0063
$(5s6s)^1S_0 - (5s6p)^1P_1$	3506.6	28518	16.19	16.18	261.7	2.78
$(5s6s)^3S_1 - (5s5p)^3P_2^*$	14140.2	7070	-3.363	-3.326	18.442	.79
$- (5s5p)^3P_1$	14534.4	6878	-3.363	-3.326	11.08	.49
$- (5s5p)^3P_0$	14721.3	6791	-3.363	-3.326	3.69	.16
$(5s6s)^3S_1 - (5s6p)^3P_2$	4934.3	2027	10.483	10.482	183.12	2.74
$- (5s6p)^3P_1$	4829.5	2071	10.483	10.482	110.0	1.61
$- (5s6p)^3P_0$	4814.7	2077	10.483	10.482	36.7	.54
$(5s^2)^1S_0 - (5s5p)^3P_1$	14504.4	6893	4.100	4.018	.0307	.00135
$(5s6s)^3S_1 - (5s5p)^1P_1$	7304.3	13623	-3.363	-3.326	.0105	.00024

Comparison with Previous Results

Resonance f-value $5s^2\ ^1S_0 - 5s5p\ ^1P_1$ $\lambda 4607$

Prokofiev	1.2
Ostrovskii, Penkin and Shabanova	$1.5 \pm .2$
Ostrovskii and Penkin	$1.54 \pm .05$
Present Calculation	2.12

Intercombination f-value $5s^2\ ^1S_0 - 5s5p\ ^3P_1$ $\lambda 6893$

Prokofiev	.00071
Present Calculation	.00135

f-value $5s5p\ ^3P - 5s6s\ ^3S$

		Bates- Damgaard	Eberhagen	Present Calculation
2 - 1	$\lambda 7070$.446	1.26	.79
1 - 1	$\lambda 6878$.275	.725	.49

References for Sr I

- 1) Prokofiev, W.
Z. Physik 50, 701 '28
measures resonance lines λ 4607 and λ 6893
- 2) Schuttevaer, J.W., de Bont, M.J., and Van den Bruek, Th. H.
Physica 10, 544, '43
measures intercombination line λ 6893
and mass relative f-values
- 3) Eberhagen, A.
Z. f. Phys. 143, 392 '55
measures many relative f-values
- 4) Ostrovskii, Yu. I., Penkin, N.P., and Shabanova, L.N.
Doklady 3, 538 '58
measure resonance line λ 4607
- 5) Ostrovskii, Yu. I., and Penkin, N.P.
Optics & Spectroscopy 11, 307 '61
measure resonance line λ 4607

Cd I

State	$\bar{\nu}$	s-node	ϵ_g	l-node	ϵ_l
$5s^2 \quad 1S_0$	0	.741	.5505	-	-
$5s5p \quad 1P$	43692.5	.716	.799	.837	.2048
$5s5p \quad 3P$	31827.0 ($3P_2$)	.720	.753	.815	.3621
$5s6s \quad 1S$	53310.2	.702	1.026	.766	.0991
$5s6s \quad 3S$	51484.0	.702	.955	.766	.1840
$5s6p \quad 1P$	59905.6	.702	1.017	.851	.0980
$5s6p \quad 3P$	58635.7 ($3P_2$)	.702	1.012	.848	.1226

transition	$\frac{\Delta\bar{\nu}}{\lambda}$	$\frac{1}{\lambda}$	$\int 1$	$\int 1, \int 2$	$\frac{s}{g}$	$\frac{gf}{s}$
$(5s^2) ^1S_0 - (5s5p) ^1P_1$	43692.5	2288	2.784	2.709	14.69	1.95
$(5s^2) ^1S_0 - (5s6p) ^1P_1$	59905.6	1669	.980	.955	1.824	.33
$(5s6s) ^1S_0 - (5s5p) ^1P_1^*$	9617.7	10397	-1.216	-1.215	1.478	.043
$(5s6s) ^1S_0 - (5s6p) ^1P_1$	6595.4	15162	14.49	14.49	209.9	4.20
$(5s6s) ^3S_1 - (5s5p) ^3P_2^*$	19657.0	5087	-2.870	-2.841	13.456	.80
$- (5s5p) ^3P_1$	20827.9	4801	-2.870	-2.841	8.08	.51
$- (5s5p) ^3P_0$	21370.0	4678	-2.870	-2.841	2.69	.17
$(5s6s) ^3S_1 - (5s6p) ^3P_2$	7151.7	13983	8.157	8.156	110.9	2.40
$- (5s6p) ^3P_1$	6977.6	14332	8.157	8.156	66.6	1.41
$- (5s6p) ^3P_0$	6906.9	14478	8.157	8.156	22.2	.47
$(5s^2) ^1S_0 - (5s5p) ^3P_1$	30656.1	3262	2.784	2.709	.0326	.00305
$(5s6s) ^3S_1 - (5s5p) ^1P_1$	7791.5	12834	-2.870	-2.841	.0179	.00042

Comparison with Previous Results

resonance f-value	$5s^2\ ^1S_0 - 5s5p\ ^1P_1$	$\lambda\ 2288$
Kuhn	1.20 ± .05	
Zemansky	1.19	
Present Calculation	1.95	

intercombination f-value	$5s^2\ ^1S_0 - 5s5p\ ^3P_1$	$\lambda\ 3261$
Kuhn:	$1.90 \cdot 10^{-3}$	
Konig & Ellett	$1.90 \cdot 10^{-3}$	
King & Stockbarger	$2.3 \cdot 10^{-3}$	
Webb & Messenger	$2.2 \cdot 10^{-3}$	
Matland	$2.3 \cdot 10^{-3}$	
Present Calculation	$3.0 \cdot 10^{-3}$	

References for Cd I

- 1) Kuhn, W.
Die Naturwiss. 14, 48 '26
measures the resonance line λ 2288
- 2) Zemansky, M. W.
Z. Physik 72, 587 '31
measures the resonance line
- 3) Filippov, A. N.
Phys. Z. Sowjetunion 1, 289 '32
measures the relative f-values for the resonance lines λ 2288
and λ 3261
- 4) Konig, H. D., and Ellett, A.
Phys. Rev. 39, 576 '32
measure the lifetime of λ 3261
- 5) King, R. E., and Stockbarger, D. C.
Ap. J. 91, 488 '40
measure absolute f-values for λ 3261, λ 3247, and λ 3274
- 6) Webb, H. W., and Messenger, H. A.
Phys. Rev. 66, 77 '44
measure the resonance lines λ 3261 and λ 2288
- 7) Matland, C. G.
Phys. Rev. 91, 436 '53
measures the line λ 3261
- 8) Van Hengstum, J. P. A., and Smit, J. A.
measure λ 3261 5^3P-5^1S , λ 5086 $6^3S_1-5^3P_2$,
 λ 4800 $6^3S_1-5^3P_1$, and λ 4678 $6^3S_1-5^3P_0$
- 9) Penkin, N. P., and Red'ko, J. P.
Optics and Spectroscopy 9, 360 '60
measure relative f-values for $5^3P_J-6^3S_1$, $J=0,1,2$

In II

State	$\bar{\nu}$	s-node	ϵ_s	l-node	ϵ_l
5s ² 1S	0	.802	1.279	-	-
5s5p 1P	63033.8	.803	1.337	.932	.707
5s5p 3P	45827 (³ P ₂)	.795	1.496	.902	.979
5s6s 1S	97025.4	.796	1.391	.823	.454
5s6s 3S	93919.0	.793	1.678	.822	.521
5s6p 1P	109775.4	.793	1.728	1.22	.329
5s6p 3P	108425.5 (³ P ₂)	.793	1.746	1.193	.363

<u>transition</u>	$\Delta\bar{v}$	λ	$\int I$	$\int I \int I$	$\frac{s}{s}$	$\frac{gf}{s}$
$(5s^2)^1S_0 - (5s5p)^1P_1$	63033.8	1586	2.553	2.527	12.77	2.44
$(5s^2)^1S_0 - (5s6p)^1P_1$	109775.4	411	.653	.645	.833	.28
$(5s6s)^1S_0 - (5s5p)^1P_1$	33991.6	2942	-1.472	-1.449	2.100	.216
$(5s6s)^1S_0 - (5s6p)^1P_1$	12750.0	7843	5.844	5.741	32.96	1.27
$(5s6s)^3S_1 - (5s5p)^3P_2$	48092	2079	-1.783	-1.776	5.255	.77
- $(5s5p)^3P_1$	50570	1977	-1.783	-1.776	3.16	.48
- $(5s5p)^3P_0$	51644	1936	-1.783	-1.776	1.05	.16
$(5s6s)^3S_1 - (5s6p)^3P_2$	14506.5	6893	5.462	5.461	49.70	2.19
- $(5s6p)^3P_1$	13918.2	7185	5.462	5.461	29.8	1.26
- $(5s6p)^3P_0$	13738.9	7279	5.462	5.461	9.95	.41
$(5s^2)^1S_0 - (5s5p)^3P_1$	43349	2307	2.553	2.527	.0713	.00938
$(5s6s)^1S_0 - (5s5p)^3P_1$	53676	1863	-1.472	-1.449	.0117	.00191
$(5s6s)^3S_1 - (5s5p)^1P_1$	30885	3238	-1.783	-1.776	.0177	.00164

Ba I

<u>state</u>	<u>$\bar{\nu}$</u>	<u>s-node</u>	<u>ϵ_s</u>	<u>l_{node}</u>	<u>ϵ_l</u>
$6s^2 \ ^1S$	0	1.681	.3426	-	-
$6s6p \ ^1P$	18060.3	1.678	.4373	2.056	.1604
$6s6p \ ^3P$	13514.7 (3P_2)	1.677	.4446	2.076	.2730
$6s7s \ ^1S$	28230.1	1.674	.5924	1.685	.0777
$6s7s \ ^3S$	26160.3	1.674	.547	1.685	.1376
$6s7p \ ^1P$	32547.1	1.673	.5707	2.041	.0830
$6s7p \ ^3P$	30987.3 (3P_2)	1.673	.5756	2.043	.1009

Transition	$\Delta\bar{\nu}$	λ	\int_1	$\int_1 \int_2$	s	gf
$(6s^2)^1S_0 - (6s6p)^1P_1^*$	18060.3	5535	4.514	4.423	39.12	2.14
$(6s^2)^1S_0 - (6s7p)^1P_1^*$	32547.1	3072	1.468	1.447	4.186	.41
$(6s7s)^1S_0 - (6s6p)^1P_1$	10169.8	9833	-.366	-.366	.134	.0041
$(6s7s)^1S_0 - (6s7p)^1P_1$	4317.0	23164	17.52	17.50	306.2	4.01
$(6s7s)^3S_1 - (6s6p)^3P_2^*$	12645.6	7906	-3.612	-3.570	21.24	.81
$- (6s6p)^3P_1$	13523.7	7393	-3.612	-3.570	12.75	.52
$- (6s6p)^3P_0$	13894.3	7195	-3.612	-3.570	4.25	.18
$(6s7s)^3S_1 - (6s7p)^3P_2$	4827.0	20717	11.195	11.193	208.8	3.06
$- (6s7p)^3P_1$	4655.3	21481	11.195	11.193	125.3	1.77
$- (6s7p)^3P_0$	4583.2	21819	11.195	11.193	41.8	.58
$(6s^2)^1S_0 - (6s6p)^3P_1$	12637	7911	4.514	4.423	.328	.0126
$(6s7s)^3S_1 - (6s6p)^1P_1$	8100	12346	-3.612	-3.570	.107	.0026

Comparison with Previous Results

Resonance f-value $6s^2 \ ^1S_0 - 6s6p \ ^1P_1 \ \lambda \ 5535$

Wessel	1.8
Ostrovskii, Penkin and Shabanova	$1.6 \pm .2$
Ostrovskii and Penkin	$1.40 \pm .05$
Present Calculation	2.14

References for Ba I

- 1) Prokofiev, W.
Z. Physik 50, 701 '28
measures relative f-values of the resonance lines λ 5535
& λ 7911
- 2) King, G.W., and Van Vleck, J.H.
Phys. Rev. 56, 464, '39
calculate relative f-values of the resonance lines
- 3) Wessel, G.
Z. Physik 126, 440 '49 and Z. Physik 130, 100 '51
measures absolute f-value of the resonance line λ 5535
- 4) Ostrovskii, Yu. I., Penkin, N.P., and Shabanova, L.N.
Soviet Physics - Doklady 3, 538 '58
measure absolute f-value of the resonance line
- 5) Ostrovskii, Yu. I., and Penkin, N.P.
Optics and Spectroscopy 9, 371 '60
measure relative f-values for 65 lines
- 6) Ostrovskii, Yu. I., and Penkin, N.P.
Optics and Spectroscopy 11, 307 '61
measure absolute f-value of the resonance line

state	$\bar{\nu}$	s-node	e_s	l-node	e_l
$6s^2\ ^1S$	0	.662	.5840	-	-
$6s6p\ ^1P$	54068.8	.616	.9017	.866	.2065
$6s6p\ ^3P$	44043.0	.623	.836	.874	.333
$6s7s\ ^1S$	63928.2	.589	1.132	.704	.1034
$6s7s\ ^3S$	71295.2	.589	1.136	.860	.0981

transition	$\Delta\bar{\nu}$	λ	$\int I$	$\int I \int I$	s	gf
$(6s^2\ ^1S_0 - (6s6p)\ ^1P_1)$	54068.8	1850	2.550	2.469	12.19	2.00
$(6s^2\ ^1S_0 - (6s7p)\ ^1P_1)$	71295.2	1402	.930	.897	1.609	.35
$(6s7s)\ ^1S_0 - (6s6p)\ ^1P_1$	9859.4	10142	-1.680	-1.679	2.818	.084
$(6s7s)\ ^1S_0 - (6s7p)\ ^1P_1$	7367.0	13574	14.30	14.29	204.3	4.56

Comparison with Previous Results

Eigenvalues:

	$6s^2$	$6s6p$	$6s7s$
Hartree and Hartree	.471		
Mishra (no exchange)	-	$\epsilon_{6p} = .2515$	$\epsilon_{7s} = .1548$
Cohen	.5665		
Present Calculation	.584	$\epsilon_{6p} \begin{matrix} 1P .2065 \\ 3P .333 \end{matrix}$	$\epsilon_{7s} \begin{matrix} 1S .1034 \\ 3S .0981 \end{matrix}$

A large number of experiments have been performed on the lines λ 2537, λ 4348, λ 4047, and λ 5461, which are described in the references cited on pp. 158-160. We haven't calculated any of these transitions.

References for Hg I

- 1) Tolman, R. C.
Phys. Rev. 23, 693 '24
measures λ 2537 transition probability
- 2) Wien, W.
Ann. d. Physik 73, 483 '24
measures λ 2537 and λ 4358 transition probabilities
- 3) Webb, H. W., and Messenger, H. A.
Phys. Rev. 33 319 '29
measure the resonance line λ 1850
- 4) Ladenburg, R., and Wolfsohn, G.
Z. Physik 63, 616 '30, and 65, 207 '30
measure transition probabilities for λ 2537, λ 1850, & λ 1190
- 5) Randall, R. H.
Phys. Rev. 35, 1161, '30
measures lifetimes for transitions λ 4047, λ 4358, λ 5461
- 6) Garrett, P. H., and Webb, H. W.
Phys. Rev. 37, 1686, '31
measures the lifetime of λ 2537
- 7) Mitchell, A. C. G.
Phys. Rev. 43, 887 '33
lifetimes for transitions λ 4047, λ 4358, & λ 5461
- 8) Wolfsohn, G.
Z. Physik 83, 234 '33 and 85, 366 '33
f-values for λ 2537, λ 1850, and λ 1338

- 9) Hartree, D.R., and Hartree, W.
Proc. Roy. Soc. London A 149, 210 '35
calculate the ground-state by SCF without exchange
- 10) King, G.W., and Van Vleck, J.H.
Phys. Rev. 56, 464 '39
calculate relative f-values for the resonance lines
- 11) Schouten, J.W., and Smit, J.A.
Physica 10, 661 '43
give absolute transition probabilities for λ 2537, λ 4078,
 λ 5461, λ 4358, and λ 4047
- 12) Lennuier, R., and Cojan, J.L.
Compt. Rend. 231, 1450 '50
measure lifetime of first 3P level for three different Hg
isotopes
- 13) Mishra, B.
Phys. Rev. 77, 153 '50
calculates $6s6p$ state by SCF, and combines with Hartree's
ground-state to get the resonance line f-value
- 14) Brossel, J.
Phys. Rev. 83, 210 '51
measures lifetime of first 3P level for Hg isotopes
- 15) Brossel, J., and Bitter, F.
Phys. Rev. 86, 308 '52
measure lifetime of first 3P level for Hg isotope

- 16) Mishra, B.
Proc. Camb. Phil. Soc. 48, 511 '52
calculates SCF excited states for Hg without exchange:
6s6p, 6s6d, 6s7s, 6s7p, and 6s7d states
- 17) Brannen, E., Hunt, F.R., Adlington, R.H., and Nicholls, R.W.
Nature 175, 810 '55
measure λ 4358 transition probability
- 18) Cohen, S.
Research Memorandum-Rand Corporation '59
relativistic SCF with exchange for the ground-state

Tl II

State	$\bar{\nu}$	s-node	ϵ_s	l-node	ϵ_l
$6s^2\ ^1S$	0	.745	1.335	-	-
$6s6p\ ^1P$	75660	.740	1.459	.975	.697
$6s6p\ ^3P$	81725	.732	1.582	.946	.940
$6s7s\ ^1S$	107996	.738	1.462	.792	.449
$6s7s\ ^3S$	105225	.720	1.784	.789	.529

Transition	$\Delta\bar{\nu}$	λ	\int_1	$\int_1\int_2$	s	gf
$(6s^2\ ^1S_0 - (6s6p)\ ^1P_1)$	75660	1321	2.391	2.360	11.14	2.56
$(6s7s)\ ^1S_0 - (6s6p)\ ^1P_1$	32336	3095	-1.563	-1.538	2.365	.232
$(6s7s)\ ^3S_1 - (6s6p)\ ^3P_2$	43500	2299	-2.025	-2.014	6.758	.891
$- (6s6p)\ ^3P_1$	52832	1892	-2.025	-2.014	4.06	.649
$- (6s6p)\ ^3P_0$	55774	1793	-2.025	-2.014	1.35	.229

- 161 -

There is not enough experimental information from Tl III to determine the Coulomb nodes for the $6s7p$ states of Tl II.

Douglas, Hartree, and Runciman have calculated the ground-state functions of $Tl II$ without exchange. They obtain an eigenvalue $\epsilon = 1.054$ for the $6s$ electrons.

Reference:

Douglas, A. S., Hartree, D. R., and Runciman, W. A.
Proc. Camb. Phil. Soc. 51, 486, '55

C. Comparison with the Coulomb Approximation, and with
Experimental Results of the National Bureau of Standards

Although the Bates-Damgaard method, as discussed in Section IV, is not expected to be justified for divalent atoms, it is useful to systematically compare results. Table VI-C contrasts the absolute values of the radial integrals $\int P_f r P_i dr$ of the Coulomb approximation with those of the nodal boundary condition (NBC) method. The Coulomb values were calculated directly from the tables of Bates and Damgaard (1). For the most part, transitions of the types $s^2 1S - sp^1P$ (lowest), $ss' 1S - sp^1P$ (excited), and $ss' 3S - sp^3P$ (excited), are not in bad disagreement. These transitions include (for example) $5s^2 1S - 5s5p^1P$, $5s6s 1S - 5s6p^1P$, and $5s6s 3S - 5s6p^3P$, all in Sr I. However, transitions $s^2 1S - sp^1P$ (excited), $ss' 1S - sp^1P$ (lowest), and $ss' 3S - sp^3P$ (lowest), often disagree by a factor of four, corresponding to a factor of 16 in the f-value. These latter transitions include, for example, $5s^2 1S - 5s6p^1P$, $5s6s 1S - 5s5p^1P$, and $5s6s 3S - 5s5p^3P$ in Sr I.

The explanation of why one group is in fair agreement, and why the other is not, undoubtedly stems from the amount of cancellation in the radial matrix elements. Cancellation is small for the first group, but larger for the second. This implies that calculations made with transitions of the second group are more sensitive to the detailed shape of the wave functions used.

Table VI-C

Ion	$2^1S - sp^1P$ (lowest)		$2^1S - sp^1P$ (excited)		$ss^1S - sp^1P$ (lowest)	
	B-D	NBC	B-D	NBC	B-D	NBC
He I	.500	.508	.231	.249	5.01	4.245
Li II	.382	--	.173	--	2.57	2.562
Mg I	2.76	3.014	.570	1.021	4.39	.797
Al II	2.305	2.487	.0278	.275	2.00	1.403
Ca I	3.57	3.832	.333	1.235	3.92	.428
Zn I	2.31	2.562	.551	.919	4.08	1.278
Ga II	2.11	2.334	.195	.387	1.913	1.442
Sr I	3.80	4.100	.316	1.332	4.14	.483
Cd I	2.43	2.784	.587	.980	3.96	1.216
In II	2.27	2.553	.251	.653	2.13	1.472
Ba I	4.14	4.514	1.01	1.468	3.35	.366
Hg I	2.08	2.550	.565	.930	3.86	1.680
Tl II	2.08	2.391	.3155	--	2.26	1.563

Ion	ss' 1s - sp ¹ P (excited)		ss' 3s - sp ³ P (lowest)		ss' 3s - sp ³ P (excited)	
	B-D	NBC	B-D	NBC	B-D	NBC
He I	1.595	--	4.37	--	.924	--
Li II	1.051	1.727	2.35	--	.395	--
Mg I	8.79	14.42	1.937	--	7.94	8.594
Al II	5.96	5.982	1.205	1.581	5.50	5.798
Ca I	2.23	--	2.295	5.083	9.25	10.022
Zn I	7.77	14.02	1.462	2.733	8.38	7.823
Ga II	5.63	5.893	1.242	1.662	5.29	5.559
Sr I	10.93	16.19	2.51	3.363	9.60	10.483
Cd I	8.20	14.49	1.915	2.870	7.63	8.157
In II	5.96	5.844	1.39	1.783	5.64	5.462
Ba I	10.08	--	2.80	3.612	9.75	11.195
Hg I	7.55	14.30	2.12	--	6.59	--
Tl II	5.75	--	1.63	--	5.33	--

The National Bureau of Standards has recently published a volume of tables entitled "Experimental Transition Probabilities for Spectral Lines of Seventy Elements" (NBS Monograph 53, 1962). Actually, relative f -values were measured, but the results were normalized by previously measured (or calculated) absolute f -values for several elements. As stated in the Monograph, relative gf -values within the spectrum of a single ion may deviate from correct values by a factor of 1.5. Absolute values may deviate by up to a factor 2.0.

All lines in common with our results are compared in Table VI-D. Some agree well, others not at all. For example, the resonance f -value of Ca I (λ 4227), from at least six previous experiments and calculations, is almost certainly at least 1.45 (see p. 132), which is a factor of five greater than the NBS value 0.28. Therefore f -values from these tables should be used with some caution, unless only fairly rough values are needed.

Table VI-D

<u>element</u>	<u>transition wavelength (Å)</u>	<u>National Bureau</u>	<u>Nodal Boundary Condition</u>
MgI	2852	1.1	1.85
	5167	.48	.14
	5173	1.4	.42
	5184	2.6	.70
CaI	4227	.28	2.02
	2399	.03	.37
	6103	.24	.154
	6124	.68	.46
	6164	1.0	.77
	6573	.00014	.00008
ZnI	2139	1.3	1.77
	4680	1.9	.16
	4722	4.9	.47
	4811	7.2	.77
SrI	2932	.0071	.356
	4607	.27	2.12
	6791	.19	.16
	6878	.53	.49
	7070	.65	.79
	6893	.0014	.0014

Table VI-D (Cont'd)

<u>element</u>	<u>transition wavelength (\AA)</u>	<u>National Bureau</u>	<u>Nodal Boundary Condition</u>
CdI	2288	.92	1.95
	3261	.0014	.0030
	4678	2.6	.17
	4801	4.9	.51
	5086	12.0	.80
InII	2306	.0025	.0094
BaI	3072	.25	.41
	5535	.90	2.14
	7195	.18	.18
	7393	.36	.52
	7906	.67	.81
	7911	.0026	.0126

D. GENERAL CONCLUSIONS

In Section B, eigenvalues and transition probabilities have been compared atom by atom with previous experimental and theoretical results. Some generalizations can be inferred from the detailed comparisons:

1) Eigenvalues

The one-electron eigenvalues can only be compared with previous SCF single-configuration calculations. The nodal boundary condition electrons are almost invariably more tightly bound than those of the usual SCF approach. As explained in Section V-C, this is to be expected. The use of experimental information roughly takes into account polarization of the core electrons, which provides an additional attractive force on the valence particle.

2) Transition Probabilities

Oscillator strengths can be compared with several sources: experimental values, standard SCF calculations (with and without exchange), and SCF calculations including core polarization and configuration interaction. In the special case of HeI, comparisons can be made with highly accurate Hylleraas-type calculations. The latter comparisons are listed on p. 115, showing surprisingly good agreement for most transitions. For this case, the nodal boundary condition method reduces to the usual single-configuration SCF approximation with exchange. The only other SCF f-value calculations which have been made among the atoms we've been treating are for MgI and CaI. For the resonance lines, both have been done

by single-configuration and by configuration-interaction methods. The nodal boundary condition f -values in each case are less than the single-configuration, but greater than the configuration-interaction results. For the resonance line of MgI, these are respectively $gf = 2.21, 1.85, \text{ and } 1.67$. For CaI, they are $gf = 2.2, 2.02, \text{ and } 1.46$. Experimental results favor the lower values. According to Ostrovskii et al, the resonance gf -values are $1.2 \pm .3$ for MgI, and $1.49 \pm .04$ for CaI. Although resonance-line f -values have not been calculated by SCF methods for other atoms of this type, there are experimental measurements for ZnI, SrI, CdI, BaI, and HgI. These are all lower than our results by about the same amount as for MgI and CaI. These comparisons therefore strongly indicate that the calculation of resonance f -values to better than 25% accuracy will require configuration-interaction methods. Also, future ordinary SCF single-configuration results will probably be slightly larger than those quoted here, and in poorer agreement with experiment.

There is another reason for believing that our resonance f -value results are up to 25% too large. The relative f -values between the triplet and singlet resonance lines (as listed in Section V-D) agree very well with experiment. But absolute measurements on f -values of the triplet (intercombination) resonance lines are generally smaller than what is found by applying our theoretical ratios to the calculated singlet f -value.

Further experimental results will be very useful in determining the accuracy of the nodal boundary condition method and

single-configuration SCF calculations in general. It should be emphasized that a measurement of a line in a particular element will help in calibrating similar transitions in all the atoms and ions of this group.

E. ASTROPHYSICAL APPLICATIONS

A number of transitions computed by the nodal boundary condition method are listed in Charlotte Moore's "A Multiplet Table of Astrophysical Interest" (43). Table VI-E collects these transitions along with our f -values. Very likely there are other lines in our tables which are now, or soon will be, of use in astrophysics. Stars of unusual abundances are being increasingly studied, so that transitions which are usually too weak may be observed. Also it may soon be possible to view a wider range of the spectrum. Aside from observations of spectra, transition probabilities are required for detailed investigation of stellar opacities.

It is of interest to compare our f -value results with those used by Goldberg, Müller, and Aller (44) in their recent analysis of element abundances in the sun. Among lines we have computed, there are surprisingly few of use in their investigations. These include two lines in CaI, three in ZnI, and three in SrI. Table VI-F lists these transitions, the f -values quoted by Goldberg, Müller, and Aller, along with the nodal boundary condition results. It is evident from a comparison that the use of our f -values would make no substantial changes in the abundance analysis for these three elements.

Thorough abundance investigations have also been carried out on B stars, for example by Aller and Jugaku (45). Among our f-values, the only ones of interest in that analysis are those for He I. They use values calculated by Trefftz, et al. (Helium reference 14), which are in fair agreement with the few we have done (see p. 115). The most important difficulty for He I was the uncertainty of measured equivalent widths, because the lines were so strong.

Table VI-2

<u>ion</u>	<u>wavelength</u>	<u>transition</u>	<u>ΔJ</u>	<u>gf</u>
LiII	5484	$1s2p^3 P - 1s2s^3 S$	2 - 1	.52
			1 - 1	.31
			0 - 1	.104
MgI	11829	$3s3p^1 P - 3s4s^1 S$	1 - 0	.016
	5184	$3s3p^3 P - 3s4s^3 S$	2 - 1	.70
	5173		1 - 1	.42
	5167		0 - 1	.14
CaI	4227	$4s^2^1 S - 4s4p^1 P$	0 - 1	2.02
	6573	$4s^2^1 S - 4s4p^3 P$	0 - 1	.00008
	10344	$4s4p^1 P - 4s5s^1 S$	1 - 0	.0054
	6164	$4s4p^1 P - 4s5s^3 S$	2 - 1	.765
	6124		1 - 1	.46
	6103		0 - 1	.15
ZnI	4810	$4s4p^3 P - 4s5s^3 S$	2 - 1	.77
	4722		1 - 1	.47
	4680		0 - 1	.16
	3076	$4s^2^1 S - 4s4p^3 P$	0 - 1	.00025
	4293	$4s4p^3 P - 4s5s^1 S$	1 - 0	-
SrI	4607	$5s^2^1 S - 5s5p^1 P$	0 - 1	2.12
	7070	$5s5p^3 P - 5s6s^3 S$	2 - 1	.79

<u>ion</u>	<u>wavelength</u>	<u>transition</u>	<u>ΔJ</u>	<u>gf</u>
	6878		1 - 1	.49
	6791		0 - 1	.16
	6893	$5s^2 1S-5s5p^3P$	0 - 1	.00135
CdI	10397	$5s5p^1P-5s6s^1S$	1 - 0	.043
	5086	$5s5p^3P-5s6s^3S$	2 - 1	.80
	4801		1 - 1	.51
	4678		0 - 1	.17
	3261	$5s^2 1S-5s5p^3P$	0 - 1	.00305
BaI	5535	$6s^2 1S-6s6p^1P$	0 - 1	2.14
	7911	$6s^2 1S-6s6p^3P$	0 - 1	.0126
	3072	$6s^2 1S-6s7p^1P$	0 - 1	.41
	7906	$6s6p^3P-6s7s^3S$	2 - 1	.81
	7393		1 - 1	.52
	7195		0 - 1	.18

Table VI-F

<u>element</u>	<u>transition</u>	<u>gf-values quoted by Goldberg, Müller, Aller</u>	<u>gf present calculation</u>
CaI	$4s^2\ ^1S_0 - 4s4p\ ^3P_1$	$4.46 \cdot 10^{-5}$ (Olsen, Routly, and King)	$8.02 \cdot 10^{-5}$
	$\lambda\ 6573$	$7.95 \cdot 10^{-5}$ (Allen)	
	$4s4p\ ^3P_0 - 4s5s\ ^3S_1$.162 (Olsen, Routly, King)	.154
	$\lambda\ 6103$.085 (Allen)	
		.0795 (Bates-Damgaard)	
		.138 (Weinstein)	
ZnI	$4s4p\ ^3P_2 - 4s5s\ ^3S_1$.813 (Schuttevaer-Smit)	.77
	$\lambda\ 4811$.603 (Bates-Damgaard)	
	$\ ^3P_1 - \ ^3S_1$.468 (Schuttevaer-Smit)	.47
	$\lambda\ 4722$.346 (B-D)	
	$\ ^3P_0 - \ ^3S_1$.145 (Schut. -Smit)	.16
	$\lambda\ 4680$.112 (B-D)	
SrI	$5s^2\ ^1S_0 - 5s5p\ ^1P_1$	1.82 (B-D)	2.12
	$\lambda\ 4607$	2.18 (Eberhagen)	
		2.29 (Unsöld)	
		1.54 (Ostrovskii)	
	$5s5p\ ^3P_2 - 5s6s\ ^3S_1$.446 (B-D)	.79
	$\lambda\ 7070$	1.26 (Eberhagen)	
	$\ ^3P_1 - \ ^3S_1$.275 (B-D)	.49
	$\lambda\ 6878$.725 (Eberhagen)	

F. Extensions and Further Applications of the Nodal Boundary Condition Method

1. Configuration Interaction

The nodal boundary condition method has been used to find approximate SCF wave functions corresponding to a single Slater determinant. That is, we have found a good approximation to those functions which are the best possible functions (from an energy standpoint), having a definite electron configuration. Arbitrarily accurate wave functions can be obtained by relaxing the latter restriction, or in other words by carrying out a configuration interaction calculation. This process was described in section III-A for SCF functions. The question of interest now is whether the nodal boundary condition functions can be used in such an expansion.

There are two general practical approaches toward the goal of finding exact functions. The first is to calculate the best wave functions (SCF) for each configuration. Then the matrix elements $\langle \psi_A | H | \psi_B \rangle$ can be evaluated, and the energy matrix diagonalized. The second approach is to use a complete set of simple analytic variational basis functions, which have larger off-diagonal elements than the SCF functions, but offer the advantage of ease of manipulation and calculation. Both these methods involve a great deal of labor, but it is clear from calculations performed that substantially better wave functions are obtained. Since even single-configuration

SCF functions are not simple to compute anyway, it is logical that one might as well proceed to do the whole problem through, superimposing several configurations.

Unfortunately, the nodal boundary condition method cannot be accurately used for such a complete configuration-interaction calculation. The reason is this: we have found nodal stability to apply usually only for s- and p-wave functions. Therefore only wave functions for configurations involving s and p electrons can be computed with any accuracy. But it is usually the case that configurations involving d electrons mix appreciably with the $(s^2)^1S$, $(sp)^1P$, and $(sp)^3P$ configurations in which we are interested. For example, Trefftz (15) has found that for calcium,

$$\psi(4^1P) = .9480 \psi(4s4p) - .3184 \psi(3d4p)$$

$$\psi(4^3P) = .9967 \psi(4s4p) + .08125 \psi(3d4p).$$

To obtain better wave functions and transition probabilities, the next step would have to be the inclusion of such competing configurations. But the problem in a configuration interaction treatment is our inability to obtain accurate d-wave functions. This trouble affects both of the general methods of obtaining accurate functions. To apply the analytic function approach via the nodal boundary condition method, one can imagine choosing a set of analytic s-functions,

p-functions, d-functions, etc., each of which is constrained to vanish at the appropriate coulomb node position, but which can be varied in other ways. But again, the proper nodes for the d-wave functions and those for higher angular momenta are not known.

We conclude that the nodal boundary condition method may be a good approximation to the full SCF calculation as long as we are satisfied with a single Slater determinant, but cannot be accurately used in the more ambitious program.

2. Additional Electron Configurations

The first obvious extension of the method is to apply it to the configurations p^2 and pp^1 . The Hartree-Fock equations are more complicated, but the same general method can be used. These configurations all involve the excitation of both valence electrons, so are usually less important than those we have calculated.

Perhaps more important would be the extension to atoms with three valence electrons. Ions having an s^2p valence ground-state configuration are very interesting. These include the isoelectronic sequences BI (CII, NIII, ...), AlI (SiII, PIII, ...), and Ga I (GeII, AsIII, ...). The coulomb nodes for some of these ions were computed and listed in section V-B. These calculations assumed that ions of this type had only a single valence electron: i. e., the s^2 subshell was kept

stationary. The coulomb nodes show a good deal of instability for some of the states, which indicates that probably the participation of the s^2 electrons should be accounted for. It would therefore be quite interesting to calculate states with configurations $s^2 p$, $s^2 s'$, and $s^2 d$ to see how much the s^2 subshell is influenced by the position of the outermost electron. The coulomb nodes for these ions would be calculated from experimental term values for the $p^6 s$ (or $d^{10} s$) ion: e.g., Al III, Si IV, The Hartree-Fock equations are not difficult, because of the two identical s -electrons. The extension to doubly-excited states, such as $ss'p$, is more complicated because three functions must be computed.

If energy prevails, work can be done on the important atoms with an $s^2 p^2$ ground state. These include Cl, SiI, GeI, SnI, and PbI. If calculations on $s^2 l$ configurations indicate that the s^2 electrons actually remain quite stable, the four-electron problem reduces essentially to a two-electron problem. However, this simplification is probably not sufficiently valid. In any case, excitations of the inner s -electrons are unimportant, so that the four-electron calculations can be restricted mainly to the configurations $s^2 p^2$ and $s^2 ps'$.

3. Other Applications

There are several other possible applications of nodal boundary condition wave functions. For any situation in which the usual SCF valence wave functions (without configuration interaction)

are adequate, and where also the behavior of the functions at small radii is unimportant, one may use nodal boundary condition functions. For example, in the calculation of quadrupole transition probabilities, one is interested in the matrix element $\langle R_f | r^2 | R_i \rangle$, which certainly depends only on the parts of the radial functions at large radii.

The inelastic scattering cross-section of a fast charged particle by an atom is computed in the Born approximation via the matrix element

$$M = \iint e^{i\vec{K} \cdot \vec{r}_1} \frac{e^2}{r_{12}} \psi_f^*(2) \psi_i(2) d\tau_1 d\tau_2 .$$

Here ψ_f and ψ_i are the final and initial wave functions of the atom, and $\vec{K} = \vec{K}_i - \vec{K}_f$ is the momentum transfer (\vec{K}_i and \vec{K}_f are the initial and final momenta of the scattered particle). This expression reduces to the single integral

$$M = \frac{4\pi e^2}{K^2} \int e^{i\vec{K} \cdot \vec{r}_2} \psi_f^*(2) \psi_i(2) d\tau_2 .$$

If we are interested in collisions involving only small momentum transfer, then in first approximation

$$M = \frac{4\pi e^2}{K^2} i \vec{K} \cdot \int \psi_f^* \vec{r} \psi_i d\tau$$

which is the same dipole moment integral needed for oscillator strengths. Then if only transitions of valence electrons are required, and if we restrict ourselves to small momentum transfer ($ka \ll 1$, where a is the atomic diameter), nodal boundary condition functions can be used.

There are also physical situations where the outer parts of the valence wave functions are distorted, while the inner parts, locked in the deep central potential, remained undisturbed. For example, nodal boundary condition functions might be useful in calculating wave functions for molecules or for electrons in a crystal lattice. In both of these cases, the outer parts of the valence functions are greatly distorted, but if the interaction energy is not too large, the inner coulomb nodes would be the same as for a single atom. Again a problem is the instability of nodes for orbital angular momenta of two (d-wave) or greater, so that calculating SCF functions using the nodal boundary condition would be generally inaccurate unless s- and p-waves formed the only significant contributions to the total wave function.

General References

1. Bates, D. R., and Damgaard, A.
Phil. Trans. R. Soc. London A242, 101, '49
2. Green, L. C., Weber, N. E., and Krawitz, E.
Ap. J. 113, 690, '51
3. Delbrück, M.
Proc. Roy. Soc. London A129, 686, '30
4. Hylleraas, E. A.
Z. Physik 54, 347, '39
See also Bibliography in reference 10.
5. Hartree, D. R., and Hartree, W.
Proc. Roy. Soc. London A164, 167, '38
6. Trefftz, E.
Z. f. Ap. 29, 287, '50
7. Hartree, D. R.
Proc. Camb. Phil. Soc. 24, 89, 111, 426, '28
8. Fock, V.
Z. Physik 62, 795, '30
9. Hartree, D. R.
The Calculation of Atomic Structures (Wiley, 1957)
10. Slater, J. C.
Quantum Theory of Atomic Structure (McGraw-Hill, 1960)
11. Biermann, L.
Z. f. Ap. 22, 157, '43
12. Biermann, L., and Lübeck, K.
Z. f. Ap. 25, 325, '48
13. Biermann, L., and Trefftz, E.
Z. f. Ap. 26, 213, '49

14. Trefftz, E.
Z. f. Ap. 26, 240, '49 and 28, 67, '50
15. Trefftz, E.
Z. f. Ap. 29, 287, '50
16. See footnote p. 36, Vol. II of reference 10.
17. Zener, C.
Phys. Rev. 36, 51, '30
18. Eckhart, C.
Phys. Rev. 36, 878, '30
19. Morse, P. M., Young, L. A., and Haurwitz, E. S.
Phys. Rev. 48, 948, '35
20. Nesbet, R. K., and Watson, R. E.
Phys. Rev. 110, 1073, '58
21. Watson, R. E.
Phys. Rev. 119, 170, '60
22. Boys, S. F.
Proc. Roy. Soc. 217, 235, '53 and refs. listed in this article
23. Boys, S. F.
Revs. Mod. Physics 32, 285, '60
24. Layzer, D.
Ann. Phys. 8, 271, '59
25. Layzer, D., and Bahcall, J.
Ann. Phys. 17, 177, '62
26. Varsarsky, C. M.
Thesis, Harvard University, 1958

27. Koopmans, T. A.
Physica 1, 104, '33
28. Hartree, D. R., and Hartree, W.
Proc. Roy. Soc. London A193, 299, '48
and Proc. Camb. Phil. Soc. 34, 550, '38
29. Hargreaves, J.
Proc. Camb. Phil. Soc. 25, 75, '28
30. Fock, V., and Petrashen, M.
Phys. z. Sowjetunion 8, 547, '35
31. Stephenson, G.
Nature 167, 156, '51
32. Filippov, A.
Zeit. f. Ph. 69, 526, '31
33. Fock, V., and Petrashen, M.
Phys. z. Sowjetunion 6, 368, '34
34. Stephenson, G.
Proc. Phys. Soc. 64A, 458, '51
35. Ostrovskii, Yu. I., and Penkin, N. P.
Optics and Spectroscopy 1, 1, '61
36. Filippov, A., and Prokofiev, W.
Zeit. f. Ph. 56, 458, '29
37. Hartree, D. R., and Hartree, W.
Proc. Roy. Soc. London A164, 167, '38
38. Condon, E. U., and Shortley, G. H.
The Theory of Atomic Spectra (Cambridge University Press,
1951, Cambridge)

39. King, G. W., and Van Vleck, J. H.
Phys. Rev. 56, 464, '39
40. Moore, C.
Atomic Energy Levels
National Bureau of Standards Circular 467 ('49)
41. Rubenstein, P. J.
Phys. Rev. 58, 1007, '40
42. Hartree, D. R., Hartree, W., and Manning, M. F.
Phys. Rev. 60, 857, '41
43. Moore, C.
A Multiplet Table of Astrophysical Interest
National Bureau of Standards
44. Goldberg, L., Müller, E. A., and Aller, L. H.
Ap. J. Supplement, Vol. 5, '60
45. Aller, L. H., and Jugaku, J.
Ap. J. Supplement, Vol. 4, '59

APPENDIX A

NUMERICAL SOLUTION OF THE EQUATIONS

In the course of this work, we have dealt with three different numerical problems. These are:

- A. The radial Schrödinger equation in a Coulomb field.
- B. The Hartree-Fock equation for the $s^2 \ ^1S_0$ state.
- C. The two coupled Hartree-Fock equations for the $sl \ ^1L_J$ and $\ ^3L_J$ states.

Problem B is a special case of problem C, but is much simpler than the general case, since the two electrons are equivalent, and because there is no exchange term.

These equations were solved numerically using a program written for the IBM 7090 computer. Appendix B will describe the programs themselves, but in this Appendix the numerical procedures will be described, as well as the general method of solution.

A. THE SCHRÖDINGER EQUATION IN A COULOMB FIELD

The radial equation to be solved is

$$P''(r) = \left[\epsilon - \frac{2C}{r} + \frac{l(l+1)}{r^2} \right] P(r)$$

where the eigenvalue ϵ is given. We require that the function $P(r)$ have the correct asymptotic form for large radii, but not that it vanish at the origin. Therefore it is appropriate to begin at large radii and integrate inwards.

The numerical procedure is the following. We begin by calculating two "starting values," P_1 and P_2 , from the asymptotic series representation given in Section IV-A, which is the Coulomb function employed by Bates and Damgaard. That is, a large value "R" is chosen for the radius such that $P(R)$ is small. Then $P_1 = P(R)$ and $P_2 = P(R-h)$ where "h" is the spacing Δr used in the numerical calculations. The equation can be integrated inward using the two first-order relations

$$1) \quad hP'(r - \frac{h}{2}) \approx P(r) - P(r-h)$$

and

$$2) \quad hP''(r) \approx P'(r + \frac{h}{2}) - P'(r - \frac{h}{2})$$

along with the Schrödinger equation itself.

It is considerably easier for a computer to solve the differential equation than it is to solve the asymptotic series representation for a large number of radii. The results should be the same within the accuracy of the calculations.

The numerical accuracy of this method was investigated by comparing computed wave functions using hydrogen eigenvalues with the exact hydrogen wave functions. It was found that the accuracy was greater than required, if a spacing $h = 0.05$ or less was used. Results remained constant at least down to $h = 0.01$, so that in the range of spacings used, round-off error was not significant. A comparison of the computed and the exact Coulomb nodes for hydrogen and ionized helium is given in the first table of Section V.

B. THE $s^2 \ 1S_0$ HARTREE-FOCK EQUATION

The equation to be solved is

$$P''(r) = \left[\epsilon - \frac{2C}{r} + \frac{2}{r} \int_0^r dr P^2(r) + 2 \int_r^\infty dr \frac{P^2(r)}{r} \right] P(r)$$

where C is the net atomic charge if both valence electrons are removed. Here again, the eigenvalue ϵ is to be specified at the start. Since $\int P^2(r) dr = 1$, we can write

$$P''(r) = \left[\epsilon - \frac{2(C-1)}{r} - \frac{2}{r} \int_r^\infty dr P^2(r) + 2 \int_r^\infty dr \frac{P^2(r)}{r} \right] P(r)$$

This is a more convenient expression for inward integration. The same basic numerical method used to solve the Coulomb potential Schrödinger equation can be used to solve this equation. Since the last two terms in the brackets are small for large radii (and their sum even smaller), Coulomb starting values are again appropriate. After integrating inwards three or four steps, the terms

$$- \frac{2}{r} \int_r^\infty dr P^2(r) + 2 \int_r^\infty dr \frac{P^2(r)}{r}$$

can be evaluated by Simpson's rule, and included in subsequent calculations of $P''(r)$ from the known $P(r)$ at each step.

There is an important difference between this equation and the Schrödinger equation with Coulomb potential. The Hartree-Fock equation is non-linear, so that if the computed s^2 function $P(r)$ is found to be unnormalized, the correct function is not $P(r)$ divided by the square

root of the normalization integral. The procedure used is to calculate $P(r)$, evaluate $N \equiv \int_0^{\infty} dr P^2(r)$, and define new starting values $P_1^{\text{new}} = P_1^{\text{old}}/\sqrt{N}$ and $P_2^{\text{new}} = P_2^{\text{old}}/\sqrt{N}$ and try again. This procedure is repeated until the computed function is correctly normalized to within 0.05%, which usually requires 6 to 8 iterations.

C. THE $s^2 1L$ AND $3L$ HARTREE-FOCK EQUATIONS

These equations are

$$P_s'' = \left[\epsilon_s - \frac{2C}{r} + \frac{2}{r} \int_0^r dr P_l^2 + 2 \int_r^{\infty} dr \frac{P_l^2}{r} \right] P_s \\ \pm \frac{1}{2l+1} \left[\frac{2}{r^{l+1}} \int_0^r dr r^l P_s P_l + 2r^l \int_r^{\infty} dr \frac{P_s P_l}{r^{l+1}} \right] P_l$$

and

$$P_l'' = \left[\epsilon_l - \frac{2C}{r} + \frac{l(l+1)}{r^2} + \frac{2}{r} \int_0^r dr P_s^2 + 2 \int_r^{\infty} dr \frac{P_s^2}{r} \right] P_l \\ \pm \frac{1}{2l+1} \left[\frac{2}{r^{l+1}} \int_0^r dr r^l P_s P_l + 2r^l \int_r^{\infty} dr \frac{P_s P_l}{r^{l+1}} \right] P_s$$

where the plus and minus signs refer to the singlet and triplet states, respectively, and $l = 0, 1, 2, \dots$. The solution of these equations is by far the most difficult of all the calculations. An almost completely different procedure from the previous methods is necessary.

For these equations, in contrast to the $s^2 1S_0$ Hartree-Fock equation, both outer and inner boundary conditions are specified for each function, so that we can solve for the wave functions and eigenvalues.

The outer boundary condition is the usual requirement that each function approach zero asymptotically for large radii. The inner boundary condition is the node position as found by the method described in Section V.

The equations can be written

$$P_s'' = \text{HART}_s(r) P_s \pm \text{FOCK}_s(r)$$

and

$$P_l'' = \text{HART}_l(r) P_l \pm \text{FOCK}_l(r)$$

where

$$\text{HART}_s(r) = \left[\epsilon_s - \frac{2C}{r} + \frac{2}{r} \int_0^r dr P_l^2 + 2 \int_r^\infty dr \frac{P_l^2}{r} \right]$$

$$\text{HART}_l(r) = \left[\epsilon_l - \frac{2C}{r} + \frac{l(l+1)}{r^2} + \frac{2}{r} \int_0^r dr P_s^2 + 2 \int_r^\infty dr \frac{P_s^2}{r} \right]$$

$$\text{FOCK}_s(r) = \frac{1}{2l+1} \left[\frac{2}{r^{l+1}} \int_0^r dr r^l P_s P_l + 2r^l \int_r^\infty dr \frac{P_s P_l}{r^{l+1}} \right] P_l$$

and

$$\text{FOCK}_l(r) = \frac{1}{2l+1} \left[\frac{2}{r^{l+1}} \int_0^r dr r^l P_s P_l + 2r^l \int_r^\infty dr \frac{P_s P_l}{r^{l+1}} \right] P_s$$

The overall procedure of solution is to first specify trial eigenvalues ϵ_s and ϵ_l , and compute trial Coulomb functions P_s and P_l , corresponding to these eigenvalues. If these eigenvalues and functions are used to evaluate $\text{HART}_l(r)$ and $\text{FOCK}_l(r)$, the equation for P_l'' can be solved, resulting in a new function P_l , and eigenvalue ϵ_l . The new ϵ_l will in general be different from the trial value because the function P_l is forced to satisfy the inner and outer boundary conditions

by varying ϵ_l . Then $HART_s(r)$ and $FOCK_s(r)$ can be found by using the initial trial values for ϵ_s and $P_s(r)$, but the new computed $P_l(r)$. Solving the equation for P_s'' , a new P_s and ϵ_s are obtained. This iterative procedure is continued until the eigenfunctions and eigenvalues (hopefully) converge.

With these equations, it is best to integrate starting from the (given) Coulomb node position, rather than from large radii inward. That is, beginning at the Coulomb node " r_c ", we can first integrate outwards to large radii to see if the function is approaching zero asymptotically. If it does not, the eigenvalue is varied until this outer boundary condition is satisfied. Then we can integrate inward from r_c to small values of r to obtain the remainder of the function. There are several advantages to this procedure over the inward integration used for the one-electron Schrödinger equation and the s^2 configuration Hartree-Fock equation. With the advent of exchange terms, it is no longer true that Coulomb-approximation starting values are adequate at large radii. The entire functions are sensitive to the starting values, so that this difficulty is important. Another advantage of beginning at the Coulomb node is related to the fact that some rather odd behavior can occur at large radii for ss' or sp singlet functions. Sometimes an "anomalous node" can appear at large radii for the most tightly bound s -electron, a fact discovered by Hartree in the calculation of wave functions for Mg I. The wave function appears ordinary for small and medium radii, but instead of gradually approaching zero as the radius is increased, it barely dips under the axis, has a minimum, and then approaches the

axis from below. This behavior is not hard to understand. The singlet equation is written

$$P_s'' = \text{HART}_s(r) P_s + \text{FOCK}_s(r) .$$

At large radii, $\text{HART}_s(r)$ is positive, and also $\text{FOCK}_s(r)$ is positive and quite large, since it contains as a factor the other wave function $P_l(r)$, which is an excited state and therefore is mostly at fairly large radii. So if P_s is slightly negative, P_s'' can still be positive, causing the function to curve up toward the axis. Therefore an extra node can occur at a large radius for the singlet function. This effect cannot occur for triplet functions because of the minus sign in the triplet equation

$$P_s'' = \text{HART}_s(r) P_s - \text{FOCK}_s(r) .$$

If we integrate outwards starting at the Coulomb node r_c , one of the two starting values is already known ($P_1 = 0$), so the slope-to-value ratio in the immediate vicinity of this point is determined. A mistake in the choice of the other starting value will then result in the computed function being unnormalized, which can be corrected in succeeding iterations. For example, if the Coulomb node for the s -function of an sp^1P state is at $r_c = 1.00$, we may begin by setting $P_2 = 0.01$. Then in general the normalization integral $\int P_s^2(r) dr = N \neq 1.0$, so that in the next iteration for P_s , we choose a starting value $P_2 = 0.01/\sqrt{N}$. The equations are non-linear, so that this substitution does not guarantee that the new $P_s(r)$ will be normalized, but the process is found to converge.

Because of the "anomalous node" difficulty, it is more convenient to integrate outwards from small radii, rather than inwards from large radii. Within a particular iteration, a wave function is calculated several times with different eigenvalues until the boundary conditions are satisfied. For slightly different eigenvalues, the main parts of the wave function at intermediate radii vary in a smooth way. But a slightly different eigenvalue can mean the appearance or disappearance of an "anomalous" node at larger radii, which can only be easily handled from outward integration. If one starts at large radii and integrates inward, the whole character of the calculation depends upon whether or not an anomalous node is present. The logic and convergence problems become very difficult.

The method of solving these two coupled equations can now be summarized. From trial eigenvalues and eigenfunctions, the subsidiary functions $HART_{\ell}(r)$ and $FOCK_{\ell}(r)$ are computed. Then, using the equation

$$P_{\ell}'' = HART_{\ell}(r) P_{\ell} \pm FOCK_{\ell}(r),$$

the function P_{ℓ} is evaluated by integrating outwards from the Coulomb node. If the asymptotic boundary condition is not satisfied, the eigenvalue ϵ_{ℓ} within the function $HART_{\ell}(r)$ is varied until the boundary condition is satisfied. This may or may not involve the appearance of an "anomalous node". Using the original P_{g} and ϵ_{g} , and the new computed P_{ℓ} , the equation

$$P_s'' = \text{HART}_s(r) P_s \pm \text{FOCK}_s(r)$$

can be solved for a new P_s . The eigenvalue ϵ_s is varied until the boundary conditions are satisfied. Then a better P_l is computed using the new P_s . This iterative procedure is continued until convergence is obtained. It is necessary that for the final iteration, the initial eigenvalues for that iteration be within 0.05% of those eigenvalues needed to satisfy the boundary conditions. Also the functions as computed must be normalized within 0.1%.

The exact description of how each of these steps is accomplished would be very lengthy. These details can be gleaned from a study of the Fortran program reproduced at the end of Appendix B.

APPENDIX B

THE COMPUTER PROGRAMS

The programs were designed to do almost all of the numerical work required in the calculation of wave functions and transition probabilities. They were written in the Fortran language, suitable for the IBM 7090 computing machine.

Six principal types of calculation can be performed with these programs for atoms or ions with one or two electrons outside closed shells. These include:

- 1) Coulomb-approximation valence functions (with given eigenvalue and angular momentum) for a single valence electron
- 2) Valence ground-state $s^2 \ ^1S_0$ functions (two valence electrons)
- 3) Valence excited-state $sl \ ^1L$ or $\ ^3L$ functions (two valence electrons)
- 4) Oscillator strengths for $l - l'$ transitions (one valence electron)
- 5) Oscillator strengths for $s^2 \ ^1S_0 \rightarrow sp \ ^1P_1$ transitions (two valence electrons)
- 6) Oscillator strengths for $sl \ ^1L \rightarrow sl' \ ^1L'$ transitions or $sl \ ^3L \rightarrow sl' \ ^3L'$ transitions (two valence electrons). In practice, l is limited to 0 or 1.

The principal purpose of this work was to calculate valence wave functions and transition probabilities for atoms and ions with two electrons outside closed shells. In carrying out this project, it was

necessary for two reasons to compute Coulomb-approximation single-electron functions. They were employed in finding Coulomb nodes for two-electron situations, and also as first trial functions for sl -configuration calculations. Since single-electron functions had to be computed anyway, it was deemed useful and convenient to have the option of computing them for their own sake, which accounts for calculation types (1) and (4). These functions should be the same as the results of using the asymptotic series representation of Bates and Damgaard (Section IV-A), and the corresponding transition probabilities should agree with the Bates-Damgaard tables. Results were compared in several cases, substantiating this expectation.

In general, for a particular day's "run", calculations can be performed with one or several of the six basic types of problem. Each calculation requires two or more input data cards. The number of input cards can be reduced if the whole "run" consists only of one-electron function calculations, or if it consists only of s^2 -configuration calculations. These are called the "efficient" one-electron mode, and the "efficient" s^2 mode, in contrast to the "general" mode. These modes were defined by the first data card for the run, which contains -1, +1, or 00 in the first two spaces, depending upon whether one wishes to use the efficient one-electron, efficient s -squared, or general mode. The necessary data-cards for the various kinds of calculation will now be listed.

INPUT DATA CARDS

A. Efficient One-Electron Mode

First card negative (-1)

For each group of six wave functions, one begins with a single card of type (1), followed by six cards of type (2).

(1)	10	10	10	10	10	10		
	E1	E2	E3	E4	E5	E6		
(2)	10	10	10	10	10	1	8	
	ELB	R1	H	N	C	NRAD	ATOM	

The numbers above each argument correspond to the number of spaces available for that argument. The quantities E1, E2, ... on the first card are the eigenvalues (in Rydbergs) for the six functions. For each of the cards (2), ELB is the angular momentum l (e.g. 1.0), R1 is the maximum radius in units of the first Bohr radius a_0 (typically R1 = 10.0, 15.0, 20.0 or 25.0), H is the spacing used (typically 0.05 or 0.025), N is the number of points (must be even), C is the net charge acting on the valence electron (1.0, 2.0, etc.), NRAD is the radial quantum number $n = 1, 2, \dots$, and ATOM is written in letters (e.g. MG II). It is necessary for the quantity N (e.g. 1000) to be written in the very last spaces available to it, and for ATOM to be written in the last 6 of the 8 spaces available to it.

This mode prints out Coulomb nodes only, and cannot print out the computed wave functions. To end the series of calculations, the very last data card for the day's run must have - .1 in the first three spaces.

B. Efficient S-Squared Mode

First card positive (+ 1)

For each group of six s^2 functions, one begins with a single card of type (1), followed by six cards of type (2).

(1)	10	10	10	10	10	10
	E1	E2	E3	E4	E5	E6
(2)	10	10	10	10	10	10
	R1	H	N	C	NRAD	ATOM

The quantities E1, ... are the one-electron eigenvalues (in Rydbergs) used for the six s^2 functions. R1, H, and N are the maximum radius, spacing and number of points. C is the net charge on the ion if one valence electron is removed. NRAD is the radial quantum number, and ATOM is the atomic symbol written in letters.

This mode also prints out Coulomb nodes only, and cannot print out wave functions. The very last data card for a day's run must have - 0.1 in the first three spaces, to end the calculations.

C. The General Mode (for arbitrary calculations)

First card zero (0)

For each individual calculation, two or three data cards are needed. Any number of calculations of any kind can be performed. To end the day's calculations, the final data card must contain - .1 in the first three spaces.

I. One-Electron Function

Two cards are required for each function. These are:

```
(1)      10      10      10      10      3
        EB    0.0    0.0    0.0    PO

(2)      10      10      10      10      10      1      8
        ELB  R1    H    N    C    NRAD  ATOM
```

EB is the eigenvalue, PO is one (1) if the wave function is to be printed out, and zero (0) if not. ELB (e.g. 1.0) is the angular momentum l . R1, H, N, and C are the maximum radius, spacing, number of points, and net charge (acting on the valence electron). NRAD is the radial quantum number $n = 1, 2, \dots$, and ATOM is written in letters (e.g. MG II). The non-decimal number N (e.g. 1000) must be placed in the very last of its available ten spaces. N must not be larger than 1200.

II. S-Squared Function

Two cards are required for each function:

```
(1)      10      10      10      10      3
        0.0    0.0    EA    0.0    PO

(2)      10      10      10      10      1      8
        R1    H    N    C    NRAD  ATOM
```

Here C = 1.0 for neutral atoms, 2.0 for 1st-ionized, etc.

III. S-L Functions

Two cards are required to compute the two functions:

(1)	10	10	10	10	3		
	EB	EBB	0.0	0.0	PO		
(2)	2	2	5	5	5	5	5
	NRADS	NRADL	ELB	R1	H	N	C
	8	3	8	3	3	8	
	SN	NS	PN	NP	MULT	ATOM	

EB and EBB are respectively the s-wave and l-wave trial eigenvalues. NRADS and NRADL are the radial quantum numbers for the s- and l-electrons. ELB = l (e.g. 1.0). SN and PN are the values for the s-wave and l-wave Coulomb nodes, while NS and NP designate which node it is. That is, the lowest-energy s-wave (l-wave) function will have NS = 1 (NP = 1), the next-lowest s-wave (l-wave) function will have NS = 2 (NP = 2), etc. MULT is the multiplicity (= 1 for singlet, = 3 for triplet states).

The quantities NRADS, NRADL, N, NS, NP, and MULT must all be placed in the last columns available to them.

IV. One-Electron F-Value

Two cards are required to compute the two functions and their f-value:

(1)	10	10	10	10	3			
	EB	0.0	EA	0.0	PO			
(2)	2	2	5	5	5	5	5	
	NRADB	NRADA	ELB	ELA	R1	H	N	
	5	3	10	8				
	C	JUMP	FREQ	ATOM				

EB and EA are the eigenvalues of the initial and final functions. NRADB and ELB are the radial quantum number and l -value for the initial function, while NRADA and ELA are the corresponding quantities for the final function. JUMP is a code designating the transition involved (see p. 204), and FREQ is the experimental line frequency in cm^{-1} .

V. $S^2 - SP \quad {}^1S_0 - {}^1P_1$ F-Value

Two cards are required to compute the three functions and the f-value:

(1)	10	10	10	10	3		
	EB	0.0	EA	EAA	PO		
(2)	2	2	5	5	5	5	
	NRADS	NRADP	R1	H	N	C	
	8	3	8	3	10	8	
	SN	NS	PN	NP	FREQ	ATOM	

EB is the eigenvalue for the s^2 configuration, and EA and EAA are the trial eigenvalues for the s- and p-wave functions, respectively. All the other arguments are explained under problem types III and IV.

VI. SL - SL' F-Value

Three cards are required to compute the four functions and the f-value:

(1)	10	10	10	10	3			
	EB	EBB	EA	EAA	PO			
(2)	2	2	2	5	5	8		
	NRADS	NRADLB	NRADLA	ELB	ELA	SNB		
	3	8	3	8	3	8	3	
	NSB	ELNB	NELB	SNA	NSA	ELNA	NELA	
(3)	5	5	5	5	3	3	10	8
	R1	H	N	C	JUMP	MULT	FREQ	ATOM

EB and EBB are the initial state s- and l-wave trial eigenvalues, and EA and EAA are the final state s- and l-wave trial eigenvalues. NRADS, NRADLB, and NRADLA are the radial quantum numbers for the s-wave, initial l-wave, and final l'-wave functions, ELB and ELA are the initial and final angular momenta l and l', SN, ELNB, and ELNA are the Coulomb node positions for the s,

initial l , and final l' states, while NS, NELB, and NELA designate which node is involved (as explained under problem type III). JUMP is the transition code given on p. 204, MULT = 1 or 3 for singlet or triplet functions, and FREQ is the experimental line frequency in cm^{-1} .

The Transition Code JUMP

(A) Single valence-electron ions

<u>transition</u>	<u>JUMP</u>
s-p $^2S_{1/2} - ^2P_{1/2}$	-1
$^2P_{3/2}$	-2
p-d $^2P_{1/2} - ^2D_{3/2}$	-3
$^2P_{3/2} - ^2D_{3/2}$	-4
$^2D_{3/2}$	-5

(B) Two valence-electron ions

<u>transition</u>	<u>JUMP</u>
s ² sp $^1S_0 - ^1P_1$	1
ss' sp $^1S_0 - ^1P_1$	2
$^3S_1 - ^3P_0$	3
3P_1	4
3P_2	5

THE SUBROUTINES

The computer program is reproduced in full (in the FORTRAN language) on pp. 223-239 . It is necessary first to discuss the purpose and contents of each subroutine, supplemented with block diagrams of those requiring a detailed description.

DIRECTOR-MAIN PROGRAM

All calculations begin with the Director. From the first data card for a complete "run," the Director determines what "mode" of computations will be carried out -- whether

- 1) efficient one-electron,
- 2) efficient s-squared, or
- 3) general

as defined on p. 197. If the "general" mode is to be used (which is usually the case), the Director finds from the first data card for each calculation what kind of calculation is to be performed, and transfers to the appropriate Sub-program (one-electron, s-squared, *sl*, one-electron f-value, or two-electron f-value).

ONE-ELECTRON (MAIN PROGRAM)

SUBROUTINE OEMP(EB, PO)

This program reads input data, calls Subroutine ONELEC (which computes a monovalent wave function), and prints out input data and computed nodes, along with the wave function, if desired.

Arguments

EB: eigenvalue

PO: print-out code

S-SQUARED (MAIN PROGRAM)

SUBROUTINE SSMP(EA, PO)

This subroutine is similar to Subroutine OEMP except that it calls Subroutine SSQRD (to compute an s^2 wave function) instead of calling ONELEC.

Arguments

EA: eigenvalue

PO: print-out code

S-L (MAIN PROGRAM)

SUBROUTINE SLMP(EB, EBB, PO)

Calls Subroutine SL (which computes s - and l -functions for 1L or 3L states), but is otherwise similar to the previous subroutine.

Arguments

EB: s -wave trial eigenvalue

EBB: l -wave trial eigenvalue

PO: print-out code

ONE-ELECTRON F-VALUE (MAIN PROGRAM)

SUBROUTINE OEFVMP(EB, EA, PO)

This subroutine reads input data, calls the ONELEC subroutine twice (to compute the initial and final wave functions), uses the OVLP function to calculate the radial integral $\int P_f r P_i dr$ and the FVALUE Subroutine to compute the line-strength and gf-value. Formats, input data, and final results are printed, along with the wave functions, if desired.

Arguments

EB: initial eigenvalue

EA: final eigenvalue

PO: print-out code

TWO-ELECTRON F-VALUE (MAIN PROGRAM)

SUBROUTINE TEFVMP(EB, EBB, EA, EAA, PO)

This Subroutine consists of two parts, one to compute s^2 -sp f-values, and one to compute $sl \rightarrow sl'$ f-values. In each case, input data is read, and formats are printed. For an s^2 -sp f-value, Subroutines SSQRD and SL are called. For an $sl - sl'$ f-value, Subroutine SL is called twice. The overlap integrals $\int P_s P_s dr$ and $\int P_l r P_l dr$ are computed from the OVLP function, and the line strength and gf-value are computed by calling Subroutine FVALUE. Finally, wave functions are printed out, if desired.

Arguments

EB: initial s-wave eigenvalue
EBB: zero (0) for s^2 -sp f-value, initial l -wave eigenvalue for
 $sl-sl'$ f-value
EA: final s-wave eigenvalue
EAA: final l -wave eigenvalue
PO: print-out code

THE ONE-ELECTRON SUBROUTINE

SUBROUTINE ONELEC(E, EL, RI, H, C, N, P, Z)

Computes normalized one-electron functions from the Coulomb-potential Schrödinger equation with given eigenvalue E.

Input arguments

E: eigenvalue
EL: angular momentum l
RI: maximum (starting) radius
H: spacing (Δr)
C: charge (C = 1 for neutral, C = 2 for first ionized, etc.)
N: number of points

Output Arguments

P: wave function
Z: node positions

THE S-SQUARED SUBROUTINE

SUBROUTINE SSQRD(E, R1, H, C, N, P, Z, PO, ETOT)

Computes normalized s^2 functions from the Hartree-Fock equation. The eigenvalue E must be specified. The subroutine also calculates the electrostatic interaction energy

$$F_0 = \int \int \psi^2(1) \frac{2}{r_{12}} \psi^2(2) d\tau_1 d\tau_2$$

and the total energy of the two electrons

$$E_{TOT} = 2E + F_0$$

Input Arguments

E: eigenvalue
 R1: maximum (starting) radius
 H: spacing
 C: charge (C = 1 for neutral,
 C = 2 for 1st ionized, etc.)
 N: number of points

Output Arguments

P: wave function
 Z: node position
 PO: electrostatic integral
 ETOT: $2E + F_0$

THE SL OUT SUBROUTINE

SUBROUTINE SL(E1, E2, EL, H, C, RB, NN, SND, PND, NS, NP,
 MU, PS, PP)

In principle, the method of solution used in this subroutine (see Appendix A) can be used for any 1L or 3L sl -configuration two-electron state. In practice, partly because the nodal boundary condition method becomes invalid for $l \gtrsim 2$, and partly because of convergence

difficulties, the program can be used only for $ss' 1S$ or $3S$ and $sp 1P$ or $3P$ states. Also only states of fairly low excitation energy were actually computed, as listed in Section VI. The program may work correctly for more highly excited states, but convergence problems may be expected to require some alteration in the procedure.

The SL subroutine is quite lengthy and complicated. It begins by using the s and l trial eigenvalues $E1$ and $E2$ to compute trial Coulomb functions via the ONELEC Subroutine. It is necessary to force the trial s -wave function to approach zero at the given Coulomb s -node, so that it looks roughly like the final result.

At this point, the first iteration begins. Subroutines MARS and VENUS are called to help in the tabulation of the $HART'_l$ and $FOCK_l$ functions for the equation

$$P''_l(r) = [\epsilon + HART'_l(r)] P_l(r) \pm FOCK_l(r) .$$

Subroutine BEGIN is called to provide starting values for the calculation. The equation is then integrated outward numerically. At each new point, it is determined whether or not one of the following "events" has taken place:

- 0) function "blows up" ($P(r) > 10.0$)
- 1) inflection point
- 2) maximum or minimum
- 3) node
- 4) end of calculation ($r = r_{max}$)
- 5) function "blows down" ($P(r) < -1.0$)

If none of these six events have occurred, the integration is continued.

If one of them has taken place, the program is routed to Subroutine EVENT, which analyzes what is going on. If the function is not behaving properly, EVENT chooses a new eigenvalue which should improve the situation. For example, if the function (while being integrated outward from the Coulomb node) has passed through an inflection point, maximum, inflection point and minimum, the function will blow up instead of approaching the axis asymptotically. EVENT lowers the eigenvalue and directs the SL program to start over again with this new eigenvalue. The process is continued until the function passes through the correct sequence of events: a) inflection point, b) maximum, c) inflection point, and d) end. The correct eigenvalue for the iteration has then been found.

As explained in Appendix A, sometimes an extra node is required at large radii for the inner s-function for singlet states.

The program determines whether such a node is necessary by finding the difference in energy between an eigenvalue which causes the function to reach a minimum (above the axis) and then blow up, and an eigenvalue which causes the function to cross the axis and then blow "down." If this energy difference is small (less than 0.05%), and if the radius at which the second function has crossed the axis is not too large ($r < r_{\max}/2$), then an extra node is required. The functions obtained for various eigenvalues in such a case are represented in figure B-1. Subroutine EXND is employed to guide the program in case such an extra node is required.

When the correct eigenvalue has been obtained, the function

is completed by integrating inward from the Coulomb node. The function is finally normalized using function SIMP to compute the integral.

The first s-wave calculation is then begun, using the same basic procedure. The iterations are continued until both functions converge, meaning then they maintain constant energies and are correctly normalized within limits given in Appendix A. All major steps in the calculations are printed out as completed.

Input Arguments

E1, E2: trial s- and l-wave eigenvalues

EL: l

H: spacing (Δr)

C: charge

RB: maximum radius

NN: number of points

SND, PND: s- and p-Coulomb nodes

NS, NP: number of nodes

MU: multiplicity (1 or 3)

Output Arguments

PS, PP: radial wave functions

Diagram for Subroutine SL

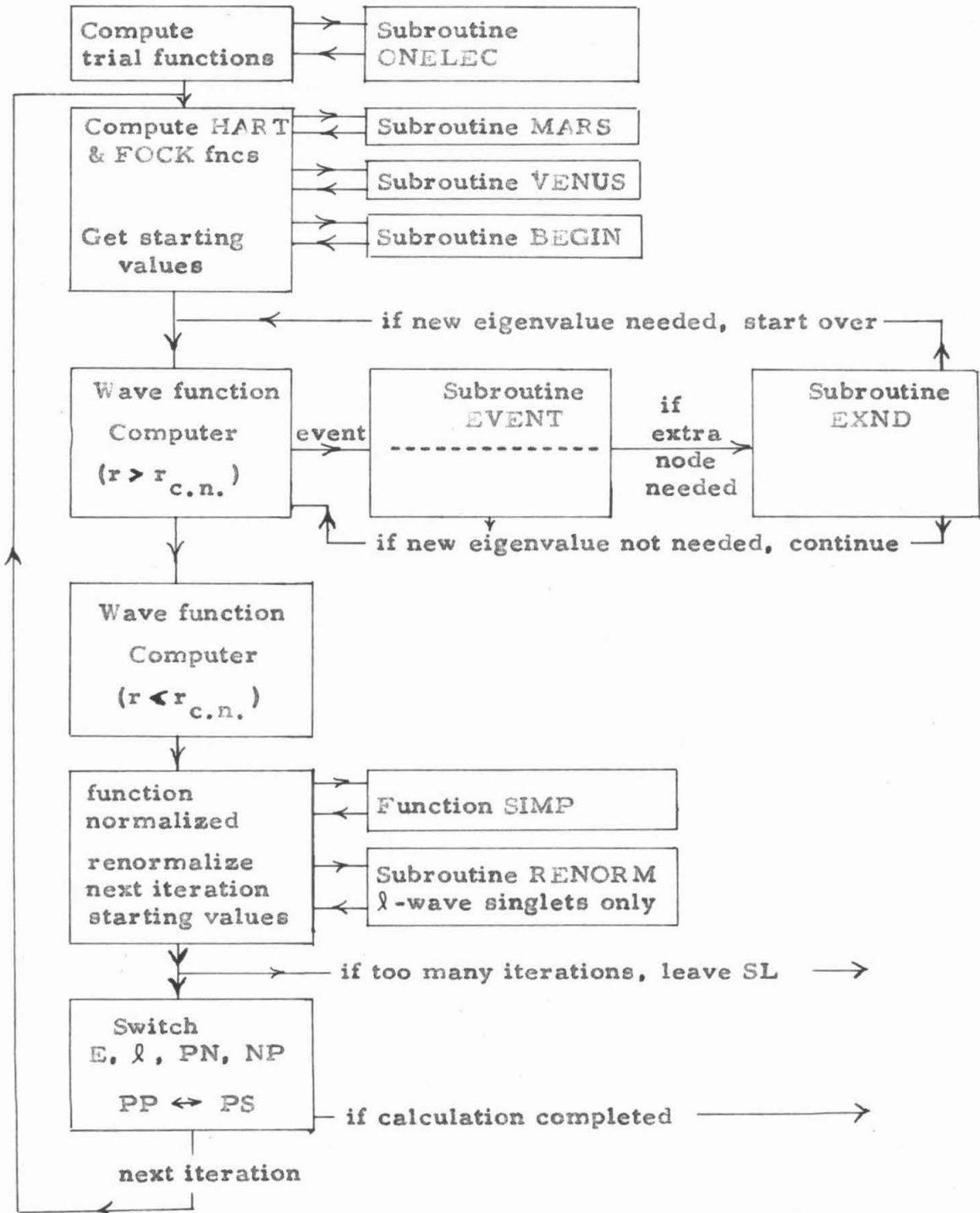
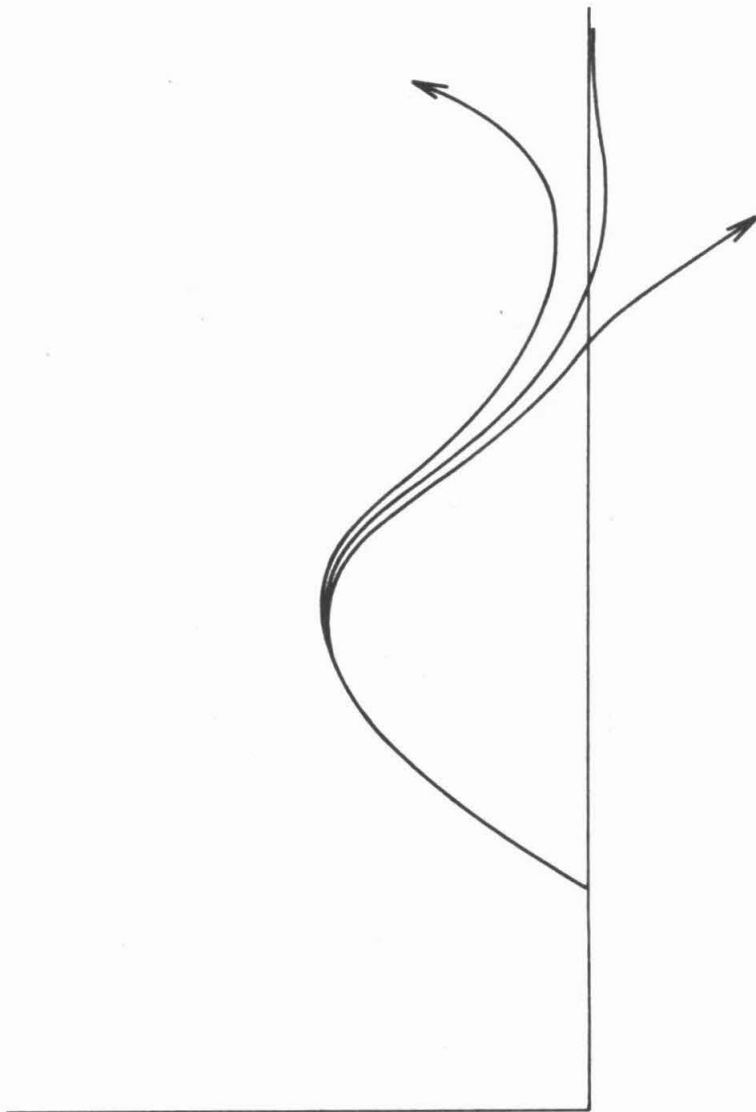


Figure B-1

Schematic diagram illustrating the appearance of an extra node at large radii for s-wave singlet functions.



THE MARS SUBROUTINE

SUBROUTINE MARS (PS, PP, R1, EL, H, N, G, RHO)

This subroutine calculates the function

$$G(r) = \frac{2}{2l+1} \left[\frac{1}{r^{l+1}} \int_r^{\infty} dr r^l P_s P_l - r^l \int_r^{\infty} dr \frac{P_s P_l}{r^{l+1}} \right]$$

and also the quantity

$$\rho = \int_0^{\infty} dr r^l P_s P_l.$$

The SL Subroutine uses $G(r)$ and ρ in the exchange term of the Hartree-Fock equation. The integrals are evaluated by Simpson's rule. The upper limits are actually $R1$, where both of the wave functions P_s and P_l are supposed to be small.

Arguments

PS, PP: radial wave functions
R1: maximum radius
EL: l
H: spacing Δr
N: number of points
G: output function $G(r)$
RHO: output ρ integral

THE VENUS SUBROUTINE

SUBROUTINE VENUS (P, R1, H, N, F)

Calculates the function

$$F(r) = \frac{2}{r} \int_r^{\infty} dr P^2(r) - 2 \int_r^{\infty} dr \frac{P^2(r)}{r}$$

which is needed in the SL Subroutine. The integrals are evaluated within the subroutine, and the upper limits are actually the maximum radius R1.

Arguments

P: input wave function P(r)
R1: maximum radius
H: spacing Δr
N: number of points
F: output function F(r)

THE F-VALUE SUBROUTINE

SUBROUTINE FVALUE (OVLP, JUMP, FREQ, STR, GF)

This subroutine computes the line strength and gf-value for a transition. Input data needed includes the radial matrix element, a code (JUMP) defining the transition (see p.), and the experimental line frequency.

Arguments

OVLP the total radial matrix element
JUMP the transition code
FREQ line frequency in cm⁻¹

STR line strength (output)

GF gf-value (output)

THE OVERLAP FUNCTION

FUNCTION OVL (H, PA, PB, R1, N, Q)

Given two radial functions PA(r) and PB(r), along with the spacing $H = \Delta r$, number of points N, and maximum radius R1, this function can calculate either $\int PA \cdot PB \, dr$ or $\int PA \cdot PB \, r \, dr$.

Arguments

H spacing

PA, PB wave functions

R1 maximum radius

N number of points

Q = 0 for $\int PA \cdot PB \, dr$; = 1 for $\int PA \cdot PB \, r \, dr$

SIMPSON'S RULE FUNCTION

FUNCTION SIMP (H, N, B)

Computes the integral of a function B(r), given the spacing H and the number of points N. The wave function calculations use an even number of points, so N must be even. Since Simpson's rule requires an odd number of points, the last function value B(N) is dropped in computing the integral, so that

$$\text{SIMP} = \frac{H}{3} (B(1) + 4B(2) + 2B(3) + \dots + 4B(N-2) + B(N-1)).$$

The neglect of the last point is not important for all calculations made with these programs.

Arguments

H: spacing
N: number of points (even)
B: function B(r)

THE FACTORIAL FUNCTION

FUNCTION FACTO(X)

Computes $x!$ for $0 \leq x \leq 1$ to within $\frac{1}{2}$ per cent accuracy.

THE STARTING VALUE SUBROUTINE

SUBROUTINE START (E, EL, R1, H, C, P1, P2)

Is used to find starting values for solution of the one-electron Schrödinger equation in a Coulomb field and of the $s^2 \ ^1S_0$ Hartree-Fock equation. This is done by solving the asymptotic series representation of the Coulomb function (using only the first three terms) for two (large) radii R1 and R1-H, where R1 is the maximum radius, and H is the spacing Δr . The representation is written in general form in Section IV-A.

Arguments

E: eigenvalue
EL: angular momentum l
R1: maximum radius
H spacing
C charge
P1, P2 computed $P(R1)$, $P(R1-H)$

THE EVENT SUBROUTINE

SUBROUTINE EVENT (NE, KIND, P, R, EIN, IN, EDB, EUB, NIT,
NEA, EOUT, IT, EDA, EUA, ND)

This subroutine is used by the SL subroutine to keep track of the progress of a function as it is being integrated outward. If the asymptotic boundary condition is not satisfied, the subroutine chooses a new eigenvalue. For example, if the function "blows up" (instead of approaching zero for large radii), a smaller eigenvalue is chosen. However, if the function crosses the axis, a larger eigenvalue is required. As mentioned in the description of the SL Subroutine, several "events" are possible, labeled by code numbers 0 to 5:

<u>Event</u>	<u>KIND (code)</u>
"blow-up"	0
inflection point	1
maximum or minimum	2
node	3
end of calculation	4
"blow-down"	5

Another code (NE) refers to the events in order. For example, starting from the Coulomb node and integrating outward, a function might go through the following sequence of events:

- (a) inflection point (NE = 1, KIND = 1)
- (b) maximum (NE = 2, KIND = 2)
- (c) inflection point (NE = 3, KIND = 1)
- (d) minimum (NE = 4, KIND = 2)

This function will blow up, so the EVENT Subroutine lowers the eigenvalue to recompute the function. The results of each choice of eigenvalues are printed out.

Input Arguments

Output Arguments

NE	event number	NEA	new event number
KIND	kind of event	EOUT	next eigenvalue
P	function	IT	new number of tries
R	radius	EDA	= EIN if EIN caused "blow-down". Otherwise, EDA = EDB.
EIN	eigenvalue used	EUA	= EIN if EIN caused "blow-up". Otherwise, EUA = EUB.
IN	number of tries	ND	code with potential for ending calculation
EDB	most recent eigenvalue causing "blow-down"		
EUB	most recent eigenvalue causing "blow-up"		
NIT	iteration number		

THE EXTRA NODE SUBROUTINE

SUBROUTINE EXND (NE, KIND, R, EIN, IN, EUB, EDB, NEA, EOUT, IT, EUA, EDA, ND)

This subroutine is quite similar to subroutine EVENT, but is only called in when an extra node is required in the s-wave function for $sl^1 L$ states. It keeps track of what events have occurred in integrating a function outward (inflection points, nodes, maxima, etc.) and chooses eigenvalues to satisfy the boundary condition, including an extra large-radius node.

Arguments

All defined under the EVENT Subroutine.

THE BEGINNING VALUE SUBROUTINE

SUBROUTINE BEGIN (PN, NP, EL, MULT, R1, H, S, RL, RM, PL,
PM, L)

This subroutine chooses the starting values to be used for each iteration of the SL Subroutine. These starting values correspond to the function values on either side of the specified Coulomb node position. For example, if the Coulomb node is at $r = .833$, and the mesh spacing used in the calculation is $\Delta r = .05$, Subroutine BEGIN provides function values PL and PM at $r = RL = .80$ and at $r = RM = .85$ such that a straight line between them crosses the axis at $r = .833$. The slope of this line depends on the type of function to be computed, and is chosen by the subroutine to try to make the resulting function normalized. After the first iteration, the starting values P' are found by $P' = P / \sqrt{N}$, where P is the starting value used in the previous iteration, and N is the normalization integral found in the previous iteration.

<u>Input Arguments</u>		<u>Output Arguments</u>	
PN	Coulomb node	RL	radius of inner starting value
NP	number of nodes		
EL	angular momentum l	RM	radius of outer starting value
MULT	multiplicity (1 or 3)	PL	starting value at RL
R1	maximum radius	PM	starting value at RM
H	spacing Δr	L	number of mesh points between PN and R1.
S	previous normalization integral		

THE RENORMALIZATION SUBROUTINES (NOS. 1 AND 2)

SUBROUTINE RENORM (S1, S2, S3, DENOM)

Two subroutines called RENORM were used in the course of these calculations. Their purpose is to speed convergence of the $ss' {}^1S_0$ functions. The majority of these functions converge using no. 1, but some require no. 2. In practice, RENORM no. 2 was compiled only if convergence was not achieved with no. 1.

The iterative calculations for these $ss' {}^1S_0$ functions are found to be overdamped, so convergence is slow. A fairly effective way to overcome this difficulty is to choose proper, or "renormalized" starting values. The usual procedure is to choose a starting value by the prescription $P' = P / \sqrt{N}$, where P is the starting value used in the previous iteration, and N is the normalization integral obtained in the previous iteration. For $ss' {}^1S$ states, this method does not sufficiently improve the normalization for the s' function, so instead, the formulae $P'_{s'} = P_{s'} / \sqrt{1.7N}$ or $P'_{s'} = P_{s'} / \sqrt{.5N}$ are used in RENORM no. 1, depending on whether the normalization integrals tend to be consistently too large or consistently too small. The Renormalization Subroutine decides which denominator is needed, and supplies it to the SL Subroutine. RENORM no. 2 uses different dividing factors, which depend on how fast the function is approaching the correct normalization.

Arguments

S1, S2, S3	three successive normalization integrals for s' functions
DENOM	denominator chosen

```
C DIRECTOR MAIN PROGRAM
100 READ INPUT TAPE 5, 101, IN
101 FORMAT(I2)
   IF(IN) 102, 1, 105
102 READ INPUT TAPE 5, 103, E1, E2, E3, E4, E5, E6
103 FORMAT(6F10.0)
   IF(E1) 11, 11, 104
104 CALL OEMP(E1, .0)
   CALL OEMP(E2, .0)
   CALL OEMP(E3, .0)
   CALL OEMP(E4, .0)
   CALL OEMP(E5, .0)
   CALL OEMP(E6, .0)
   GO TO 102
105 READ INPUT TAPE 5, 106, F1, F2, E3, F4, E5, E6
106 FORMAT(6F10.0)
   IF(E1) 11, 11, 107
107 CALL SSMP(E1, .0)
   CALL SSMP(E2, .0)
   CALL SSMP(E3, .0)
   CALL SSMP(E4, .0)
   CALL SSMP(E5, .0)
   CALL SSMP(E6, .0)
   GO TO 105
  1 READ INPUT TAPE 5, 2, EB, EBB, EA, EAA, PO
  2 FORMAT(4F10.0, F3.1)
   IF (EA) 11, 3, 6
  3 IF (EBB) 11, 4, 5
  4 CALL OEMP(EB, PO)
   GO TO 1
  5 CALL SLMP(EB, EBB, PO)
   GO TO 1
  6 IF (EAA) 11, 7, 10
  7 IF (EB) 11, 8, 9
  8 CALL SSMP(EA, PO)
   GO TO 1
  9 CALL OEFVMP(EB, EA, PO)
   GO TO 1
 10 CALL TEFVMP(EB, EBB, EA, EAA, PO)
   GO TO 1
 11 CALL EXIT
C TO END RUN, MAKE ANY ENERGY NEGATIVE
  END
```

```
C S SQUARED MAIN PROGRAM
SUBROUTINE SSMP(EA, PO)
  DIMENSION P(1200), Z(5)
300 READ INPUT TAPE 5, 301, R1, H, N, C, NRAD, ATGM
301 FORMAT(2F10.0, I10, F10.0, I1, A8)
   CALL SSQRD(EA, R1, H, C, N, P, Z, FO, ETCT)
   IF(PO) 304, 308, 304
304 WRITE OUTPUT TAPE 6, 305
3050 FORMAT(75H RADIUS FUNCTION RADIUS
  1 FUNCTION )
   R = R1
   M = N-1
   DO 307 I = 1, M, 2
   C = R -H
   Y1 = P(I)
   Y2 = P(I + 1)
   WRITE OUTPUT TAPE 6, 306, R, Y1, C, Y2
306 FURMAT(4E20.P)
307 R = R-(2.0*H)
308 RETURN
  END
```

```
C ONE ELECTRON MAIN PROGRAM
SUBROUTINE OEMP(EB, PO)
DIMENSION P(1200), Z(5)
200 READ INPUT TAPE 5, 201, ELH, R1, H, N, C, NRAD, ATOM
201 FORMAT(3F10.0, 110, F10.0, 11, A8)
CALL ONELEC (EB, ELB, R1, H, C, N, P, Z)
WRITE OUTPUT TAPE 6, 202
202 FORMAT (22H ONE ELECTRON FUNCTION/)
Z1 = Z(1)
Z2 = Z(2)
Z3 = Z(3)
Z4 = Z(4)
Z5 = Z(5)
WRITE OUTPUT TAPE 6, 203, ATOM, NRAD, ELB, EB, R1, H, N, C
2030FORMAT(A8, 6H N = 11, 6H L = F3.1, 11H ENERGY = F10.8,
113H RYD R1 = F5.1, 6H H = F5.3, 6H N = 15, 6H C = F5.3//)
WRITE OUTPUT TAPE 6, 209, Z1, Z2, Z3, Z4, Z5
209 FORMAT(10H NODES AT F10.6, 4F10.6//)
IF(PC) 204, 208, 204
204 WRITE OUTPUT TAPE 6, 205
2050FORMAT(75H RADIUS FUNCTION RADIUS
1 FUNCTION )
R = R1
M = N-1
DO 207 I = 1, M, 2
Q = R-H
Y1 = P(I)
Y2 = P(I+1)
WRITE OUTPUT TAPE 6, 206, R, Y1, Q, Y2
206 FORMAT(4E20.8)
207 R = R - ( 2.0*H)
208 RETURN
```

```
C S L MAIN PROGRAM
SUBROUTINE SLMP(EB, EBB, PO)
DIMENSION PS(1200), PP(1200)
4000READ INPUT TAPE 5, 401, NRADS, NRADL, ELB, R1, H, N, C,
ISN, NS, PN, NP, MULT, ATOM
401 FORMAT(2I2, 3F5.0, 15, F5.0, F8.0, 13, F8.0, 13, 13, A8)
WRITE OUTPUT TAPE 6, 403, ATOM, NRADS, NRADL, ELB, NS, SN, NP, PN
4030FORMAT(13H SL FUNCTIONS//A8, 7H NS = 11, 7H NL = 11,
16H L = F3.1, 9H NUMBER 11, 11H S NODE AT F15.8, 9H NUMBER 11,
211H L NODE AT F15.8 //)
WRITE OUTPUT TAPE 6, 409, R1, H, N, C
409 FORMAT(6H R1 = F5.2, 6H H = F5.3, 6H N = 15, 6H C = F5.3//)
CALL SL(EB, EBB, ELB, H, C, R1, N, SN, PN, NS, NP, MULT, PS, PP)
IF(PC) 404, 408, 404
404 WRITE OUTPUT TAPE 6, 405
405 FORMAT(55H RADIUS S FUNCTION P FUNCTION)
R = R1
DO 407 I = 1, N
Q = PS(I)
Y = PP(I)
WRITE OUTPUT TAPE 6, 406, R, Q, Y
406 FORMAT(3F18.8)
407 R = R-H
408 RETURN
END
```

C

```
                TWO ELECTRON F-VALUE
SUBROUTINE TEFVMP(EB, EBR, EA, EAA, PC)
    DIMENSION PA(1200), PB(1200), PC(1200), Z(5), PD(1200)
    WRITE OUTPUT TAPE 6, 599
599  FORMAT(1H1)
600  IF(EBB) 700, 601, 700
601  READ INPUT TAPE 5, 602, NRADS, NRADP, R1, H, N, C, SN, NS,
    1PN, NP, FREQ, ATOM
602  FORMAT(2I2, 2F5.0, 15, F5.0, F8.0, 13, F8.0, 13, F10.0, A8)
    WRITE OUTPUT TAPE 6, 605
605  FORMAT(36H S-SQUARED TO SP OSCILLATOR STRENGTH //)
    OWRITE OUTPUT TAPE 6, 606, ATOM, NRADS, NRADS, NRACP, R1, H, N, C,
    1NS, SN, NP, PN, FREQ
606  OFORMAT(18, 12, 13HS-SQUARED TO 12, 3HS 12,
    122HP TRANSITION R1 = F5.2, 5H H = F5.3, 6H N = 15,
    26H C = F5.3//, 9H THE NO. 12, 14H S-NODE IS AT F7.4,
    39H THE NO. 12, 14H P-NODE IS AT F7.4, 18H THE FREQUENCY IS F10.0//)
    CALL SSQORD(EB, R1, H, C, N, PA, Z, FO, ETOT)
    Z1 = Z(1)
    Z2 = Z(2)
    Z3 = Z(3)
    Z4 = Z(4)
    Z5 = Z(5)
    WRITE OUTPUT TAPE 6, 607, EB, Z1, Z2, Z3, Z4, Z5, FO, ETOT
607  OFORMAT(20H S-SQUARED ENERGY = F9.6, 16H WITH NODES AT F7.4,
    14F7.4, 6H FO = F7.4, 15H TOTAL ENERGY = F7.4//)
    CALL SL(EA, EAA, 1.0, H, C, R1, N, SN, PN, NS, NP, 1, PB, PC)
    O1 = OVLP(H, PA, PC, R1, N, 1.0)
    O = O1*OVLP(H, PA, PB, R1, N, 0.0)
    CALL FVALUE(O, 1, FREQ, STR, GF)
    WRITE OUTPUT TAPE 6, 609, O1, O, STR, GF
609  OFORMAT(18H RADIAL INTEGRAL = F9.5, 17H TOTAL OVERLAP = F9.5,
    112H STRENGTH = F9.5, 7H GF = F9.5//)
    IF(PC) 610, 614, 610
610  WRITE OUTPUT TAPE 6, 611
611  OFORMAT(81H RADIUS S SQUARED FUNCTION FINAL S FUN
    1CTIGN FINAL P FUNCTION // )
    R = R1
    DO 613 I = 1, N
    C = PA(I)
    X = PB(I)
    Y = PC(I)
    WRITE OUTPUT TAPE 6, 612, R, Q, X, Y
612  FORMAT(4E20.8)
613  R = R-H
614  RETURN
700  READ INPUT TAPE 5, 701, NRADS, NRADLB, NRADLA, ELB, ELA,
    1SNB, NSB, ELNB, NELB, SNA, NSA, ELNA, NELA
701  FORMAT(3I2, 2F5.0, F8.0, 13, F8.0, 13, F8.0, 13, F8.0, 13 )
    READ INPUT TAPE 5, 702, R1, H, N, C, JUMP, MULT, FREQ, ATOM
702  FORMAT(2F5.0, 15, F5.0, 2I3, F10.0, A8)
    WRITE OUTPUT TAPE 6, 703
703  FORMAT(31H SL1 TO SL2 OSCILLATOR STRENGTH //)
    WRITE OUTPUT TAPE 6, 704, ATOM, NRADS, NRADLB, ELB, NRADLA, ELA
704  OFORMAT(18, 5H N = 12, 6H FOR THE STATIONARY S-WAVE ELECTRON.
    11H THE TRANSITION IS FROM N = 12, 5H L = F3.1, 8H TO N = 12,
    2 5H L = F3.1 //)
    OWRITE OUTPUT TAPE 6, 705, R1, H, N, C, NSB, SNB, NELB, ELNB,
    1NELA, ELNA, MULT, JUMP, FREQ
705  OFORMAT(6H R1 = F5.2, 6H H = F5.3, 6H WITH 14, 16H POINTS C =
    1F5.3, 11H THE NUMBER 12, 17H S-NODE IS AT R = F7.4 //, 11H THE NUMB
```

```
2ER 12,24H L-NODE BEFORE IS AT R = F7.4, 15H AND THE NUMBER 12,  
323H L-NODE AFTER IS AT R = F7.4//, 19H THE MULTIPLICITY = 12,  
416H THE JUMP CODE = 12,20H AND THE FREQUENCY = F10.1// )  
CALL SLIEB,EBB,ELB,H,C, R1, N, SNB, ELNB, NSB, NELB, MULT, PA,PB)  
CALL SLIEA,EAA,ELA,H,C, R1, N, SNA, ELNA, NSA, NELA, MULT,PC,PD)  
O1 = OVLP(H, PB, PC, R1, N, 1.0)  
O = O1*OVLP(H, PA, PC, R1, N, 0.0)  
CALL FVALUE(O, JUMP, FREQ, STR, GF)  
WRITE OUTPUT TAPE 6, 706, O1, O, STR, GF  
7060FORMAT(19H RADIAL INTEGRAL = F9.5, 17H TOTAL OVERLAP = F9.5//,  
112H STRENGTH = F9.5, 6H GF = F9.5////)  
IF(PO) 707, 711, 707  
707 WRITE OUTPUT TAPE 6, 708  
7080FORMAT(101H RADIUS INITIAL S FUNCTION INITIAL L F  
UNCTION FINAL S FUNCTION FINAL L FUNCTION // )  
R = R1  
DO 710 I = 1, N  
Q = PA(I)  
W = PB(I)  
X = PC(I)  
Y = PD(I)  
WRITE OUTPUT TAPE 6, 709, R, Q, W, X, Y  
709 FORMAT(5E20.8)  
710 R = R-H  
711 RETURN  
END
```

```
C ONE ELECTRON F-VALUE  
SUBROUTINE OEFVMP(EB, EA, PO)  
DIMENSION PB(1200), PA(1200), Z(5)  
5000READ INPUT TAPE 5, 501, NRADB, NRADA, ELB, ELA, R1, H, N, C,  
1JUMP, FREQ, ATOM  
501 FORMAT(2I2, 4F5.0, 15, F5.0, 13, F10.0, A8)  
WRITE OUTPUT TAPE 6, 503  
503 FORMAT(1H1 32H ONE ELECTRON OSCILLATOR STRENGTH //)  
WRITE OUTPUT TAPE 6, 504, ATOM, NRADB, ELB, EB, NRADA, ELA, EA  
5040FORMAT(A8, 6H N = 11, 6H L = F3.1, 13H WITH ENERGY F15.8,  
113H RYD TO N = 11, 6H L = F3.1, 13H WITH ENERGY F15.8, 4H RYD//)  
CALL ONELEC(EB, ELB, R1, H, C, N, PB, Z)  
WRITE OUTPUT TAPE 6, 515, R1, H, N, C, JUMP, FREQ  
5150FORMAT(7H R1 = F5.2, 6H H = F5.3, 6H N = 15, 6H C = F5.3,  
110H JUMP = 13, 15H FREQUENCY IS F8.1//1  
Z1 = Z(1)  
Z2 = Z(2)  
Z3 = Z(3)  
Z4 = Z(4)  
Z5 = Z(5)  
WRITE OUTPUT TAPE 6, 505, Z1, Z2, Z3, Z4, Z5  
505 FORMAT(24H THE FIRST HAS NODES AT F10.6, 4F10.6//)  
CALL ONELEC(EA, ELA, R1, H, C, N, PA, Z)  
Z1 = Z(1)  
Z2 = Z(2)  
Z3 = Z(3)  
Z4 = Z(4)  
Z5 = Z(5)  
WRITE OUTPUT TAPE 6, 506, Z1, Z2, Z3, Z4, Z5  
506 FORMAT(25H THE SECOND HAS NODES AT F10.6, 4F10.6//)  
O = OVLP(H, PA, PB, R1, N, 1.0)  
CALL FVALUE(O, JUMP, FREQ, STR, GF)  
WRITE OUTPUT TAPE 6, 507, O, STR, GF  
5070FORMAT(1H0 18HRADIAL INTEGRAL = F12.8, 14H STRENGTH = F9.5,  
18H GF = F9.5////)  
IF(PO) 508, 512, 508  
508 WRITE OUTPUT TAPE 6, 509  
509 FORMAT(55H RADIUS INITIAL FUNCTION FINAL FUNCTION)  
R = R1  
DO 511 I = 1, N  
Q = PB(I)  
Y = PA(I)  
WRITE OUTPUT TAPE 6, 510, R, Q, Y  
510 FORMAT(3E20.8)  
511 R = R-H  
512 RETURN  
END
```

C

```
          S-SQUARED SUBROUTINE
SUBROUTINE SSQRD(E, R1, H, C, N, P, Z, FO, ETCT)
DIMENSION P(1200), PSQR(1200), Z(5), QUAC2(1200)
COMMON PSQR, QUAD2
Z(1) = 0.0
Z(2) = 0.0
Z(3) = 0.0
Z(4) = 0.0
Z(5) = 0.0
K = 1
CALL START(E, 0.0, R1, H, C, P1, P2)
P(1) = P1
P(2) = P2
50 PSQR(1) = P(1)**2
   PSQR(2) = P(2)**2
   DP = P(1)-P(2)
   R = R1-(2.0*H)
   DDP = (H**2)*(E-(2.0*C)/(R+H))*P(2)
   DP = DP-DDP
   P(3) = P(2)-DP
   TAB1A = 0.0
   TAB2A = 0.0
   TAB1B = 0.0
   TAB2B = 0.0

   PSQR(3) = P(3)**2
   J = 1
   QUAD2(1) = 0.0
   QUAD2(2) = 0.0
   M = N-2
   DO 55 I = 3, M, 2
   QUAD1 = (H/3.0)*(PSQR(I)+(4.0*PSQR(I-1))+PSQR(I-2))+TAB1A
   QUAD2(I) = (H/3.0)*((PSQR(I)/R)+4.0*(PSQR(I-1)/(R+H))
   1+(PSQR(I-2)/(R+(2.0*H))))+TAB2A
   TAB1A = QUAD1
   TAB2A = QUAD2(I)
   DDP = (H**2)*(E-((2.0*C)/R)-(2.0*QUAD1/R)+(2.0*QUAD2(I)))*P(I)
   DP = DP-DDP
   P(I+1) = P(I)-DP
   QUAD1 = (H/3.0)*(PSQR(I+1)+(4.0*PSQR(I))+PSQR(I-1))+TAB1B
   QUAD2(I+1) = (H/3.0)*((PSQR(I+1)/(R-H))+4.0*(PSQR(I)/R)
   1+(PSQR(I-1)/(R+H)))+TAB2B
   TAB1B = QUAD1
   TAB2B = QUAD2(I+1)
   DDP = (H**2)*(E-(2.0*C/(R-H))-(2.0*QUAD1/(R-H))+(2.0*QUAD2(I+1)))
   1*P(I+1)
   DP = DP-DDP
   P(I+2) = P(I+1)-DP
   R = R-(2.0*H)
   PSQR(I+1) = P(I+1)**2
   PSQR(I+2) = P(I+2)**2
   IF(P(I)*P(I+1)) 52, 52, 51
51 IF(P(I+1)*P(I+2)) 53, 53, 55
52 Z(J) = R + H - (H*P(I+1))/(P(I) - P(I+1))
   GO TO 54
53 Z(J) = R - (H*P(I+2))/(P(I+1) - P(I+2))
54 J = J+1
55 CONTINUE
S = SIMP(H, N, PSQR)
A = ABSF(1.0 - S)
IF(.0005 - A) 56,57, 57
56 P(1) = P(1)/SQRTF(S)
   P(2) = P(2)/SQRTF(S)
   K = K+1
   GO TO 59
57 DO 58 I = 1, N
58 PSQR(I) = PSQR(I)*QUAD2(I)
   FO = 4.0*SIMP(H, N, PSQR)
   ETOT = (2.0*E)+FO
   RETURN
59 IF(K - 10) 50, 50, 1000
1000 WRITE OUTPUT TAPE 6, 1001
1001 FORMAT(37H ERROR IN S SQRD TOO MANY ITERATIONS )
   CALL EXIT
   END
```

```
C      ONE ELECTRON SUBROUTINE
SUBROUTINE ONELEC(E, EL, R1, H, C, N, P, Z)
DIMENSION P(1200), PSQR(1200), Z(5)
COMMON PSQR
Z(1) = 0.0
Z(2) = 0.0
Z(3) = 0.0
Z(4) = 0.0
Z(5) = 0.0
CALL START(E, EL, R1, H, C, P1, P2)
P(1) = P1
P(2) = P2
PSQR(1) = P(1)**2
PSQR(2) = P(2)**2
DP = P(1) - P(2)
R = R1-H
J = 1
M = N-1
DO 41 I = 2, M
DDP = (H**2)*((E+(EL*(EL+1.0))/(R**2))-(2.0*C1/R)*P(I))
DP = DP-DDP
P(I+1) = P(I)-DP
PSQR(I+1) = P(I+1)**2
R = R-H
IF(P(I+1)*P(I)) 40, 40, 41
40 Z(J) = R - (H*P(I+1))/(P(I) - P(I+1))
J = J+1
41 CONTINUE
S = SIMP(H, N, PSQR)
DO 42 I = 1, N
42 P(I) = P(I)/SQRT(S)
RETURN
END
```

```
C      THE MARS SUBROUTINE
SUBROUTINE MARS(PS, PP, R1, EL, H, N, G, RHO)
DIMENSION PS(1200), PP(1200), B1(1200), B2(1200), G1(1200),
IG2(1200), G(1200)
COMMON B1, B2
R = R1
DO 18 I = 1, N
B1(I) = (R**EL)*PS(I)*PP(I)
18 R = R-H
R = R1
DO 19 I = 1, N
B2(I) = PS(I)*PP(I)/(R**(EL+1.0))
19 R = R-H
TAB1A = 0.0
TAB1B = 0.0
G1(1) = 0.0
G2(1) = 0.0
G1(2) = 0.0
G2(2) = 0.0
TAB2A = 0.0
TAB2B = 0.0
M = N-1
DO 20 I = 3, M, 2
G1(I) = (H/3.0)*(B1(I)+4.0*B1(I-1)+B1(I-2))+TAB1A
TAB1A = G1(I)
G1(I+1) = (H/3.0)*(B1(I+1)+4.0*B1(I)+B1(I-1))+TAB1B
TAB1B = G1(I+1)
G2(I) = (H/3.0)*(B2(I)+4.0*B2(I-1)+B2(I-2))+TAB2A
TAB2A = G2(I)
G2(I+1) = (H/3.0)*(B2(I+1)+4.0*B2(I)+B2(I-1))+TAB2B
20 TAB2B = G2(I+1)
R = R1-(2.0*H)
C = 2.0/(2.0*EL+1.0)
G(1) = 0.0
G(2) = 0.0
DO 21 I = 3, N, 1
G(I) = C*((G1(I)/(R**(EL+1.0)))-(R**EL)*G2(I))
21 R = R-H
RHO = TAB1A
RETURN
END
```

```
C THE VENUS SUBROUTINE
SUBROUTINE VENUS (P, R1, H, N, F)
DIMENSION P(1200), F1(1200), F2(1200), F(1200)
COMMON F1, F2
TAB1A = 0.0
TAB1B = 0.0
TAB2A = 0.0
TAB2B = 0.0
F1 (1) = 0.0
F1 (2) = 0.0
F2 (1) = 0.0
F2 (2) = 0.0
M = N-1
DO 22 I = 3, M, 2
F1(I) = (H/3.0)*((P(I)**2)
1+(4.0*(P(I - 1)**2))
2+ (P(I - 2)**2)) + TAB1A
TAB1A = F1(I)
F1 (I+1) = (H/3.0) * ((P(I+1) **2)
1+4.0 * (P(I) **2) + (P(I-1)**2)) + TAB1B
TAB1B = F1 (I+1)
Y = I
F2 (I) = (H/3.0) * (((P(I)**2) / (R1 - (Y-1.0) * H))
1+ 4.0 * ((P(I-1)**2) / (R1-(Y-2.0)*H))
2+ ((P(I-2)**2) / (R1-(Y-3.0)*H))) + TAB2A

TAB2A = F2 (I)
F2 (I+1) = (H/3.0) * (((P(I+1)**2) / (R1-Y*H))
1+ 4.0 * ((P(I)**2) / (R1-(Y-1.0)*H))
2+ ((P(I-1)**2) / (R1-(Y-2.0)*H))) + TAB2B
22 TAB2B = F2(I+1)
R = R1 - (2.0*H)
F(1) = 0.0
F(2) = 0.0
DO 23 I = 3, N, 1
F(I) = 2.0 * ((F1(I) / R) - F2(I))
23 R = R-H
RETURN
END
```

```
C FACTORIAL FUNCTION
FUNCTION FACTO (X)
Y = (0.461*X*(X - 1.0)) + 1.0
A = ABSF(X-0.461)
IF(A - 0.15) 94, 94, 90
90 IF(A - 0.461) 91, 91, 94
91 IF (X-0.461) 92, 93, 93
92 FACTO = Y-0.005
GO TO 95
93 FACTO = Y + 0.005
GO TO 95
94 FACTO = Y
95 RETURN
END
```

```
C THE OVERLAP FUNCTION
FUNCTION OVLP(H, PA, PB, R1, N, Q)
DIMENSION PA(1200), PB(1200), B(1200)
COMMON B
IF(Q) 13, 13, 15
13 DO 14 I = 1, N
14 B(I) = PA(I)*PB(I)
GO TO 17
15 R = R1
DO 16 I = 1, N
B(I) = R*PA(I)*PB(I)
16 R = R-H
17 OVLP = SIMP(H, N, B)
RETURN
END
```

```
C   STARTING VALUE SUBROUTINE
SUBROUTINE START (E, EL, R1, H, C, P1, P2)
EN = C/ SQRTF (E)
Y = 1.0
A = 1.0
30 IF (EN+EL-A) 32, 32, 31
31 Y = Y*(EN+EL-A+1.0)
A = A+1.0
GO TO 30
32 X = EN+EL-A+1.0
F = Y*FACTO(X)
Z = 1.0
H = 1.0
IF(EN - EL - 2.0) 36, 36, 33
33 IF (EN-EL-B-1.0) 35, 35, 34
34 Z = Z* (EN-EL-B)
B = B + 1.0
GO TO 33
35 X = EN-EL-B
G = F*Z* FACTO (X)
GO TO 39
36 IF (EN-EL+B-2.0) 37,38,38
37 Z = Z* (EN-EL-1.0+B)
H = B+1.0
GO TO 36
38 X = EN-EL+B-2.0
IF(Z) 70, 71, 70
70 G = F*FACTO(X)/Z
39 S = EN* LOGF (2.0*C/EN)
T = (EXPF(S)* SQRTF(C))/(EN*SQRTF(G))
B1 = EN*((EL*(EL + 1.0)) - (EN*(EN - 1.0)))/(2.0*C)
B2 = EN* B1 * ((EL * (EL+1.0)) - ((EN-1.0) * (EN-2.0)))/(4.0*C)
B3 = EN * B2 * ((EL * (EL+1.0))-((EN-2.0)*(EN-3.0)))/(6.0*C)
U1 = EN * LOGF (R1)
P1 = T * (EXPF(U1-C*R1/EN))*(1.0+(B1/R1)
1+(B2/(R1**2)) + (B3/(R1**3)))
R2 = R1 - H
U2 = EN * LOGF (R2)
P2 = T * (EXPF (U2-C*R2/EN)) * (1.0+(B1/R2)
1+ (B2/(R2**2)) + (B3/(R2**3)))
RETURN
71 WRITE OUTPUT TAPE 6, 72
72 FORMAT(26H ERROR IN START, Z IS ZERO)
CALL EXIT
END
```

```
C   SIMPSONS RULE FUNCTION
FUNCTION SIMP ( H, N, B)
DIMENSION B (1200)
S = 0.0
M = N-2
DO 80 I = 2, M, 2
80 S = S + B (I)
S = 2.0 * S
K = N-3
DO 81 I = 3, K, 2
81 S = S + B (I)
SIMP = (H/3.0)*((2.0*S) +B(1) + B(N-1))
RETURN
END
```

C

THE EVENT SUBROUTINE

```
OSUBROUTINE EVENTINE, KIND, P, R, EIN, IN, EDB, EUB, NIT,
INEA, ECUT, IT, EDA, EUA, ND )
ENIT = NIT
EDA = EDB
EUA = EUB
EOUT = EIN
ND = 0
IF(NE - 2) 1, 10, 20
1 IF(KIND - 1) 2, 58, 5
2 IT = IN + 1
EOUT = EIN/(1.0 + 0.2*EIN)

GO TO 59
5 IF(KIND - 3) 6, 2, 2
6 IT = 1
NEA = 2
GO TO 60
10 IF(KIND - 1) 11, 15, 12
12 IF(KIND - 3) 11, 11, 2
11 IT = IN + 1
EOUT = (1.0 + 0.2 * EIN) * EIN
GO TO 59
15 IT = 1
NEA = 3
GO TO 60
20 IF(KIND - 1) 21, 21, 23
21 NEA = 3
IT = IN
GO TO 60
23 IF(KIND - 3) 30, 40, 25
25 WRITE OUTPUT TAPE 6, 26, EIN, P, R
260FORMAT(F8.5, 44H MAXIMUM INFLECTION PT MONOTONIC TO P = F7.5,
1 10H AT R = F8.5 ///)
ND = 1
IT = IN
NEA = 4
GO TO 60
30 IT = IN + 1
EUA = EIN
IF(EDB) 31, 31, 35
31 EOUT = EIN/(1.0 + (0.1/((ENIT - 1.0) ** 2)))
GO TO 36
35 EOUT = (EUA + EDB)/2.0
36 WRITE OUTPUT TAPE 6, 37, EIN, P, R
370FORMAT(F8.5, 44H MAXIMUM INFLECTION PT MINIMUM WITH P = F7.5,
1 10H AT R = F8.5 )
GO TO 59
40 IT = IN + 1
41 EDA = EIN
IF(EUB) 42, 42, 45
42 EOUT = (1.0 + (0.1/((ENIT - 1.0) ** 2))) * EIN
GO TO 46
45 EOUT = (EUB + EDA)/2.0
46 WRITE OUTPUT TAPE 6, 47, EIN, R
47 FORMAT(F8.5, 43H MAXIMUM INFLECTION PT AND NODE AT R = F8.5 )
GO TO 59
58 IT = IN
59 NEA = 1
60 RETURN
END
```

```
C          EXTRA NODE SUBROUTINE
OSUBROUTINE EXNDINE, KIND, R, EIN, IN, EUB, EDB, NEA,
1EOUT, IT, EUA, EDA, ND )
  EUA = EUB
  EDA = EDB
  ND = 0
  EOUT = EIN
  NEA = 1
  IT = IN
  IF(NE - 5) 1, 10, 30

1 IF(KIND - 2) 2, 8, 4
2 WRITE OUTPUT TAPE 6, 3, EIN, R
3 FORMAT(F8.5, 37H EXTRA NODE INFLECTION POINT AT R = F8.5 )
  EDA = EIN
  IT = IN + 1
  EOUT = (EIN + EUB)/2.0
  GO TO 45
4 WRITE OUTPUT TAPE 6, 5, R
5 FORMAT(F8.5, 47H EXTRA NODE FOLLOWED BY BLOW UP OR END AT R = F8.5 )
  IT = 20
  GO TO 45
8 NEA = NE + 1
  GO TO 45
10 IF(KIND - 3) 11, 20, 12
11 NEA = NE + 1
  GO TO 45
12 WRITE OUTPUT TAPE 6, 13, EIN, R
13 FORMAT(F8.5, 38H EXTRA NODE MINIMUM MONOTONIC TO R = F8.5)
  ND = 1
  GO TO 45
20 WRITE OUTPUT TAPE 6, 21, EIN, R
21 FORMAT(F8.5, 34H EXTRA NODE MINIMUM NODE AT R = F8.5 )
  EUA = EIN
  IT = IN + 1
  EOUT = (EIN + EDB)/2.0
  GO TO 45
30 IF(KIND - 3) 31, 35, 40
31 WRITE OUTPUT TAPE 6, 32, EIN, R
32 FORMAT(F8.5, 38H EXTRA NODE MIN INFLEC MAXIMUM AT R = F8.5 )
  IT = IN + 1
  EOUT = (EIN + EUB)/2.0
  GO TO 45
35 WRITE OUTPUT TAPE 6, 36, EIN, R
36 FORMAT(F8.5, 35H EXTRA NODE MIN INFLEC NODE AT R = F8.5 )
  ND = 2
  GO TO 45
40 WRITE OUTPUT TAPE 6, 41, EIN, R
41 FORMAT(F8.5, 40H EXTRA NODE MIN INFLEC MONOTONIC TO R = F8.5 )
  ND = 1
  GO TO 45
45 RETURN
  END
```

```

C          F-VALUE SUBROUTINE
SUBROUTINE FVALUE(OVLP, JUMP, FREQ, STR, GF)
  IF(JUMP) 900, 900, 901
  JUMP = -JUMP
  GO TO (902, 903, 903, 904, 905, 905, 906, 907), JUMP
901 GO TO (908, 909, 910, 911, 912, 913, 914, 915, 916, 917,
  1718, 919), JUMP
902 C = 2.0/3.0
  GO TO 920
903 C = 4.0/3.0
  GO TO 920
904 C = 4.0/15.0
  GO TO 920
905 C = 12.0/5.0
  GO TO 920
906 C = 6.0/35.0
  GO TO 920
907 C = 24.0/7.0
  GO TO 920
908 C = 2.0
  GO TO 920
909 C = 1.0
  GO TO 920
910 C = 1.0/3.0
  GO TO 920
911 C = 1.0
  GO TO 920
912 C = 5.0/3.0
  GO TO 920
913 C = 2.0
  GO TO 920
914 C = 2.0/3.0
  GO TO 920
915 C = 1.0/2.0
  GO TO 920
916 C = 3.0/2.0
  GO TO 920
917 C = 1.0/30.0
  GO TO 920
918 C = 1.0/2.0
  GO TO 920
919 C = 14.0/5.0
920 STR = C*(OVLP**2)
921 GF = .0000030324*FREQ*STR
  RETURN
  END

```

```

C          BEGINNING VALUE SUBROUTINE
SUBROUTINE BEGIN(PN, AM, EL, MULT, TAB, RL, H, S, RL, RP, PU, PP, DI)
  K = R1
  L = 1
  DIV = 1.0
  1 R = R - P
  L = L + 1
  IF(R = PN) 2, 2, 1
  2 C = .0
  3 IF(L = PN) 4, 4, 5
  4 C = C + P
  GO TO 3
  5 RM = C
  6 R = C - H
  IF(RN = 0.5) 14, 14, 10
  14 IF(L1) 16, 16, 18
  15 IF(TAB) 16, 16, 17
  16 DIV = 0.45
  GO TO 13
  17 DIV = 0.07
  GO TO 13
  18 IF(MULT = 1) 6, 6, 13
  9 DIV = 50.0
  GO TO 13
  10 IF(L2) 13, 11, 13
  11 IF(LP = 1) 12, 12, 13
  12 DIV = 0.25
  13 PU = .01 * LRL = PN/LH * DIV * SQRT(S1)
  PM = .01 * LRM = PN/LH * DIV * SQRT(S1)
  RETURN
  END

```

C THE RENORMALIZATION SUBROUTINE NO. 1
SUBROUTINE RENORM(S1, S2, S3, DBNOM)
G = 1.0
Q1 = S1 - 1.0
Q2 = S2 - 1.0
Q3 = S3 - 1.0
IF(Q1 * Q2) 8, 8, 1
1 IF(Q2 * Q3) 8, 8, 3
3 IF(Q3 - .05) 4, 5, 5
4 IF(Q3 + .03) 6, 6, 8
5 DENOM = 1.5
GO TO 9
6 DBNOM = 0.7
GO TO 9
8 DBNOM = 1.0
9 RETURN
END

C THE RENORMALIZATION SUBROUTINE NO. 2
SUBROUTINE RENORM(S1, S2, S3, DBNOM)
G = 1.0
Q1 = S1 - 1.0
Q2 = S2 - 1.0
Q3 = S3 - 1.0
IF((Q1 + Q2) * (Q2 + Q3)) 8, 8, 1
1 IF(Q1 * Q3) 8, 8, 2
2 IF(ABSFLQ1) - ABSFLQ2) 8, 8, 3
3 IF(ABSFLQ3) - .05) 8, 8, 4
4 CAV = ((Q1/Q2) + (Q2/Q3))/2.0

I = 1
5 F = 1.0 + (Q3/(CAV**I))
IF(ABSFLF - 1.0) - .05) 7, 7, 6
6 G = F * G
I = I + 1
GO TO 5
7 DENOM = SQRTF(G)
GO TO 9
8 DBNOM = 1.0
9 RETURN
END

```

      THE SL OUT SUBROUTINE
0SUBROUTINE SL(E1, E2, EL, H, C, RB, NN, SNO, PNO, NS, NP, MU,
1PS, PP)
GDIMENSION PS(1200), PP(1200), GL(1200), FOCK(1200), P(1200),
IHART(1200), PSQR(1200), ZS(5), ZP(5)
COMMON PSQR
DENCH = 1.0
S1 = 1.0
S2 = 1.0
S3 = 1.0
RHO1 = 0.0
RHO2 = 0.0
RI = RH
N = NN
SN = SNO
PN = PNO
MULT = MU
NTRY = 0
NIT = 1
SU = 1.0
SIMPS = 1.0
TAB = 1.0
NRHO = 0
EL2 = BU
EL1 = C.C
CALL CNELECC(E1, O.C, RI, H, C, N, PS, ZS)
CALL UNBLECC(E2, EL, RI, H, C, N, PP, ZP)
LFIN = 0
R = RI
DO 12 I = 1, N
  IF(R - SN(12, I)) 10
10 IF(R - SN - 1.0) 11, 11, 12
11 PS(I) = (R - SN)*PS(I)
12 R = R - H
54 IF(TAB) 61, 61, 55
55 WRITE OUTPUT TAPE 6, 56, NIT
56 FORMAT(17H ITERATION NUMBER 12 /)
  NIT = NIT + 1
  IF(EL2 = 1.0) 61, 57, 59
57 WRITE OUTPUT TAPE 6, 58, PN
58 FORMAT(34H H-WAVE FUNCTION WITH NODE AT R = F8.5//)
  GO TO 63
59 WRITE OUTPUT TAPE 6, 60, PN
60 FORMAT(34H D-WAVE FUNCTION WITH NODE AT R = F8.5//)
  GO TO 63
61 WRITE OUTPUT TAPE 6, 62, PN
62 FORMAT(34H S-WAVE FUNCTION WITH NODE AT R = F8.5//)
63 TAB = - TAB
```

```
IN = 1
ECH = - 1.0
EUB = - 1.0
NBX = -1
NSTRAD = 0
CALL MARSL RS, RP, R1, EL, H, N, G, RHO )
EN2 = E2
LOP = C
R = R1
IF(MULT - 1) 28, 28, 15
15 IF(BL2) 28, 16, 28
16 IF(RHC1) 18, 17, 18
17 RHC1 = RHO
GO TO 28
18 IF(RHC2) 20, 19, 20
19 RHC2 = RHO
GO TO 28
20 WRITE OUTPUT TAPE 6, 21, RHO
21 FORMAT(18H UNAVERAGED RHO = F8.5 //)
RHO = (RHC1 + RHC2 + RHO) / 3.0
RHC1 = RHO2
RHC2 = RHO1
RHO = RHO1
28 DO 101 I = 1, N
FOCK(I) = RS(I)*(((2.0*RHO)/(((2.0*BL)+1.0))+(R**4*(BU+1.0))))-G(I)
101 R = R + F
102 CALL VENUS(RS, R1, H, N, F)
R = R1
DO 103 I = 1, N
HART(I) = -(2.0*G/R) + ((EL2 + (EL2 + 1.0)) / (R**2)) - F(I)
103 R = R + F
CALL BEGIN(PN, NP, BL2, MULT, TAP, R1, H, SU, RU, RM, PU, PM, LU)
37 WRITE OUTPUT TAPE 6, 64, PM, RM, RHO
64 FORMAT(21H STARTING VALUE P = F10.7, 7H AT R = F8.5, 5H RHO = F8.5 //)
NIX = C
NATT = 0
WRITE OUTPUT TAPE 6, 65
65 FORMAT(40H ENERGY EVENTS //)
104 NB = 1
106 ODP = - 1.0
OP = PM - PL
R = RM
J = 1
PR(LL) = PL
PR(LL - 1) = PM
113 DO 153 I = 3, LL
L = LL - I + 2
ODPB = ODP
OPB = OP
IF(MBLTI 114, 114, 111)
111 IF(MGLT - 1) 114, 112, 113
112 ODP = (H**2) * (((EN2 + HART(L)) * PR(L)) + FOCK(L))
GO TO 115
113 ODP = (H**2) * (((EN2 + HART(L)) * PR(L)) - FOCK(L))
GO TO 115
114 ODP = (H**2) * ((EN2 + HART(L)) * PR(L))
115 R = R + F
OP = OP + ODP
PR(L - 1) = PR(L) + OP
```

```
IF(CCPB * CDP) 125, 125, 116
116 IF(CPB * DP) 126, 126, 117
117 IF(PP(L - 1) * RP(L)) 127, 127, 118
118 IF(ABS(PR(L - 1)) - 20.0) 119, 128, 128
119 IF(NP - 1) 120, 120, 121
120 IF(PP(L - 1) + 1.0) 129, 129, 121
121 IF(R + (FZ.1) - R1) 153, 153, 122
122 KIND = 4
GO TO 130
125 KIND = 1
GO TO 130
126 KIND = 2
GO TO 130
127 KIND = 3
GO TO 130
128 KIND = 9
GO TO 130
129 KIND = 5
GO TO 130
130 IF(NP - J) 133, 133, 131
131 IF(KIND - 3) 158, 132, 158
132 J = J + 1
WRITE OUTPUT IARE 6, 136, R
136 FORMAT(20H FIRST NODE AT R = F8.5 )
IF(NIX - 30) 400, 900, 310
400 NIX = NIX + 1
GO TO 153
133 W = PP(L)
IF(TAH) 137, 137, 134
134 IF(XARSR(MULT) - 1) 135, 135, 137
135 IF(NE - 3) 137, 500, 502
500 IF(KIND - 3) 504, 501, 504
501 RND = R
K3 = 3
GO TO 505
502 IF(NEX) 137, 137, 514
504 K3 = C
505 IF(K3 - 3) 137, 507, 137
507 IF(EBH) 137, 137, 508
508 IF(EDB) 137, 137, 509
509 IF(ABS(EUR - EDH) - (.0005 * EDH)) 510, 137, 137
510 IF(RND - (.25 * R1)) 511, 137, 137
511 NEX = 1
NE = 4
GO TO 153
514 CALL EXND(LNE, KIND, W, R, EN2, IN, EDB, EDH, NEA, EOL,
117, EGA, EDA, ND )
IX = II
IF(RND) 510, 515, 520
515 IF(II - 8) 151, 517, 516
516 RN = RND
GO TO 178
517 WRITE OUTPUT IARE 6, 518
518 FORMAT(32H SEVERAL TRIES WITH AN EXTRA NODE )
IF(II - 20) 178, 519, 178
519 R = RND
GO TO 178
520 IF(RND - 1) 230, 230, 178
137 CALL EVNT(LNE, KIND, W, R, EN2, IN, EDB, EUB, NEA,
```

```
INBA, BCUT, IT, BDA, EOA, ND )
ENBR = EN2
IM = IT
IF(NE - 1) 150, 230, 230
150 IF(IT - 20) 151, 151, 300
151 IF(EN2 - BCUT) 155, 152, 155
152 NB = NEA
158 IF(KIND - 1) 153, 116, 153
153 CONTINUE
IF(NP - J) 230, 230, 154
154 EN2 = BN2/2.0
GO TO 104
155 EN2 = BCUT
NATT = NATT + 1
IF(NATT - 30) 145, 145, 310
145 EUR = EOA
EDB = EDA
IF(NEX) 159, 159, 190
159 IF(NE - 2) 104, 104, 160
160 IF(BDB) 162, 162, 161
161 IF(EUB) 162, 162, 170
162 LOP = LOP + 1
163 IF(LOP - 2) 104, 165, 165
165 EN2 = BN2 + 2.0 * (BA2 - ENBR)
GO TO 104
170 NSTRAD = NSTRAD + 1
IF(NSTRAD - 10) 104, 175, 178
175 EN2 = ECB
GO TO 104
178 RN = R
179 R = R1
DO 183 IF = 1, N
IF(R - RN) 183, 182, 182
182 PR(I) = 20
183 R = R - F
WRITE OUTPUT TAPE 6, 185, RN
185 FORMAT(60H ASYMPTOTIC CONDITION NOT MET FUNCTION ZEROED PAST
1 R = F8.5 / / / /)
GO TO 230
190 NSTRAD = NSTRAD + 1
IF(NSTRAD - 12) 104, 104, 178
243 CP = PM - PL
R = RL
DO 251 L = 1, N
DPP = (F**2) * ((EN2 + HAPT(L)) * PP(L))
CP = CP - DPP
PR(L + 1) = PP(L) - CP
IF(R - 0.5) 249, 249, 251
249 IF(R) 249, 249, 250
250 PR(L + 1) = 2.0 * R * PP(L + 1)
251 R = R - F
DO 252 F = 1, N
252 PSQR(I) = PR(I)**2
S = SIMR(H, N, PSQR)
DO 253 F = 1, N
253 PR(I) = PR(I)/SQRT(FS)
WRITE OUTPUT TAPE 6, 254, S
254 FORMAT(26H NORMALIZATION INTEGRAL = F8.5 / / / /)
IF(TAR) 255, 255, 256
```

```
255 SIMPL = S * SU
    SU = SIMPS
400 IF(NIT - 3) 260, 401, 401
401 IF(S1 - 1.0) 403, 402, 403
402 S1 = S
    GO TO 260
403 IF(S2 - 1.0) 406, 404, 406
404 S2 = S
    GO TO 260
406 IF(S3 - 1.0) 407, 408, 407
407 S1 = S2
    S2 = S3
408 S3 = S
    CALL RNFNRM(S1, S2, S3, DENOM)
    GO TO 260
256 SIMPS = S * SU
    SU = SIMPL * DENOM
260 IF(LABSLEN2 - E2) - .0025 * E2) 261, 270, 270
261 WRITE OUTPUT TAPE 6, 262
2620 FORMAT(86H  MEETS CONDITION WITH AN ENERGY WITHIN 22 PERCENT OF Y
    THIS ITERATIONS INITIAL ENERGY  //// )
    IF(LBL) 268, 269, 268
268 IF(ABSFLS - 1.0) - .005) 267, 267, 265
269 IF(LABSFLS - 1.0) - .03) 267, 267, 274
274 WRITE OUTPUT TAPE 6, 275
275 FORMAT(52H FUNCTION NOT NORMALIZED WITHIN 2 PERCENT; PROCEED; //)
    GO TO 270
265 WRITE OUTPUT TAPE 6, 266
266 FORMAT(52H FUNCTION NOT NORMALIZED WITHIN 25 PERCENT; PROCEED; //)
    GO TO 270
267 NTRY = NTRY + 1
    IF(NTRY - 2) 279, 263, 263
263 WRITE OUTPUT TAPE 6, 264
264 FORMAT(25H  FUNCTIONS ESTABLISHED //// )
    GO TO 300
270 NTRY = 0
    IF(NIT - 25) 273, 273, 271
271 WRITE OUTPUT TAPE 6, 272
272 FORMAT(44H  TOO MANY ITERATIONS  CN TO NEXT PROBLEM )
    GO TO 310
273 E2 = EN2
279 A = E2
    C2 = E1
    E1 = A
    A = E12
    E12 = E11
    E11 = A
    A = PN
    PN = SA
    SN = A
    I = AP
    AP = NS
    NS = I
300 DO 280 I = 1, N
    A = PP(I)
    PP(I) = PS(I)
280 PS(I) = A
    IF(UFIN) 54, 54, 310
308 LRIN = 1

    IF(TAR) 310, 310, 309
309 WRITE OUTPUT TAPE 6, 301
301 FORMAT(50H TWENTY TRIES WITHOUT PROGRESS  CN TO NEXT PROBLEM )
310 RETURN
    END
```